STUDIES ON THE CHAOTIC DYNAMICS OF PERIODICALLY FORCED WEAK BROWNIAN SPHEROIDS IN SIMPLE SHEAR FLOW

Thesis submitted to
the Cochin University of Science and Technology
in partial fulfilment of the requirements
for the degree of
DOCTOR OF PHILOSOPHY
in
TECHNOLOGY

by

C. V. ANIL KUMAR

under the supervision of

Dr T. R. RAMAMOHAN

Computational Materials Science, Unit I
Regional Research Laboratory
(Council of Scientific and Industrial Research)
Thiruvananthapuram - 695 019, India

October 1997

COUNCIL OF SCIENTIFIC AND INDUSTRIAL RESEARCH [CSIR]
क्षेत्रीय अनुसंधान प्रयोगशाला, तिरुवनन्तपुरम्-695 019
REGIONAL RESEARCH LABORATORY
Trivandrum- 695 019, INDIA.

50

CERTIFICATE

This is to certify that the thesis entitled **"Studies on the chaotic dynamics of periodically forced weak Brownian spheroids in simple shear flow"** is an authentic record of the research work carried out by **Mr. C. V. Anil Kumar** under my supervision in partial fulfilment of the requirements for the degree of **Doctor of Philosophy** of the **Cochin University of Science and Technology** and further that no part thereof has been submitted elsewhere for any other degree.

T. R. Ramamohan
06/10/1997

T. R. Ramamohan
(Supervisor)

Contents

List of Figures

List of Tables

Preface

The advanced computational capacities of the new generation computers have opened up a new area in the field of nonlinear dynamics, namely, **CHAOS**. Non-linear dynamics is common in nature. However physicists have been concentrating on linear dynamics for the last three centuries. Henry Poincaré (1854-1912) laid the foundations of the modern theory of chaos by the mathematical study of nonlinear dynamics. The theory of nonlinear dynamics has now grown in many directions and scientists have interpreted chaotic behavior in an attempt to understand the complex behaviour of nonlinear dynamical systems. The key fact to be considered is that the behaviour of a system may not be simple even though the governing laws are simple. For example, models of real systems such as simple electrical circuits, sets of differential equations (Lorenz 1963), biological population dynamics (May 1976) *etc.* can exhibit complex behaviour as the control parameter is varied (Hilborn 1994).

Chaos introduces a fundamental uncertainty in the sense that a deterministic prediction of chaotic dynamics requires infinite precision in the knowledge of initial conditions. In practice initial conditions can be known only to a finite precision. Small errors due to the limitation of precision in the knowledge of the initial conditions are multiplied in chaotic systems and result in overwhelming consequences in the long run. The sensitive exponential divergence of trajectories due to small initial effects is known as the *butterfly effect*. This sensitive dependence on initial conditions in deterministic systems rules out the possibility of long term prediction of the behaviour of systems showing chaos. The

presence of complexity and chaos is common. The study of chaos enables us to understand the complex behaviour of such systems. Chaotic dynamics also usually implies dramatic qualitative and quantitative changes in a system as the control parameter is varied. Due to these reasons scientists and engineers are fascinated by chaos.

The problem considered in this thesis is the dynamics of small dipolar spheroids of various aspect ratios in simple shear flow, under the action of periodically varying external force fields. The dynamics of periodically forced spheroids is the simplest case of a class of problems which have not received any attention in the chaos literature. The problem discussed in this work is the first demonstration that the dynamics and hence rheological properties of such suspensions can be chaotic. Based on the understanding of the problem considered, suitable techniques can be developed to calculate the rheological properties, thermal conductivities, rheo-optical properties *etc.* This work also points out a fundamental weakness in the approach of Strand (1989).

The relevant literature and review on chaotic dynamics and rheology are described briefly along with the introduction in chapter 1. The scientific and technological importance of the problem considered is also explained in that chapter.

The development of the theory is summarized in chapter 2. The equations of the dynamics of periodically forced particles of finite aspect ratio in simple shear flow are presented in this chapter both in Cartesian and spherical co-ordinate systems. The necessary assumptions for the mathematical formulation of the model and the computational procedure are also given in the chapter.

The existence of chaotic parametric regimes is described in the third chapter of this thesis. A potential application to segregate particles from a suspension of particles of different aspect ratios using the strong dependence on the results in the chaotic regime on the aspect ratio of the particles and the wide range of

orientations, thus obtained, is suggested in this chapter. A possible design for such a separator is also suggested in this chapter.

Chapter 4 describes the existence of a new type of class I intermittency, namely, a non-hysteretic form of class I intermittency with nearly regular behaviour interrupted by chaotic out breaks with nearly regular reinjection period. The scaling behaviour near the onset of bifurcation shows the existence of a typical class I intermittency. A new scaling behaviour away from the tangent bifurcation is also demonstrated in this chapter.

In chapter 5 a new algorithm for controlling chaotic dynamics is suggested and its applicability in the problem of chaotic dynamics of periodically forced spheroids in simple shear flow is demonstrated. It is also demonstrated that controlling chaotic dynamics of periodically forced spheroids can lead to better separation of particles than otherwise possible.

Some advantages of the novel control technique over two other methods are also demonstrated. To demonstrate these advantages, the novel algorithm has been successfully applied in three different models. The results obtained with the novel control technique in these models are compared with those obtained with the two other methods. These results are explained in detail in chapter 6.

The conclusions of this thesis and new directions for future work in this area are given in the last chapter.

The results described in chapters 3, 4, 5 and 6 have been published in internationally reputed journals. **The list of publications** resulting from this thesis is given at the end of the thesis.

Chapter 1

Introduction

The study of the motion of a single solid particle or particles of arbitrary shape in a Newtonian fluid has fascinated many scientists and engineers (Brenner 1974, Kim and Karrila 1991 and references therein) and finds application in the development of new techniques and processes for the preparation of composites, polymer solutions, electro-rheological fluids *etc.* There are many situations in nature and technology involving the motion of solid particles subjected to the shearing motion of the suspending fluid. The understanding of the rheological properties of such systems is essential to develop new processes and applications. Suspensions of macromolecules, emulsion and paint technology, transport and processing of slurries and ferro fluid rheology can be effectively studied by the application of suitable theories of suspension rheology. Ferrofluids, namely stabilized suspensions of small magnetic particles in a non-magnetic solvent have many industrial applications like rotary seals, inertia dampers, magnetic domain detectors, concentration of drugs at body sites *etc.* (Strand and Kim 1992). An excellent review of suspensions is given by Brenner (1972).

The rheological properties of a suspension may be greatly influenced by the dynamics of individual particles suspended in the fluid. This influence on the rheological properties allows the possibility of the construction of many novel electromechanical devices which have potential applications in the automotive, aerospace and other industries (Ginder and Sproston 1996) using suspensions

of charged particles. The physical properties of a suspension such as bulk fluid stress or optical properties depend on the instantaneous orientations of the suspended particles and can be examined through an averaging process (Strand and Kim 1992). It is thus of great interest to study the dynamics of individual particles in a suspending fluid. An extensive review of nonlinear dynamics is beyond the scope of this thesis. As an introduction we will present the development of the subject from a collection of selected works, review papers and books which are relevant to the goal of this thesis.

1.1 A brief review of rheology

Rheology deals with the science of deformation and flow, especially of non-Newtonian fluids. Navier (1795-1836) and Stokes (1819-1903) together developed the equations governing motion in Newtonian fluids of constant density and viscosity. Many other researchers like Lord Rayleigh (1842-1919), Boussinesq (1842-1929), Darcy (1803-1858) *etc.* have also contributed significantly to the development of the subject. Albert Einstein (1879-1955) analyzed the problem of the disturbance caused by the presence of spherical particles suspended in a Newtonian fluid. He demonstrated that the apparent increase in the viscosity of the suspension was proportional to the volumetric concentration of the solid particles (Einstein 1906 and 1911). Einstein considered a sufficiently dilute system such that the motion of one particle was not influenced by the disturbances created by other particles. An extension of the theory of the rheology of suspensions of spherical particles to suspensions of ellipsoidal particles in the absence of rotary Brownian motion was developed by Jeffery (1922). A historical review of the development of the theory of the motion of small particles in Newtonian fluids and its applications have been presented by Happel & Brenner (1986) in their book, *Low Reynolds number hydrodynamics with special applications to particulate media.* Strand (1989) has given a comprehensive literature survey pertaining to the suspension rheology of dipolar non-Brownian

particles with and without the presence of externally induced forces. His work is concerned with the rheology of dilute suspensions of rigid particles suspended in a Newtonian solvent. The effects of particle shape on the dynamics and rheology of such suspensions in the absence of hydrodynamic interactions is modelled in his work. Most of the fundamental concepts and methods used in the study of suspension rheology are explained in the review papers of Brenner (1972, 1974).

The dynamics of suspensions of small dipolar particles stabilized by surface active agents in a variety of linear flows under the effect of alternating or rotating external fields has been studied by a number of authors and a number of practical applications such as magnetofluidization (Buevich *et al.*, 1984), magnetostriction of ferromagnetic particle suspensions (Ignatenko *et al.*, 1984), the growth of single crystals from a melt by Czochralski's method (Zibold *et al.*, 1986), rheological properties of ferromagnetic colloids (Tsebers, 1986) and the characterization of magnetorheological suspensions (Cebers, 1993a, Cebers, 1993b, Kashevskii, 1986, Petrikevich and Raikher Yu L, 1984, Shul´man *et al.*, 1986) *etc.* have been discussed. Some of the above authors consider rotatory external fields which can be considered as a superposition of two orthogonal alternating fields.

The dynamics of particles in a variety of linear flows is analyzed by a number of authors (Altan *et al.*, 1989, Anczurowski and Mason, 1967, Bretherton, 1962, Leal and Hinch, 1971, Macmillan, 1989). Szeri *et al.* (1992) have analyzed the motion of rigid particles in time dependent flows. However their results are qualitatively different from those considered in this work in the sense that they preclude the possibility of chaotic motions, since their equations reduce to a set of two first order nonlinear ordinary differential equations. The above authors (Altan *et al.*, 1989, Anczurowski and Mason, 1967, Bretherton, 1962, Leal and Hinch, 1971, Macmillan, 1989) have considered the dynamics of a particle without external force fields. A detailed calculation of the trajectory of

rigid particles under the action of a constant external force is also reported in the literature (Ramamohan *et al.* 1991). Strand (1989) has developed a theory of the dynamics and rheology of nonspherical particles in oscillating external force fields in simple shear flow. However the technique of Fourier expansion in higher harmonics of the driving frequency of the external field, he has used, will yield incorrect results in the case of chaotic dynamics or dynamics containing subharmonic frequencies. This would correspond to the limit of weak Brownian motion(*i.e.* $q_c \not\ll 1$) as noted by Strand(1989). Recently, Ramamohan *et al.* (1994) introduced a class of problems, namely, the dynamics of periodically forced small particles in flows other than uniform flows. They analyzed the dynamics of a slender rigid rod in a simple shear flow under the action of a sinusoidal driver. For further reading on the subject of rheology of suspensions the reader is referred to

1. Dynamics of Polymeric Liquids Vol. I and Vol. II
   R. B. Bird, R. C. Armstrong and O. Hassager
   Wiley-Interscience Publications, New York (1987).
2. Low Reynolds number Hydrodynamics
   J. Happel and H. Brenner
   Martinus Nijhoff Publishers (1986).
3. Microhydrodynamics: Principles and Selected Applications
   S. Kim and S. J. Karrila
   Butterworth - Heinemann series in Chemical Engineering, Stoneham, MA, 1991.
4. Rheology of a Dilute Suspension of Axisymmetric Brownian Particles
   H. Brenner
   Int. J. Multiphase Flow. Vol. 1 195-341, Pergamon Press (1974).
5. Dynamic Rheological and Rheo-optical Properties of dilute suspensions of dipolar Brownian Particles
   S. R. Strand
   Ph. D Thesis, The University of Wisconsin, Madison (1989).

1.2 A brief review of chaotic dynamics

One of the main contributions of the twentieth century- the discovery of chaos destroyed the earlier belief that the behaviour of a deterministic system can always be predicted in the long term. A sensitive dependence of the solutions of a system of equations on initial conditions is the dominant characteristic of a chaotic system. This means that trajectories evolving from two distinct but arbitrary close initial conditions diverge exponentially. There is always noise or measurement error in experiments and in computer simulations of physical systems. The small errors due to the noise will change the observed behaviour of a chaotic system because of sensitive dependence on initial conditions. Hence the behaviour of a chaotic system becomes unpredictable in the real sense, in the long term. Experimental and numerical studies show that chaotic behaviour exists in many nonlinear systems such as fluids, plasmas, electric circuits, chemical reactions, celestial mechanics, acoustical systems, ecological systems, physiological systems (Hao Bai-lin 1988) and so on. A list of biological examples can be found in the recent book of Glass and Mackey (1988). Chaotic phenomena have been reported in almost all scientific disciplines ranging from engineering to medicine. Scientists and engineers are currently exploring the features of chaotic phenomenon for applications in industry and technology (Parker and Chua 1989).

An observed irregularity in the time evolution of a system doesn't necessarily imply chaos. It is thus essential to clarify whether chaos exists or not in the system from recorded data. A positive Lyapunov exponent, wide band power-spectrum, fractional dimensions *etc.* are some indications of the existence of chaotic behaviour. Among them the existence of a positive Lyapunov exponent is the most reliable measure. Two initially adjacent points in a chaotic attractor evolve with time such that their trajectories show exponential divergence. This exponential divergence is characterized by a positive Lyapunov exponent. The

maximum Lyapunov exponent gives the maximum rate of divergence of two initially close trajectories. A positive Lyapunov exponent indicates the possibility of existence of chaos. The phenomenon of sensitivity to initial conditions is one of the main characteristics of a chaotic system. Hence the existence or non-existence of chaotic behaviour can be visualized by plotting time series of two trajectories starting from initially close conditions.

Reconstruction of attractors and modelling of systems from chaotic data are two important areas of research in the field of chaos (Anishchenko 1995). Distinguishing between deterministic chaos and random noise is another important problem in this area. A step-by-step recipe for the implementation of a procedure to detect the difference is given in Hao Bai-lin (1988)

Many interesting physical systems are modelled by ordinary differential equations. Autonomous ordinary differential equations with at least three variables or non-autonomous ordinary differential equations with at least two variables are the minimum requirements for the possibility of the existence of chaos (Hao Bai-lin 1988). The Lorenz equations were one of the first sets of ordinary differential equations showing irregular behaviour (Lorenz 1963). In this work we present a set of non-autonomous differential equations showing complex behaviour.

Chaos is ubiquitous in natural phenomenon and man-made devices (Sprott 1993). Chaos is desirable or undesirable depending on the situation. Certain physical and biological systems use chaotic behavior (Schiff *et al.* 1994). In certain cases chaos needs to be eliminated or controlled to avoid failure as in mechanical systems. Controlling a chaotic system is one recent development in nonlinear dynamics. The method suggested in the work of Ott *et al.* (1990) has generated lot of interest in this area. The possibility of stabilizing a predetermined unstable periodic orbit from the infinity of such orbits in a chaotic attractor by small perturbations is the unique feature of the OGY method.

Thereafter a number of algorithms have been reported which control or synchronize chaos. A recent review of the work in this area is given by Lindner and Ditto (1995). It is reported in the literature that when two chaotic signals are synchronized the resultant signal will be non-chaotic. Violent chaotic motion on the dynamics of a rolling railway wheel set at higher velocity is also reported in the literature(Knudsen *et al.* 1992 and Knudsen *et al.* 1994). The chaotic motions of the rolling railway wheelset could be neutralized by synchronizing it with the chaotic behaviour of the rheological parameters after translating them into mechanical signals.

The new mechanisms and properties of a chaotic system can be utilized effectively for the development of new processing technologies. The introduction of *chaos* and the theory of *nonlinear dynamics* has contributed a lot to the understanding of the challenging problem of turbulence.

A list of the relevant literature from the field of chaos is given below for further reading.

1. Bibliography on chaos (Directions in chaos Vol. 5)
   Zhang Shu - Yu
   World Scientific, Singapore (1991).
2. Universality in chaos
   P. Cvitanovic
   Adam Hilger, Bristol, England (1989).
3. Deterministic chaos, an introduction
   H. G. Schuster
   VCH Verlagsgesellschaft mbH, Weinheim, FRG (1989).
4. Order within chaos
   P. Bergé, Y. Pomeau and C. Vidal
   Wiley, New York (1986).
5. Chaos in dynamical systems
   E. Ott
   Cambridge University Press, Cambridge, U.K. (1993).

6. Applied non-linear dynamics- analytical, computational and experimental methods
A. H. Nayfeh and B. Balachandran
John Wiley and sons, Inc, New York (1995).

7. Characterization of chaos
D. M. Heffernan, P. Jenkins, M. Daly, B. J. Hawdon and J. O'Gorman
Int. J. Theor. Phys. 31 (8) 1345-1362 (1992).

8. Ergodic theory of chaos and strange attractors
J. P. Eckmann and D. Ruelle
Rev. Mod. Phys. 57 617-656 (1985).

9. Chaos and nonlinear dynamics
Robert C. Hilborn
Oxford University Press, New York (1994).

1.3 The importance of the problem

As can be seen from the relevant literature cited above, it is of interest to

1. study the dynamics of periodically forced particles with a view to develop robust theories for potential applications such as magnetorheological suspensions, magnetostriction of ferromagnetic particle suspensions, magnetodielectric material suspensions, ferromagnetic colloidal suspensions *etc.*

2. develop new theories to aid in the of development of new suspensions with desired properties.

3. modify the processing conditions of suspensions to improve the performance of the process.

4. develop techniques for effective separation of particles by aspect ratio to yield well characterized suspensions for testing theories of the above processes and for developing suitable theories for suspensions of particles of various aspect ratios and sizes.

5. to study the possibility of controlling the chaos present in the dynamics of periodically forced particles with a view to develop potential applications such as control of magnetorheological suspensions, magnetostriction of ferromagnetic particle suspensions, magnetodielectric material suspensions, ferromagnetic colloidal suspensions and the possibility of computer controlled intelligent rheology.

6. develop new techniques for control of chaos and to demonstrate the applicability of the technique in physical systems.

7. demonstrate the existence of new types of behavior such as new types of Class I intermittency, *etc.* in such processes.

8. develop new products and devices making use of the understanding achieved by such analysis.

In order to separate out the effects of the particle size and shape on the properties of the suspension, it would be desirable to obtain suspensions of particles having a narrow distribution of shapes and sizes. A narrow distribution of sizes can be obtained through appropriate separation techniques such as filtration. However we are not aware of any technique to separate particles having the same size but different shapes.

In what follows, we present the results of our analysis on the dynamics of spheroids of various aspect ratios immersed in a simple shear flow, subjected to periodic and constant force fields as a first step in achieving the objectives outlined above. We also demonstrate the existence of chaotic parametric regimes in our solutions, thus invalidating the approach used by Strand (1989) in the limit of weak Brownian motion(*i.e.* $q_c \not\ll 1$). Based on the general theory of the dynamics of particles, immersed in linear flows subjected to external force fields as developed by Brenner (1974), we develop the equations for the dynamics of spheroids in linear flows and demonstrate the existence of chaotic

parametric regimes. During the course of these computations, we observed a strong dependence of the attractor on the shape of the particle as characterized by its aspect ratio in the chaotic parametric regimes. We discuss the use of this strong dependence on the aspect ratio as a tool to separate particles of different shapes but having the same size. The existence of chaotic parametric regimes also allows the possibility of control of chaos to further finetune the separation of particles by aspect ratio.

In addition to the technological interest in this problem we have also discussed certain aspects of this problem that are of interest to the nonlinear dynamics community, namely it is an example of one of the very few physically realizable chaotic systems showing the phenomenon of a non hysteretic form of Class I intermittency with nearly regular reinjection period. The intermittent transition between a laminar phase and chaotic outbreaks has recently been the subject of much study both in physical systems and also in sets of ODE's. The associated set of ODE's derived in this work represents one of the very few ODE systems describing the phenomenon of Class I intermittency with nearly regular reinjection period. The so-called intermittency refers to a state in which nearly regular behaviour is intermittently interrupted by chaotic outbreaks (bursts) at irregular intervals (Bergé *et al.* 1986). In almost all previous computational and experimental studies of Class I intermittency the bursting process was irregular. Recently Price and Mullin (1991) experimentally observed a new type of intermittency mechanism in a variant of the Taylor-Couette flow problem. One of the main features of their observation was the existence of a hysteretic form of intermittency with extreme regularity of the bursting. In a set of equations representing the dynamical behaviour of stream wise rolls, existence of intermittency behaviour was reported by Aubry *et al.* (1988). Their model displays evidence of regular intermittency of class II followed by a subcritical Hopf bifurcation.

In this work we report the non hysteretic form of Class I intermittency with the nearly regular behaviour interrupted by chaotic outbreaks (bursts) with nearly regular reinjection period. We also present appropriate return maps to explain the behaviour observed in this work. The system also shows certain interesting features such as new scaling behaviour away from the onset of intermittency and the number of the bursts during a particular realization varying smoothly with the control parameter. We discuss and compare the model of Class I intermittency with the new type of intermittency. The comparison with the theoretical predictions of Class I intermittency shows scaling typical of Class I intermittency. The average length of the burst also scales with the control parameter with zero slope.

There has been considerable interest recently in the use of chaos and controlling chaos as a tool to develop new processing technologies (Zumbrunnen 1996). Practically speaking chaos may be desirable or undesirable depending on the application desired. In many practical situations, in order to improve system performance, the chaotic system must be controlled to a periodic orbit or to a steady state. Thus techniques of controlling chaotic systems have received increased attention in the recent literature. In a physical apparatus, one can imagine that the system dynamics is to be changed in some way so that improved performance is obtained. One can achieve this by making appropriate changes in the system to achieve the desired objective. Similar or otherwise unattainable objectives can be attained by operating the system in a chaotic regime and then applying suitable control of chaos techniques. Since a chaotic attractor is a closure of unstable periodic orbits of different periods, any of these orbits can be stabilized to attain the desired objective by suitable control algorithms.

We propose an algorithm for control of chaos in this work. The method proposed is comparatively easy to implement experimentally and needs almost no information about the system. We have also demonstrated that controlling

the chaotic dynamics of periodically forced particles by the new control technique leads to the possibility of better separation than is otherwise possible. Utilizing the flexibility of controlling chaotic dynamics in a desired orbit irrespective of initial state, it is demonstrated that it is theoretically possible to separate particles much more efficiently than otherwise possible from a suspension of particles having different shapes but similar sizes especially for particles of aspect ratio $r_e > 1.0$. The strong dependence of the controlled orbit on the aspect ratio of the particles demonstrated in this work may have many applications such as the development of new processing technologies. The existence of chaotic parametric regimes in the problem considered in this work and the possibility of control of its chaotic behaviour (Ott *et al.* 1990) allows the possibility of many applications including the development of computer controlled intelligent rheology. Since the chaotic phase space is an unlimited reservoir of periodic solutions (Güémez *et al.* 1994) a particle of a particular aspect ratio can be forced to oscillate in any one of the orbits and can be picked up from there effectively. Though the results presented herein represent a preliminary analysis of the problem considered in dilute suspensions, the existence of chaos and hence its controllability and the strong dependence of the results on the aspect ratio of the controlled orbit suggest that these results may have many potential applications. As an example, we also focus on the more efficient separation of particles by aspect ratio through control of chaos.

The novel algorithm of controlling chaos based on parametric perturbation shows some advantages over other methods. One of the main advantages of the novel control technique proposed is the possibility of pre-targeting the length of the control period by suitably engineering the control technique. We have also demonstrated some other advantages of the novel technique such as the possibility of switching behaviour, pre-targeting the period, stabilizing high period solutions *etc.* over two well-known algorithms such as control by periodic parametric perturbation and control by addition of a second weak periodic force.

We have also demonstrated the applicability of the novel technique in models of physical systems. We have also successfully implemented the new algorithm in a rather difficult problem such as the control of the dynamics and the rheological parameters of periodically forced suspensions of slender rods in simple shear flow and also in the Bonhoeffer-Van der Pol (BVP) oscillator (Rajasekar and Lakshmanan 1993).

Chapter 2

The Dynamics of a Periodically Forced Spheroid in Simple Shear Flow

2.1 Introduction

There is considerable literature on the dynamics of particles in a variety of linear flows (Altan *et al.*, 1989, Leal and Hinch, 1971 and references therein). They have considered the dynamics of a particle without external force fields. Szeri *et al.* (1992) have analyzed the motion of rigid particles in time dependent flows. However their results are qualitatively different since they preclude the possibility of chaotic motions, since their equations reduce to a set of two first order nonlinear ordinary differential equations. Strand and Kim (1992) have recently developed a theory of the dynamics and rheology of nonspherical particles in constant external force fields in simple shear flow. Strand (1989) has developed a theory of the dynamics and rheology of nonspherical particles in oscillating external force fields in simple shear flow. However the technique of Fourier expansion in higher harmonics of the driving frequency of the external field, he has used, will yield incorrect results in the case of chaotic dynamics or dynamics containing subharmonic frequencies. A brief review of rheology is given in the first chapter of this thesis. This chapter explains the development of equations of a model of the dynamics of suspensions of small dipolar

spheroids of finite aspect ratio in simple shear flow under the effect of externally induced periodic fields.

2.2 Assumptions in the model

A number of reasonable assumptions are necessary in any mathematical formulation of a fluid dynamic system to simplify the mathematics and to analyze the characteristic behaviour of the system. The equations governing strongly viscous behavior (sufficiently slow flow) are called the creeping motion (Stokes) equations (Happel & Brenner 1986). In reality there is no fluid flow system without inertial effects and exhibiting only viscous effects. The ratio of inertial forces to viscous forces is called the *Reynolds number.* In strongly viscous flow, the Reynolds number is very small. In this work, it is assumed that the flow is sufficiently slow so that the inertial terms are negligible compared to viscous terms in the mathematical formulation, *i. e.* is the Reynolds number is taken as zero in the development of the model. This assumption is realistically validated, since there are many multiparticle suspensions involving sufficiently slow flow or sufficiently small particles that the Reynolds number is negligibly small.

It is also assumed that the number of particles per unit volume is small enough that the motion of an individual particle is not affected by motion of other particles. Such suspensions not involving particle-particle interactions are called dilute suspensions. The dynamics of a single particle suspension is considered in this analysis.

One more assumption made in this work for a fruitful analysis is regarding Brownian motion. The equations solved numerically in this work are obtained by neglecting Brownian motion. However there will be round off errors in the solution of the equations by numerical computation. This round off error can be considered as a white noise or weak Brownian motion. Therefore our

computational analysis is valid in the case of weak Brownian motion, even though the governing equations are formulated by neglecting Brownian motion. The effect of Brownian motion is characterized by a non-dimensional number called the *Peclet number*. The Peclet number is defined by (Brenner 1974)

$$P_e = \frac{\dot{\gamma}}{D_r}$$

where,

$$\dot{\gamma} = \text{The shear rate}$$
$$D_r = \text{Rotary diffusivity}$$

By definition it is clear that the Peclet number is large for Weak Brownian motion. Hence our analysis is valid in the case of very high Peclet number.

Experimental data is available in good agreement with theoretical predictions made under these assumptions (Happel & Brenner 1986).

2.3 The development of the model

The general equation governing the effect of an externally induced torque on small particles possessing fore-aft symmetry immersed in linear flows, as developed by Brenner (1974) is given by:

$$\boldsymbol{L} = \mu_o[{}^c\hat{\mathbf{K}} \cdot (\boldsymbol{V} - \boldsymbol{U}) + {}^r\hat{\mathbf{K}} \cdot (\boldsymbol{\omega} - \boldsymbol{\Omega}) + \hat{\tau} : \mathbf{S}] \tag{2.1}$$

where ${}^c\hat{\mathbf{K}}$, ${}^r\hat{\mathbf{K}}$, $\hat{\tau}$ are intrinsic properties of the particle, which depend upon the geometric configuration of its wetted surface, $\boldsymbol{L}$ is the torque about the center of the particle exerted by the fluid on the particle, $\boldsymbol{U} - \boldsymbol{V}$ is the translational

slip velocity, $\boldsymbol{\Omega} - \boldsymbol{\omega}$ is the rotational slip velocity, μ_o is the viscosity of the fluid and $\mathbf{S}$ is the rate of deformation tensor given by $\mathbf{S} = \frac{1}{2}\left[\nabla \boldsymbol{V} + \nabla \boldsymbol{V}^{\mathrm{T}}\right]$. Here the negative of the torque, $-\boldsymbol{L}$ can be considered as the externally induced torque on the particle, since when an external torque is applied on the particle, the particle exerts the same torque on the fluid and hence the torque exerted by the fluid on the particle is equal in magnitude but opposite in direction. The components of the above equation 2.1 can be expressed as

$$L_i = \mu_o[{}^{c}\hat{K}_{ij}(V_j - U_j) + {}^{r}\hat{K}_{ij}(\omega_j - \Omega_j) + \hat{\tau}_{ijk}S_{jk}] \tag{2.2}$$

where ${}^{c}\hat{K}_{ij} = 0$ for any particle possessing fore-aft symmetry, $\boldsymbol{L} = (L_1, L_2, L_3)$, $\boldsymbol{\Omega} = (\Omega_1, \Omega_2, \Omega_3)$, $\boldsymbol{\omega} = (\omega_1, \omega_2, \omega_3)$, $\boldsymbol{V} = (V_1, V_2, V_3)$ and $\boldsymbol{U} = (U_1, U_2, U_3)$. Let $\boldsymbol{u} = (u_1, u_2, u_3)$ be the unit vector determining the orientation of the particle. Using Brenner's notation (Brenner 1974) we have

$$\begin{aligned}
{}^{r}\hat{K}_{ij} &= 6V_p{}^{r}K_{ij} \\
\hat{\tau}_{ijk} &= 6V_p\tau_{ijk} \\
{}^{r}K_{ij} &= u_iu_j{}^{r}K_{\parallel} + (\delta_{ij} - u_iu_j){}^{r}K_{\perp} \\
\tau_{ijk} &= -(\epsilon_{ijl}u_lu_k + \epsilon_{ikl}u_lu_j)\tau
\end{aligned} \tag{2.3}$$

In the expressions 2.3, ${}^{r}K_{ij}$ and τ_{ijk} are dimensionless quantities, ${}^{r}K_{\parallel}, {}^{r}K_{\perp}$ and τ depend upon the geometric configuration of wetted surface of the particle, V_p denotes the particle volume, δ_{ij} is the Kronocker delta function and ϵ_{ijk} is the permutation symbol. The Kronocker delta function and the permutation symbol are defined by

$$\begin{aligned}
\delta_{ij} &= 1 \quad \text{if } i = j \\
&= 0 \quad \text{if} i \neq j
\end{aligned}$$

and

$$\begin{aligned} \epsilon_{ijk} &= 1 \quad \text{if } ijk = 123, 231, 312 \\ &= -1 \quad \text{if } ijk = 213, 321, 132 \\ &= 0 \quad \text{if any two symbols are equal} \end{aligned} \tag{2.4}$$

Applying the above expressions, the equations 2.2 can be reduced to

$$\begin{aligned} L_i &= 6V_p\mu_o \left[\left(u_i u_j{}^T K_{\parallel} + (\delta_{ij} - u_i u_j)^T K_{\perp} \right) (\omega_j - \Omega_j) \right. \\ &\quad \left. - \left(\epsilon_{ijl} u_l u_k + \epsilon_{ikl} u_l u_j \right) \tau S_{jk} \right] \end{aligned} \tag{2.5}$$

2.4 Simple shear flow

In this section, we find the equations governing the dynamics of periodically forced particles possessing fore-aft symmetry suspended in a simple shear flow.

Let $\dot{\gamma}$ be the shear rate, y is the $y-$ coordinate and $\boldsymbol{i_x}$ is the unit vector in the x-direction. Then the undisturbed flow field of simple shear flow is given by

$$\begin{aligned} \boldsymbol{V} &= \dot{\gamma} y \boldsymbol{i_x} \\ &= (\dot{\gamma} y, 0, 0) \end{aligned} \tag{2.6}$$

Hence, the velocity gradient tensor is given by

$$\begin{aligned} \mathbf{G} &= \nabla \boldsymbol{V} \\ &= \left(\boldsymbol{i_x} \frac{\partial}{\partial x} + \boldsymbol{i_y} \frac{\partial}{\partial y} + \boldsymbol{i_z} \frac{\partial}{\partial z} \right) \dot{\gamma} y \boldsymbol{i_x} \\ &= \dot{\gamma} \boldsymbol{i_y} \boldsymbol{i_x} \end{aligned}$$

where $\nabla = \left(\boldsymbol{i_x} \frac{\partial}{\partial x} + \boldsymbol{i_y} \frac{\partial}{\partial y} + \boldsymbol{i_z} \frac{\partial}{\partial z} \right)$

Hence the rate of shear tensor is given by

$$\begin{aligned} \mathbf{S} &= \frac{1}{2}(\mathbf{G}+\mathbf{G}^T) \\ &= \frac{1}{2}\dot{\gamma}(\boldsymbol{i}_x\boldsymbol{i}_y + \boldsymbol{i}_y\boldsymbol{i}_x) \end{aligned}$$

$$\text{Hence,} \qquad S_{12} = S_{21} = \frac{\dot{\gamma}}{2}$$

$$S_{11} = S_{13} = S_{22} = S_{23} = S_{31} = S_{32} = S_{33} = 0 \quad (2.7)$$

where S_{ij} are the components of $\mathbf{S}$. The vorticity tensor is defined by

$$\begin{aligned} \boldsymbol{\omega} &= \frac{1}{2}(\nabla \times \boldsymbol{V}) \\ &= (0, 0, -\frac{\dot{\gamma}}{2}) \end{aligned} \quad (2.8)$$

The equation of motion then reduces to

$$\begin{aligned} L_1 &= -6V_p\mu_o\left[[Au_1^2 + {}^rK_\perp]\Omega_1 + Au_1u_2\Omega_2 + Au_1u_3(\frac{\dot{\gamma}}{2}+\Omega_3) + u_1u_3\dot{\gamma}\tau\right] \\ L_2 &= -6V_p\mu_o\left[Au_1u_2\Omega_1 + [Au_2^2 + {}^rK_\perp]\Omega_2 + Au_2u_3(\frac{\dot{\gamma}}{2}+\Omega_3) - u_2u_3\dot{\gamma}\tau\right] \\ L_3 &= -6V_p\mu_o\left[Au_1u_3\Omega_1 + Au_2u_3\Omega_2 + [Au_3^2 + {}^rK_\perp](\frac{\dot{\gamma}}{2}+\Omega_3)\right. \\ &\quad \left. +(u_2^2 - u_1^2)\dot{\gamma}\tau\right] \end{aligned} \quad (2.9)$$

where $A = {}^rK_{\|} - {}^rK_\perp$ and $\boldsymbol{L} = (L_1, L_2, L_3)$.

The above equations 2.9 can be written in the matrix form,

$$6V_p\mu_o \begin{pmatrix} [Au_1^2 + {}^rK_\perp] & Au_1u_2 & Au_1u_3 \\ Au_1u_2 & [Au_2^2 + {}^rK_\perp] & Au_2u_3 \\ Au_1u_3 & Au_2u_3 & [Au_3^2 + {}^rK_\perp] \end{pmatrix} \begin{pmatrix} 0 - \Omega_1 \\ 0 - \Omega_2 \\ -\left(\frac{\dot{\gamma}}{2} + \Omega_3\right) \end{pmatrix}$$

$$= \begin{pmatrix} L_1 + 6V_p\mu_o u_1u_3\dot{\gamma}\tau \\ L_2 - 6V_p\mu_o u_2u_3\dot{\gamma}\tau \\ L_3 + 6V_p\mu_o(u_2^2 - u_1^2)\dot{\gamma}\tau \end{pmatrix}$$

Solving the above matrix equation by matrix inverse method for Ω_1, Ω_2 and Ω_3, we get a set of equations:

$$
\begin{aligned}
\Omega_1 &= ({}^rK_\perp)^{-1}\left[-(6V_p\mu_o)^{-1}L_1 + A(6V_p\mu_o{}^rK_\parallel)^{-1}u_1(\boldsymbol{u}\cdot\boldsymbol{L}) - u_1u_3\dot{\gamma}\tau\right] \\
\Omega_2 &= ({}^rK_\perp)^{-1}\left[-(6V_p\mu_o)^{-1}L_2 + A(6V_p\mu_o{}^rK_\parallel)^{-1}u_2(\boldsymbol{u}\cdot\boldsymbol{L}) + u_2u_3\dot{\gamma}\tau\right] \\
\Omega_3 &= ({}^rK_\perp)^{-1}\left[-(6V_p\mu_o)^{-1}L_3 + A(6V_p\mu_o{}^rK_\parallel)^{-1}u_3(\boldsymbol{u}\cdot\boldsymbol{L})\right. \\
&\quad \left.-(u_2^2 - u_1^2)\dot{\gamma}\tau\right] - \frac{\dot{\gamma}}{2} \qquad (2.10)
\end{aligned}
$$

where $\boldsymbol{u}\cdot\boldsymbol{L} = u_1L_1 + u_2L_2 + u_3L_3$. Realizing that $\dot{\boldsymbol{u}} = \boldsymbol{\Omega}\times\boldsymbol{u} = \epsilon_{ijk}\Omega_j u_k$, the following equations are obtained in u_1, u_2, u_3

$$
\begin{aligned}
\dot{u_1} &= ({}^rK_\perp)^{-1}u_2(1-2{u_1}^2)\dot{\gamma}\tau + \frac{\dot{\gamma}}{2}u_2 - (6V_p\mu_o{}^rK_\perp)^{-1}(u_3L_2 - u_2L_3) \\
\dot{u_2} &= ({}^rK_\perp)^{-1}u_1(1-2{u_2}^2)\dot{\gamma}\tau - \frac{\dot{\gamma}}{2}u_1 - (6V_p\mu_o{}^rK_\perp)^{-1}(u_1L_3 - u_3L_1) \\
\dot{u_3} &= -2({}^rK_\perp)^{-1}u_1u_2u_3\dot{\gamma}\tau - (6V_p\mu_o{}^rK_\perp)^{-1}(u_2L_1 - u_1L_2) \qquad (2.11)
\end{aligned}
$$

Note that u_1, u_2, u_3 denote the x, y, z components of the unit vector $\boldsymbol{u}$ along the axis of symmetry which determines the orientation of the spheroids, respectively. If for example we consider a situation where an electric or magnetic field is imposed on the particle, the torque induced on the particle $(-\boldsymbol{L})$ is given by $\boldsymbol{L} = \boldsymbol{k}\times\boldsymbol{u}$ in the case of a constant force field and $\boldsymbol{L} = \boldsymbol{k}\times\boldsymbol{u}\cos(\omega t)$ in the case of a periodic force field. $\boldsymbol{k}$ can be considered to be the orientation independent part of the torque or its magnitude. It can also be considered as a vector representing the interaction between the external field and a dipole either induced in the body or one already present in the body, as, for example, a single domain magnetic particle. Let k_1, k_2 and k_3 be the x, y, z components of $\boldsymbol{k}$, ω be the frequency of the driver and t be the time. Substituting the expression

$$
\boldsymbol{k}\times\boldsymbol{u} = (u_3k_2 - u_2k_3, u_1k_3 - u_3k_1, u_2k_1 - u_1k_2) \qquad (2.12)
$$

in 2.11, the equations governing the dynamics are obtained as

$$\begin{aligned} \dot{u_1} &= ({}^rK_\perp)^{-1}u_2(1-2{u_1}^2)\dot{\gamma}\tau + \frac{\dot{\gamma}}{2}u_2 + (6V_p\mu_o{}^rK_\perp)^{-1}a_1 \\ \dot{u_2} &= ({}^rK_\perp)^{-1}u_1(1-2{u_2}^2)\dot{\gamma}\tau - \frac{\dot{\gamma}}{2}u_1 + (6V_p\mu_o{}^rK_\perp)^{-1}a_2 \\ \dot{u_3} &= -2({}^rK_\perp)^{-1}u_1u_2u_3\dot{\gamma}\tau + (6V_p\mu_o{}^rK_\perp)^{-1}a_3 \end{aligned} \tag{2.13}$$

in the case of a constant force field and

$$\begin{aligned} \dot{u_1} &= ({}^rK_\perp)^{-1}u_2(1-2{u_1}^2)\dot{\gamma}\tau + \frac{\dot{\gamma}}{2}u_2 + (6V_p\mu_o{}^rK_\perp)^{-1}a_1\cos(\omega t) \\ \dot{u_2} &= ({}^rK_\perp)^{-1}u_1(1-2{u_2}^2)\dot{\gamma}\tau - \frac{\dot{\gamma}}{2}u_1 + (6V_p\mu_o{}^rK_\perp)^{-1}a_2\cos(\omega t) \\ \dot{u_3} &= -2({}^rK_\perp)^{-1}u_1u_2u_3\dot{\gamma}\tau + (6V_p\mu_o{}^rK_\perp)^{-1}a_3\cos(\omega t) \end{aligned} \tag{2.14}$$

in the case of a periodic force field, where

$$\begin{aligned} a_1 &= u_3(u_3k_1 - u_1k_3) - u_2(u_1k_2 - u_2k_1) \\ a_2 &= u_1(u_1k_2 - u_2k_1) - u_3(u_2k_3 - u_3k_2) \\ a_3 &= u_2(u_2k_3 - u_3k_2) - u_1(u_3k_1 - u_1k_3) \end{aligned}$$

2.5 The factor B

The orientational dynamics of periodically forced small spheroids in simple shear flow has been analyzed for $|B| \leq 1$, where $B = (r_e^2 - 1)/(r_e^2 + 1)$ and we observed chaotic dynamics of the particle under the action of a sinusoidal driver.

2.6 The spheroid

The equations presented in the above section are the general equations governing the dynamics of axi-symmetric particles possessing fore-aft symmetry under the action of a periodic force suspended in simple shear flow. The constants

${}^{r}K_{\perp}$ and τ in the equations are functions of the material constants. The material constants are again functions of the aspect ratio r_e. Suitable expressions for the material constants appearing in the equations governing the dynamics for various axisymmetric particles possessing fore-aft symmetry are available in the literature (Brenner 1974) in terms of the geometrical configuration of the wetted surface of the particle (*i.e.* in terms of the particle aspect ratio, r_e). We substitute the expressions for the constants in the equations depending upon the shape of the particle under study. Hence the equations can be used as such for various particle shapes like oblate and prolate spheroids; dumbells; circular disks; symmetrical double cone; circular cylinder *etc.* by using the appropriate expressions for the material constants occurring in the equations.

As a first case of the development and analysis of the problem under study, we study the dynamics of periodically forced spheroids in simple shear flow. Since most particles can be approximated as spheroids (Bretherton 1962), the analysis presented in this work has wide applicability. The relevant material constants for spheroids as given in Brenner (1974) are

$$\begin{aligned} {}^{r}K_{\perp} &= \frac{2(r_e^2+1)}{3(r_e^2\alpha_{\parallel}+\alpha_{\perp})} \\ N &= \frac{2(r_e^2-1)}{5(r_e^2\alpha_{\parallel}+\alpha_{\perp})} \\ \tau &= \frac{5}{6}N \\ \alpha_{\perp} &= \frac{r_e^2}{(r_e^2-1)}(1-\beta) \\ \alpha_{\parallel} &= \frac{2}{(r_e^2-1)}(r_e^2\beta-1) \end{aligned} \tag{2.15}$$

in which

$$\begin{aligned} \beta &= \frac{\ln[r_e+(r_e^2-1)^{1/2}]}{r_e(r_e^2-1)^{1/2}} \quad \text{if } r_e > 1 \\ \beta &= \frac{\cos^{-1}(r_e)}{r_e(1-r_e^2)^{1/2}} \quad \text{if } r_e < 1 \end{aligned}$$

where the particle axis ratio, r_e of the spheroid is defined as $r_e = a/b$, a = polar radius and b = equatorial radius. The volume of a spheroid is given by

$$V_p = \frac{4\pi}{3}ab^2$$

The material constants can be derived for long slender bodies by taking the limiting case $r_e \longrightarrow \infty$. The material constants are same as the material constants in Strand and Kim (1992). The equations reduce to the equations of the dynamics of long slender rods in simple shear flow as developed by Ramamohan *et al.* (1994) in the limiting case.

2.7 The dimensionless equation

The quantities $\dot{\gamma}, \mu_o, V_p, k_1, k_2, k_3$ and ω appearing in the above sets of equations 2.13 and 2.14 are dimensional quantities. It is convenient to characterize the system by means of dimensionless quantities to reduce the number of parameters to the essential minimum. The particle axis ratio of the spheroid is defined as $r_e = a/b$, as stated above. All the quantities that appear in the analysis will be scaled as follows:

$$\begin{aligned} \text{Length} \quad &: \quad a \\ \text{Velocity} \quad &\quad \sqrt{2}a[\mathbf{S} : \mathbf{S}]^{1/2} \\ \text{Time} \quad &\quad J/\sqrt{2}[\mathbf{S} : \mathbf{S}]^{1/2} \\ \text{Frequency} \quad &\quad \sqrt{2}[\mathbf{S} : \mathbf{S}]^{1/2}/J \\ \text{volume} \quad &\quad a^3 \\ \text{Torque} \quad &\quad \sqrt{2}a^3[\mathbf{S} : \mathbf{S}]^{1/2}\mu_o \end{aligned} \tag{2.16}$$

Here $J/\dot{\gamma}$ is the Jeffery period (Jeffery, 1922) defined as

$$J/\dot{\gamma} = 2\pi\dot{\gamma}^{-1}(r_e + {r_e}^{-1})$$

After scaling all quantities that appear in the analysis as above, we get the following equations

$$\begin{aligned} \dot{u_1} &= Pu_2(1-2{u_1}^2)+Qu_2+Ra_1 \\ \dot{u_2} &= Pu_1(1-2{u_2}^2)-Qu_1+Ra_2 \\ \dot{u_3} &= -2Pu_1u_2u_3+Ra_3 \end{aligned} \tag{2.17}$$

in the case of a constant force field and

$$\begin{aligned} \dot{u_1} &= Pu_2(1-2{u_1}^2)+Qu_2+Ra_1\cos(\omega t) \\ \dot{u_2} &= Pu_1(1-2{u_2}^2)-Qu_1+Ra_2\cos(\omega t) \\ \dot{u_3} &= -2Pu_1u_2u_3+Ra_3\cos(\omega t) \end{aligned} \tag{2.18}$$

in the case of a periodic force field.

$$\begin{aligned} \text{where,}\quad a_1 &= u_3(u_3k_1-u_1k_3)-u_2(u_1k_2-u_2k_1) \\ a_2 &= u_1(u_1k_2-u_2k_1)-u_3(u_2k_3-u_3k_2) \\ a_3 &= u_2(u_2k_3-u_3k_2)-u_1(u_3k_1-u_1k_3) \\ P &= \frac{\pi(r_e^2-1)}{r_e},\quad Q=\frac{\pi(r_e^2+1)}{r_e},\quad R=\frac{3r_e^3[(2r_e^2-1)\beta-1]}{8(r_e^2-1)}, \\ \beta &= \frac{\ln[r_e+(r_e^2-1)^{1/2}]}{r_e(r_e^2-1)^{1/2}} \text{ or } \frac{\cos^{-1}(r_e)}{r_e(1-r_e^2)^{1/2}} \end{aligned}$$

with β depending on the axis ratio r_e being > 1 or < 1, $\dot{\boldsymbol{u}}$ is the rate of change of the orientation vector; u_i is actually $u_i/|\boldsymbol{u}|$ since we have derived equations 2.17 and 2.18 based on the assumption that $\boldsymbol{u}$ is a unit vector. As can be seen, the equations 2.18 depend on the aspect ratio of the particle and also depend on the magnitude and frequency of the external force field. In the subsequent chapters we analyze the dynamics of periodically forced spheroids in detail. We note that equation 2.18 satisfies the condition $\boldsymbol{u}\cdot\dot{\boldsymbol{u}}=0$. This implies that as u_1, u_2 and u_3 evolve with time, from the given initial condition $|\boldsymbol{u}|=1$, the

magnitude of the vector $\boldsymbol{u}$ remains at unity. Thus the three equations listed above can be reduced to a system of two nonlinear nonautonomous ODEs. This system of equations 2.18 was converted into five coupled autonomous first order equations, with two constants of integration by a standard transformation, Hao Bai-lin (1989). However the method of Hao Bai-lin (1989) leads to some numerical errors during long computations. To avoid this we use the equations 2.18 for our calculations.

2.8 The limiting value of ω

The Stokes equations are obtained from the Navier-Stokes equations by setting the Reynolds number equal to zero. Experimental observations show that the theoretical predictions based on the Stokes equations are in good agreement with experiments on systems with very low Reynolds number. This shows that simulations based on the Stokes equations are valid for experiments of very low Reynolds numbers. The maximum value of the Reynolds number for which predictions based on the Stokes equations are valid is about 0.1. Hence our analysis is valid for low Reynolds number. The Reynolds number R_e is given by

$$R_e = \frac{lv\rho}{\mu}$$

where,

l = a characteristic length of the system

v = a characteristic velocity of the flow field

ρ = The density of the viscous fluid

μ = The viscosity of the fluid

In our analysis two expressions $l\dot{\gamma}$ and $l\omega$ can be considered as the characteristic velocities of the flow. Hence two different expressions for the same Reynolds number will be obtained by substituting $l\dot{\gamma}$ and $l\omega$ separately. Since the frequency (ω) of the external force is scaled with respect to J and the reciprocal of the shear rate $\dot{\gamma}$, it can be expressed as

$$\omega = \omega^* \frac{\dot{\gamma}}{J}$$

where ω^* is the scaled frequency of the external driver. Therefore the two expressions for the same Reynolds number can be written as

$$\begin{aligned} R_e &= \frac{l^2\dot{\gamma}\rho}{\mu} \leq R_e \text{ (critical)} \\ R_e &= \frac{l^2\dot{\gamma}\rho}{\mu}\frac{\omega^*}{J} \leq R_e \text{ (critical)} \end{aligned} \tag{2.19}$$

Comparing these expressions, we can find that the maximum possible value of ω^*/J for which the quasi-static Stokes equations are valid is 1. Therefore the value of the scaled quantity ω^* for which our analysis is valid is such that

$$\frac{\omega^*}{J} \leq 1$$

It can be concluded that the maximum scaled value of ω^*, corresponding to the limit where the quasi-static Stokes' equations are valid corresponds to J, since the frequency of the driver is scaled with respect to the Jeffery period and the incident velocity is scaled with respect to the average shear rate. In the dimensionless equations 2.18 given in the section 2.7, ω^* is denoted as ω for convenience.

2.9 The equations in spherical coordinates

The equations for u_1, u_2 and u_3 can be converted into equations for θ and ϕ where θ is the azimuthal angle and ϕ is the polar angle corresponding to a given

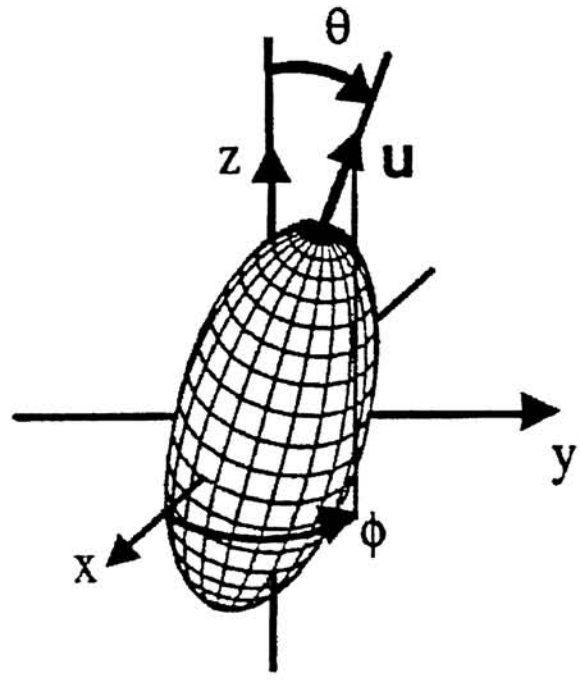

Figure 2.1: The coordinate system.

vector $\boldsymbol{u}$ (shown in Fig. 2.1) by the relations

$$\begin{aligned} \theta &= \tan^{-1}\left(\frac{\sqrt{{u_1}^2 + {u_2}^2}}{u_3}\right) \\ \phi &= \tan^{-1}(u_2/u_1) \end{aligned} \tag{2.20}$$

The equations for u_1, u_2 and u_3 under the above transformation change as

$$\begin{aligned} \frac{d\theta}{dt} &= \frac{P}{2}\sin 2\theta \sin 2\phi + R[\cos\theta\cos\phi\ k_1 + \cos\theta\sin\phi\ k_2 - \sin\theta\ k_3]\cos(\omega t) \\ \frac{d\phi}{dt} &= P\cos 2\phi - Q + R\left[\frac{-\sin\phi\ k_1 + \cos\phi\ k_2}{\sin\theta}\right]\cos(\omega t) \end{aligned} \tag{2.21}$$

We note that the equation for $\dot{\phi}$ has a singularity at $\theta = 0$. This singularity probably appears because when $\theta = 0$, $u_1 = u_2 = 0$ as is evident from Fig. 2.1 To remove the singularity we consider the following equations

$$\begin{aligned}
\frac{d\theta}{dt} &= \frac{P}{2}\sin 2\theta \sin 2\dot{\phi} + R[\cos\theta\cos\phi\ k_1 + \cos\theta\sin\dot{\phi}\ k_2 - \sin\theta\ k_3]\cos(\omega t) \\
\frac{d\phi_1}{dt} &= \frac{P}{2}\phi\cos\theta\sin 2\theta\sin 2\dot{\phi} + \sin\theta(P\cos 2\phi - Q) + R[(-\sin\phi\ k_1 + \cos\phi\ k_2) \\
&\quad +\phi(\cos^2\theta\cos o\ k_1 + \cos^2\theta\sin\phi\ k_2 - \sin\theta\cos\theta\ k_3)]\cos(\omega t) \qquad (2.22)
\end{aligned}$$

where $\phi_1 = (\phi\sin\theta)$.

2.10 The computational procedure

The three sets of equations 2.18, 2.21 and 2.22 were solved independently using a standard 4^{th} order Runge Kutta method with adaptive step size (Press *et al.*, 1986). The accuracy of the computations was checked by requiring that the magnitudes of u_1, u_2 and u_3 remain within 0.1% of the initial value and also by requiring that the solutions obtained by integrating equations 2.18, 2.21 and 2.22 gave similar attractors and equal Lyapunov exponents. It was generally noted that a tolerance of 0.001% in the integrator (Press *et al.*, 1986) was required to achieve this precision. The Lyapunov exponents of the equations were calculated using the scheme of Kantz (1994). The equations for $\dot{\theta}$ and $\dot{\phi}$ when integrated numerically, did not lead to any problems with the singularity at $\theta = 0$ and we obtained the same results as that obtained by the other two sets of equations.

We note that the equations for $\dot{\theta}$ and $\dot{\phi}$ reduce to Jeffery's (1922) equations in the absence of the external force field. We also note that the above equations for $\dot{\theta}$ and $\dot{\phi}$ decouple in the absence of k_1 and k_2. Hence the presence of an external force field with either k_1 or k_2 is necessary to obtain chaotic solutions in this system.

Chapter 3

Chaotic Dynamics with a Potential Application to Particle Separation

3.1 Introduction

In the previous chapter, we described the formulation of a set of equations governing the dynamics of periodically forced spheroids in simple shear flow based on a model given by Brenner (1974). The control parameters that can be varied in equations 2.18 and 2.21 are k_1, k_2, k_3, ω and r_e. The evolution can be simulated in a computer for different values of these control parameters. In what follows we vary one of the control parameters in 2.21 by keeping the others constant for a systematic simulation. A number of chaotic regimes have been established by the simulation for these parameters.

3.2 Existence of chaotic regimes

As a first step in analyzing the properties of the equations derived in this work, we set $k_1 = k_3 = 0$ and varied k_2 between 0.0 and 20.0 for $r_e = 1.6$ and between 0.0 and 100.0 for $r_e = 0.4$ and kept ω equal to J. We expect the greatest complexity of the solutions of these equations for this particular choice of parameters, since k_2 is responsible for the greatest opposition to the

hydrodynamic torque due to the imposed shear flow field. At $k_2 = 0$, Jeffery's results are reproduced and all solutions of the equations starting from different initial conditions tend towards a fixed point in the stroboscopic plot.

We ran the program for 2500 points of the Poincaré section (stroboscopic plot) and deleted the first 2250 points to remove the transients. All runs were started with the initial conditions $\theta = \phi = 45°$. For each trajectory we evaluated 100 points in each cycle which resulted in 25000 points of the trajectory after the transients are removed. We obtained identical results when $\dot{\phi}$ was replaced by $-\dot{\phi}$. As a test case when we ran the program for $\theta = 90°$ the trajectory plot reduced to a continuous curve, indicating regular behaviour for all the values of k_2 considered. At $k_2 = 0.03$ for $r_e = 1.6$, the attractor slowly begins to broaden from a continuous curve and the Lyapunov exponent first becomes positive. There are a number of regular regimes in between the chaotic regimes. In our system, chaos usually appears as a broadening of the attractor as can be seen from the example given in Fig. 3.1. In certain regimes as in Ramamohan *et al.*, (1994) the attractor broadens to such an extent that a subset of the phase space is completely filled. Ramamohan *et al.* (1994) have analyzed the orientational dynamics of periodically forced slender rigid rods in simple shear flow under the action of a sinusoidal driver. Our equation 2.21 reduces to equations 2.6, 2.8 and 2.9 of Ramamohan *et al.* (1994) after suitable scaling and letting r_e tend to ∞. Ramamohan *et al.* (1994) also kept $k_1 = k_3 = 0$ and varied k_2 between 0 and 1 ω was kept equal to 1 in Ramamohan (*et al.*, 1994). In Ramamohan (*et al.*, 1994) at $k_2 = 0.005$ the attractor slowly begin to broaden compared to $k_2 = 0.03$ for $r_e = 1.6$ in this work. Ramamohan *et al.* (1994) observed transient chaos at $k_2 = 0.25$. However for $r_e = 1.6$ we first obtained transient chaos at $k_2 = 4.5$. In this work we have tentatively identified chaotic regimes of the parameter k_2 namely for $r_e = 1.6$. Based on a similar analysis we obtained a chaotic regime for $r_e = 0.4$.

One paper resulting from this work has been accepted for presentation in an international conference. **ICTAM** held in JAPAN, 1996.

3.3 Results on separation technique

During our computations, we noted that the results of the computations are very sensitive to the aspect ratio of the particle in some parameter regimes as given in Fig. 3.2 for $\omega = J$. In the case of constant external fields (*i. e.* $\omega = 0$) in the same parametric regimes we obtained regular behaviour. For $r_e > 1.0$, we obtained nearly the same fixed point in the Poincaré section for all initial conditions in the case of a constant force field. This suggested the possibility of separating particles based on this observation.

To develop quantitative results based on this observation, we divided the range of possible orientations namely $[-90°\ ,\ 90°]$ in both θ and ϕ variables into 7 equal intervals resulting in 49 equal sized grids. We then computed the evolution of initially uniformly distributed particles of different aspect ratio within the range of r_e equal to 0.2 to 2 in steps of 0.2. We followed the evolution of the initially uniformly distributed particles within the above range of particle axis ratios under the effect of constant, periodic and zero force fields. We followed the evolution of the ensemble of particles from 3001 to 5000 points of the Poincaré section in the case of periodic, constant and zero forces. In all cases we calculated the number of particles in each grid on every 4^{th} iteration of the Poincaré section of the evolution equations resulting in a total of 500 values for periodic, constant and zero forces. We noted the grids in which the total number of particles was greater than or equal to 5 and also noted the number of particles in each grid only if the particle occurred in that grid in more than 10 iterations in all the cases. We denote these values as r_e, l_1 and l_2, where r_e, l_1 and l_2 denote the aspect ratio, total number of occurrences of the grid and total number of particles in the grid on the average respectively and

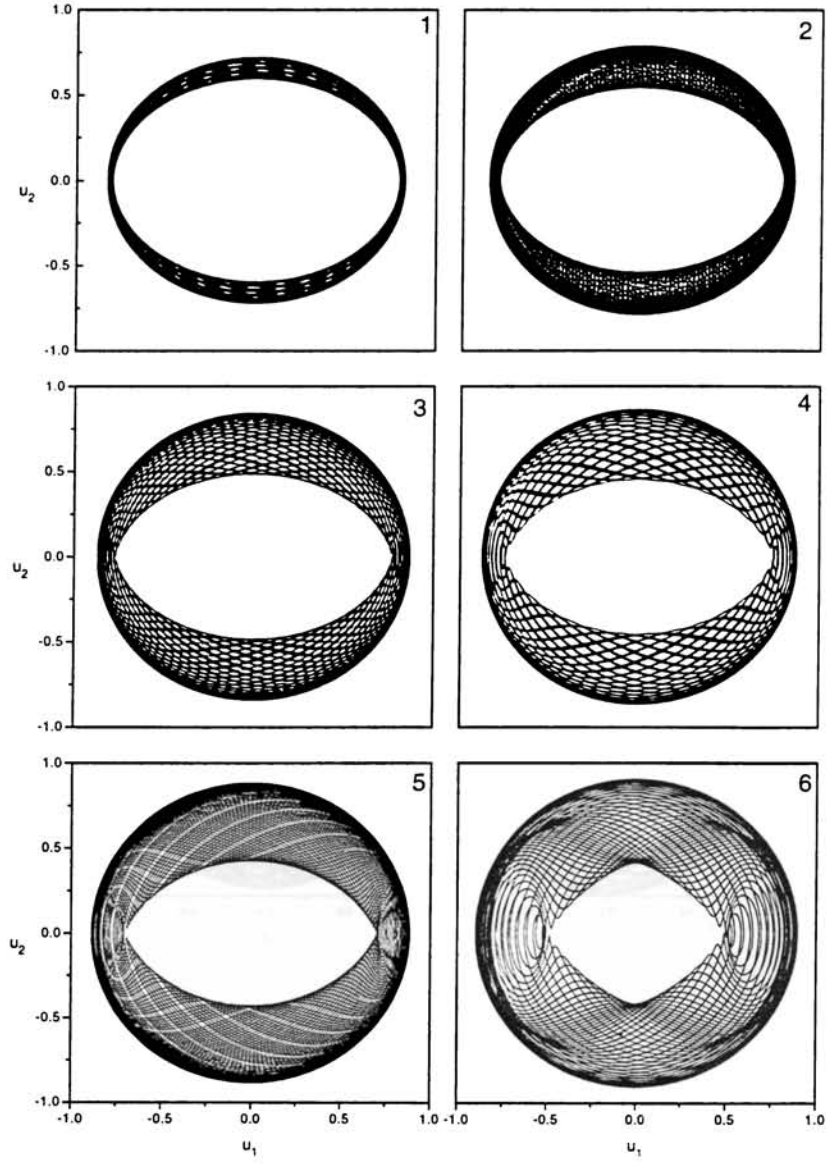

Figure 3.1: The trajectory plot of u_1 vs. u_2 for initial conditions $\theta = 45°$, $\phi = 45°$, $\omega = J = 2\pi(r_e + r_e^{-1})$, $r_e = 1.6$ and (1) k_2=1.0 (2) k_2=2.0 (3) k_2=3.0 (4) k_2=3.5 (5) k_2=4.0 (6) k_2=4.5.

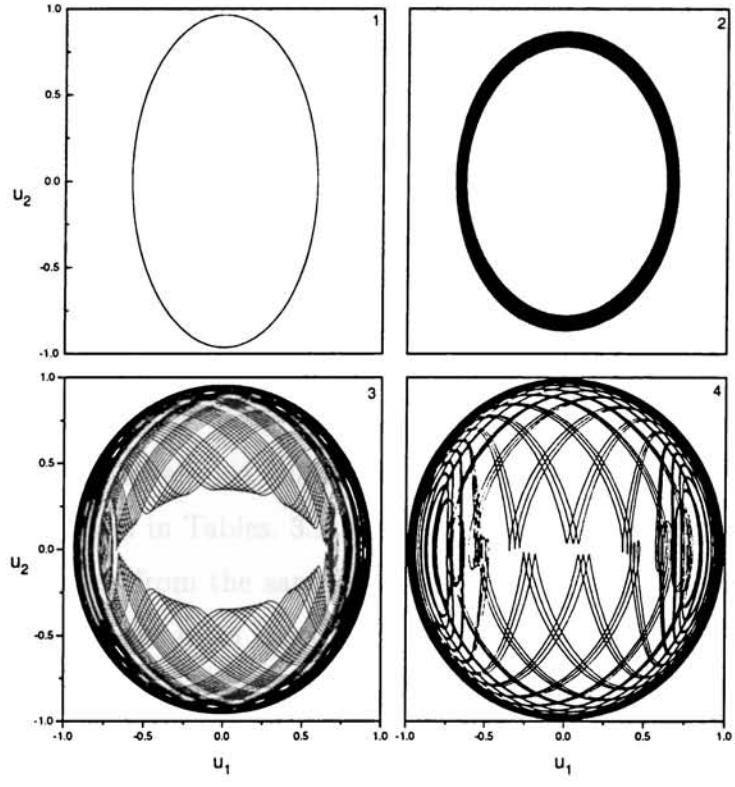

Figure 3.2: The attractor (trajectory plot) for $k_1 = k_3 = 0$, $k_2 = 10$, initial conditions $\theta = 45°$, $\phi = 45°$, $\omega = J = 2\pi(r_e + r_e^{-1})$ (1) $r_e = 0.2$ (2) $r_e = 0.6$ (3) $r_e = 1.2$ (4) $r_e = 1.6$

prepared tables for these values. Since our preliminary computations indicated the greatest sensitivity of the results to the aspect ratio at $k_2 = 10$, we ran the program for k_2 equal to 9.5, 10 and 10.5 for periodic and constant forces.

In the case of constant forces, all the attractors for different aspect ratios resulted in a continuous curve and the maximum Lyapunov exponent was zero for all initial conditions, indicating regular behavior. Similar results were obtained for zero forces. In the case of periodic forces, the attractors resulted in a broadening of the torus or a completely filled subset of the phase space and the maximum Lyapunov exponent was positive, indicating chaotic behavior. The Lyapunov exponent of the time series was calculated using the Kantz (1994) method. For aspect ratios greater than or equal to 2, all the attractors reduce to a continuous curve for all initial conditions and forces k_2 =9.5, 10 and 10.5, indicating regular behavior. The tables for the cases of $k_2 = 9.5, 10$ and 10.5, considered for both periodic and constant forces and for zero force were prepared for a detailed analysis of the separation technique. A sample of the tables are given in Tables. 3.1 and 3.2.

As can be seen from the sample tables, there is a possibility of separation of particles by aspect ratio based on a judicious combination of periodic and constant forces. A detailed analysis of all the tables indicates that particles of aspect ratio 0.2 alone can be separated from a mixture containing particles of different aspect ratios by applying a constant force $k_2 = 0$, since particles of aspect ratio 0.2 alone occur on some extreme grids on the boundary of the tables. This suggests that particles of this aspect ratio alone can be separated by applying a zero force. In the case of particles of aspect ratio 0.4 a constant force between 9.5 and 10.5 appears to be sufficient for separating these particles alone. For separating particles of aspect ratio 0.6, it is desirable to apply a constant force between 9.5 and 10.5. Here particles of this aspect ratio alone occur in the centre grids for constant forces. Based on a similar analysis, periodic forces leading to chaotic dynamics or constant forces leading to regular dynamics of

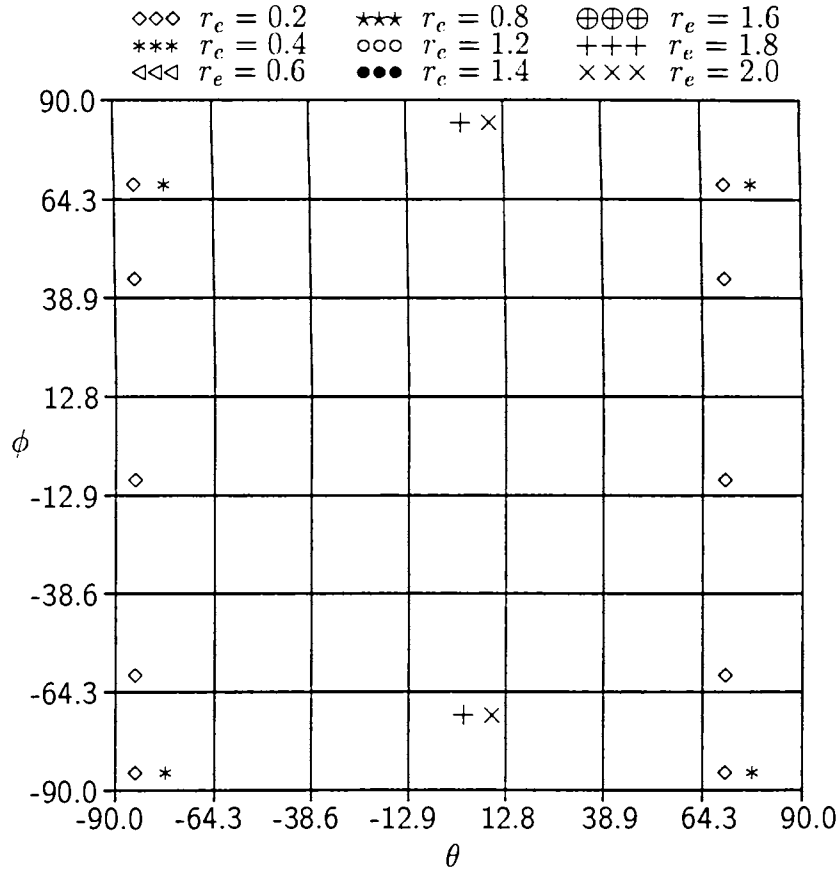

Table 3.1: Distribution of the evolution of initially uniformly distributed particles of different aspect ratios for the case $k_2 = 0$, $\omega = 0$, $5 \leq l_1 \leq 49$ and $10 \leq l_2 \leq 500$, where l_1 is the total number of particles in the grid on the average and l_2 is the total number of occurrences of the grid.

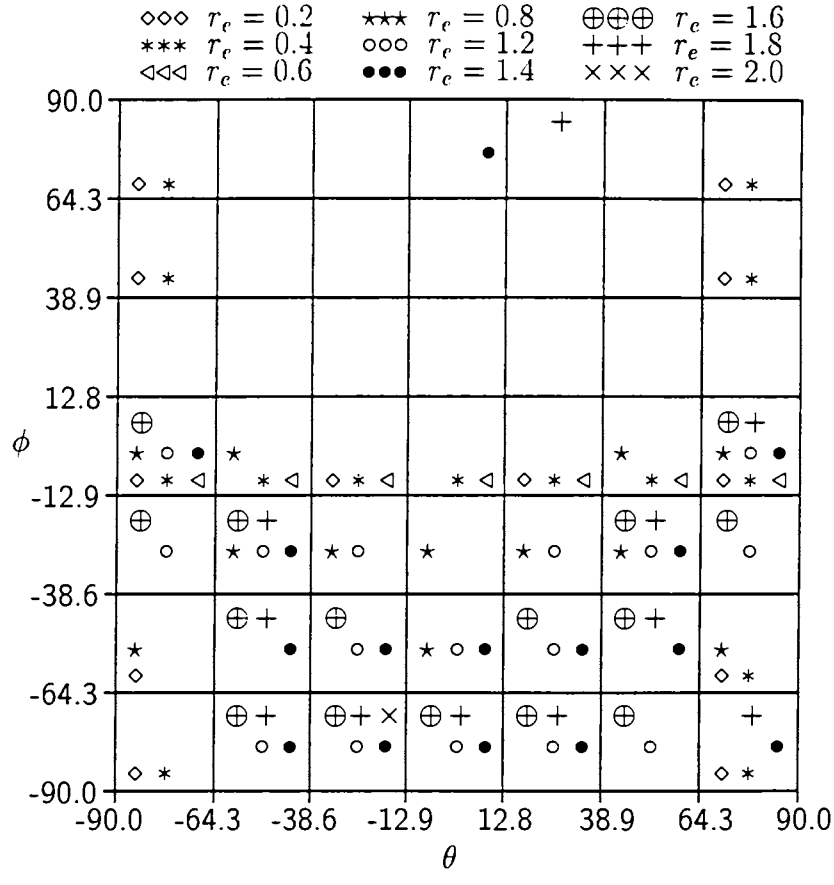

Table 3.2: Distribution of the evolution of initially uniformly distributed particles of different aspect ratios for the case $k_2 = 10.0$, $\omega = J = 2\pi(r_e + r_e^{-1})$, $5 \leq l_1 \leq 49$ and $10 \leq l_2 \leq 500$, where l_1 is the total number of particles in the grid on the average and l_2 is the total number of occurrences of the grid.

the particles can separate particles of aspect ratio 0.8 alone. However in this case, a constant force is preferable to a periodic force, since such particles are spread over a large number of grids in the case of a periodic force.

Further analysis of the tables indicate that the considered forces are not preferable for separating particles of aspect ratio 1.2 alone. A similar analysis shows that for particles of aspect ratio 1.4 a periodic force is desirable to separate particles from a mixture containing this particle. For particles of aspect ratio greater than or equal to 1.6 individual separation may not be possible. However there is a possibility of separating particles of aspect ratio 1.8 by applying a periodic force of magnitude k_2=10, with the limitation that the occurrence of these particles alone are sensitive to small changes in the magnitude of the periodic force. For particles of higher aspect ratio, particles appear in combination with particles of lower aspect ratio in all cases. Hence if particles of lower aspect ratios have been separated out as explained earlier, particles of higher aspect ratios can be separated from the mixture. In general periodic forces are preferable to constant forces and zero forces for separating particles of aspect ratio $r_e > 1$. However for particles of aspect ratio $r_e \geq 1.6$ individual separation is not possible in this analysis.

It has been generally noted that chaotic behavior gives better separation than regular behavior, especially in the case of particles having aspect ratio greater than or equal to 1.6. A possible design for this separation of particles with different aspect ratios based on the differences in the orientation of the particle may consist of a base plate having grooves along different orientations so that when the particles are oriented in such directions, they settle in a particular groove and can be separated out.

We believe that there is both important new physics and the possibility of new technology in such separations, since they could lead to better characterization of real suspensions for a study of their physical properties. This work also demonstrates the existence of chaotic parametric regimes in the problem

considered. This result may have considerable impact on the analysis of the practical applications referred to in the introduction. None of the authors dealing with the practical application of this problem have considered the existence of chaotic parametric regimes in their work.

One paper resulting from this work has been published in **Rheol. Acta** (1995), Germany. This paper has also been Listed in the Current World Literature section of **Current Opinion in Colloid and Interface Science 1/4**, 1996.

Chapter 4

A New Class I Intermittency

4.1 Introduction

After the discovery of chaos there arose lots of questions regarding the routes to the development of chaotic behaviour. What is the scenario behind the transition from regular behaviour to the chaotic behaviour as the control parameter is varied ? Are there any universal patterns or sequences for this transition ? Different routes to chaos have been reported in the chaos literature. The period doubling route to chaos, quasi periodic route to chaos, intermittency route to chaos, crisis induced intermittency route to chaos *etc.* are some of the widely accepted scenarios. These routes to chaos are the ways in which the laminar flow loses stability and becomes chaotic. Manneville and Pomeau (1979) introduced the intermittency route to chaos in the Lorenz equations. The so-called intermittency occurs when nearly regular behaviour (laminar flow) is intermittently interrupted by chaotic outbreaks (bursts) at irregular intervals. As the control parameter is increased (or decreased), the strength of the chaotic burst also increases and finally the system ends up in fully chaotic behaviour. One of the routes to chaos is the class I intermittency route to chaos.

4.2 Class I intermittency

The scenarios describing the creation or destruction of a chaotic attractor as a parameter is varied are also important in the field of dynamical systems. It is interesting to see what happens in a dynamical system as the control parameter is changed. If the trajectories in phase space of a dynamical system before and after a specified value of the control parameter are qualitatively different, then the qualitative difference is called a bifurcation. The transition from a stable periodic orbit to an unstable periodic orbit is a qualitative change. If branches of stable and unstable periodic orbits coincide at a particular value of the control parameter, then such a bifurcation is called cyclic-fold bifurcation. Assume that a dynamical system is under the influence of cyclic-fold bifurcation at a particular value (say λ) of the control parameter in such a way that the attractor is a limit cycle for all values of the control parameter less than the particular value, λ. At the same time it is impossible to determine the system behaviour for values greater than λ by local bifurcation analysis.

The behaviour after bifurcation can be analyzed by numerical computations. One possibility is that the attractor before bifurcation may be switched onto a new attractor in which the old attractor will be a proper subset of the new attractor. The analysis of the time series obtained by computer simulation shows that an orbit in the attractor after the bifurcation point stays back near the destroyed limit cycle for a long time and is interrupted by chaotic bursts. The orbit near the destroyed limit cycle is called the laminar phase and the chaotic burst between the laminar phases is called the turbulent phase. As the control parameter is increased (or decreased in some other cases) the average time spent by the chaotic bursts in the attractor tends to infinity the attractor become fully chaotic. This type of transition from periodic behaviour to chaotic behaviour via a cyclic-fold bifurcation is called the intermittency route to chaos of class I. The existence of the mechanism that reinjects the trajectory lying

in the chaotic bursts to the vicinity of the limit cycle is necessary for the intermittency route to chaos. If not, the orbit will never revisit the vicinity of the limit cycle. A detailed treatment of different types of intermittency routes to chaos is available in the literature (Pomeau and Manneville 1980; Hilborn 1994; Nayfeh and Balachander 1995). We observed a new type of class I intermittency in the dynamics of periodically forced spheroids in simple shear flow which is discussed in the following section.

4.3 Results on the new class I intermittency

In this section we report a physically realizable system in which the possibility of an interesting and novel type of Class I intermittency, namely, a non hysteretic form of Class I intermittency with nearly regular behaviour interrupted by chaotic outbreaks (bursts) with nearly regular reinjection period is demonstrated. The bursting process was irregular in almost all previous computational and experimental studies of Class I intermittency. Price and Mullin (1991) have observed experimentally a similar type of phenomenon in which a hysteretic form of intermittency with extreme regularity of the bursting is observed. The system described in this section appears to be one of the very few ODE systems describing a physically realizable system showing a non hysteretic form of Class I intermittency with nearly regular behaviour interrupted by chaotic outbreaks (bursts) with nearly regular reinjection period. We also present appropriate return maps to explain the behaviour observed in this work. The system also shows certain interesting features such as new scaling behaviour away from the onset of intermittency and the number of the bursts during a particular realization varying smoothly with the control parameter. We discuss and compare the model of Class I intermittency with the new type of intermittency. The comparison with the theoretical predictions of Class I intermittency shows scaling typical of Class I intermittency. The average length of the burst also scales with the control parameter with zero slope.

The phenomenon of Class I intermittency with nearly constant reinjection period, we observed in this work was obtained in the parametric regime $10.6 \leq k_2 \leq 12.44$. We report the results for $0.01 \leq \theta \leq 40°$ and for all values of ϕ in steps of 20° which results in 15 initial conditions for a given parameter value. The evolution of the particle upto 2150 cycles was computed and the results are presented for $r_e = 1.6, \omega = J = 2\pi(r_e + r_e^{-1})$, and $k_1 = k_3 = 0$,. For the trajectory we evaluated 100 points in each cycle which resulted in 215000 points and deleted 200000 points (2000 cycles) as transients. It was found to be sufficient to concentrate on the remaining 15000 points of the trajectory to study the new behaviour, because when the number of iterations was doubled the only change in the observed behaviour was a doubling in the number of bursts with no other change in the dynamics. We expect the greatest complexity of the solutions of the above equations for this particular choice of parameters, since k_2 is responsible for the greatest opposition to the hydrodynamic torque due to the imposed shear flow field. For $k_2 = 0$, Jeffery's results are reproduced and all solutions of the equations starting from different initial conditions tend towards a fixed point in the stroboscopic plot. Upon changing k_2 we observed a number of chaotic regimes of the parameter k_2 as well as a number of regular regimes in between the chaotic regimes. The phenomena we wish to report in this work lies in the parameter regime $10.6 \leq k_2 \leq 12.44$. We also confine ourselves to the value of $0.01 \leq \theta \leq 40°$ and $0° \leq \phi \leq 90°$ in steps of 20°. This choice of initial conditions and range of k_2 results in interesting behaviour with clear evidence for the new behaviour, namely Class I intermittency with nearly constant reinjection period. For all values of k_2, θ and ϕ within the above range, the system shows similar behaviour.

The analysis of the time series and the attractor shows the existence of a tangent bifurcation which leads to the novel behaviour of Class I intermittency with nearly constant reinjection period. The maximum Lyapunov exponents of both the time series of the bursts (denoted by **X**) and the laminar phase

(denoted by **Y**) were positive and entirely different. Fig. 4.1 shows a superposition of the trajectories corresponding to the laminar phase and the bursts and Fig. 4.2 shows the corresponding time series. During the bursts, the trajectory moves away from the vicinity of the laminar region as is evident from Fig. 4.1. The maximum Lyapunov exponent for the bursts was nearly constant for all θ, ϕ and k_2 considered and was equal to 0.21, indicating that the bursts show the same type of chaotic behaviour everywhere in the system. At the same time the maximum Lyapunov exponent for the laminar phase decreases with increasing k_2 and finally ends up in a periodic behaviour at $k_2 = 12.46$. The system is more sensitive to initial conditions near the chaotic bursts (Type **X**) and less sensitive to initial conditions near the laminar phase (Type **Y**) as can be seen from the time series of trajectories for slightly different initial conditions given in Fig. 4.3.

The existence of the intermittency behaviour in the system was further confirmed by solving the evolution equations 2.18 and 2.21 in single and double precision. The trajectories obtained from equation 2.21 in single and double precision and from equation 2.18 in single precision for the same set of parameters and initial conditions are given in Fig. 4.4. There will be small changes in the evolutions obtained from the numerical computations in single and double precision due to round off error. Hence if the orbit is in a chaotic attractor, the time series obtained here will diverge exponentially as is evident from Fig. 4.4. However all the time series obtained show the same intermittency behaviour. As k_2 is increased near the onset of tangent bifurcation the bursts remain chaotic with nearly the same Lyapunov exponent equal to 0.21. The Lyapunov exponents of the laminar phase were small compared to that of the bursts and decreased slowly and became nearly zero as k_2 is increased near the onset of tangent bifurcation as can be seen from Table. 4.1. Table 4.1 shows that the maximum Global Lyapunov exponent (GE) on the average lies between the maximum Local Lyapunov exponent (LE) of the laminar phase and the chaotic

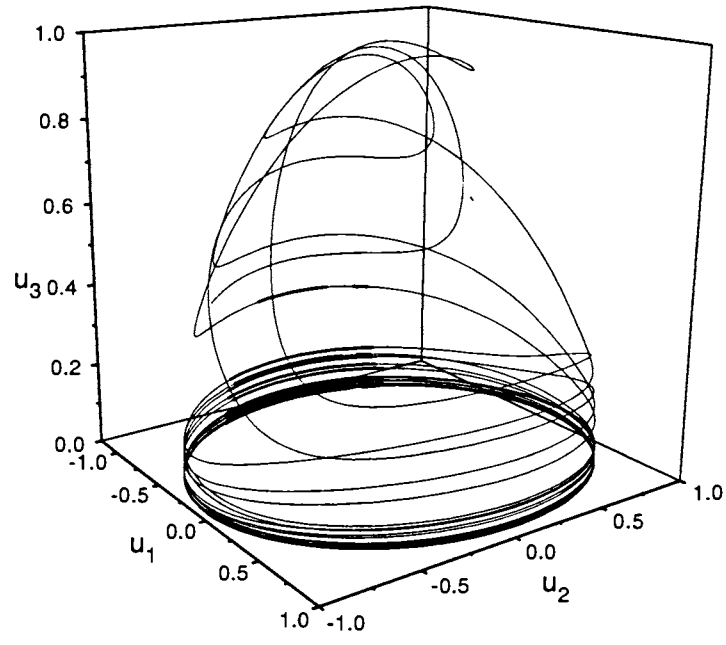

Figure 4.1: Typical phase space trajectory of the attractor showing the laminar phase as well as the chaotic burst for $k_2 = 12.2$, initial conditions $\theta = \phi = 20°$, $\omega = J = 2\pi(r_e + r_e^{-1})$, $r_e = 1.6$.

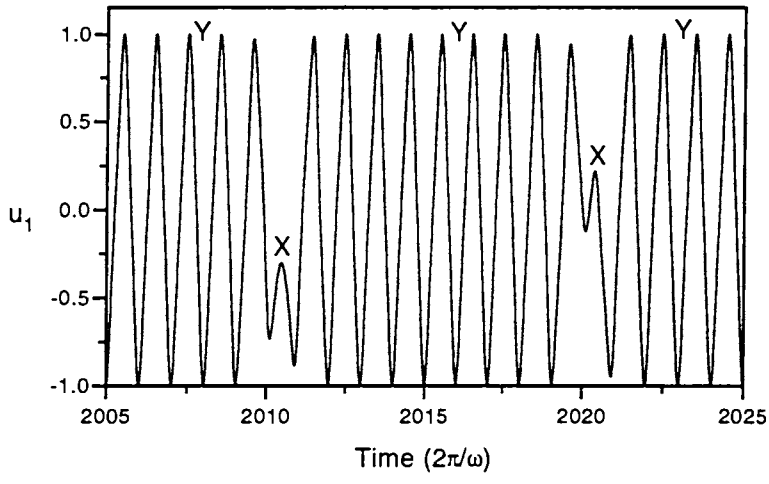

Figure 4.2: The time series of u_1 of the trajectory shown in Fig. 4.1

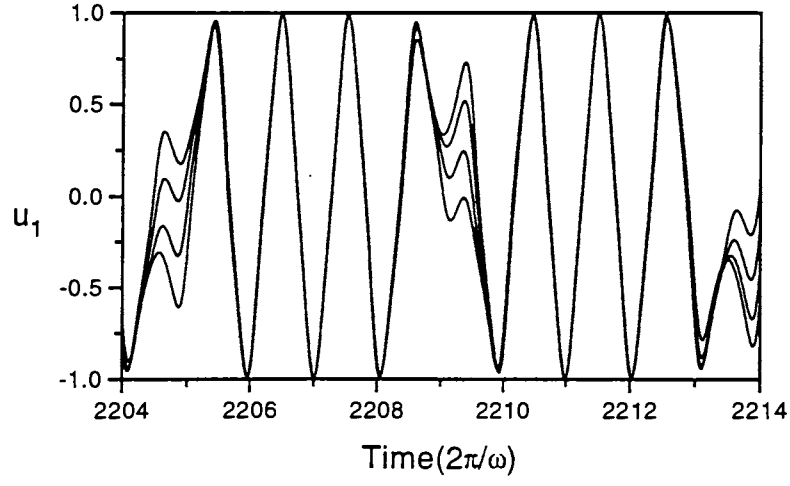

Figure 4.3: Time series of different trajectories for $k_2 = 11.2$, slightly different initial conditions $\theta = 20.0°$, $20.1°$, $20.2°$, $20.3°$, $\phi = 20°$, $\omega = J = 2\pi(r_e + r_e^{-1})$, $r_e = 1.6$.

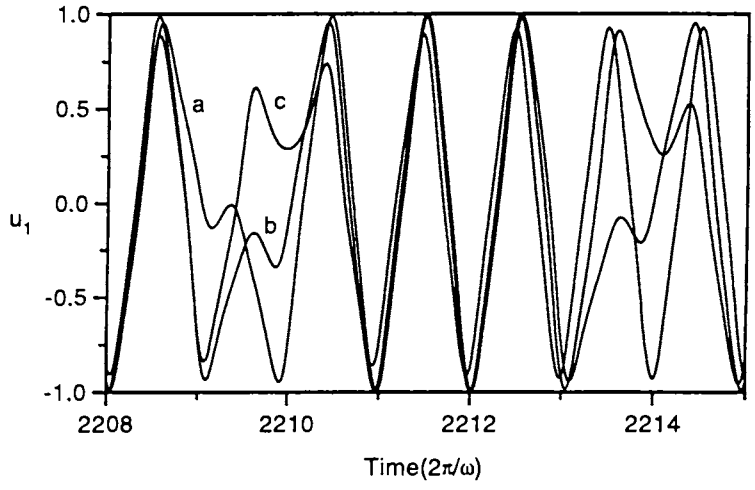

Figure 4.4: Time series of trajectories obtained for from the equations 2.21 in single and double precision (denoted by a and b respectively) and from the equations 2.18 in single precision (denoted by c) for the same set of parameters and initial conditions. $\theta = \phi = 20°$, $\omega = J = 2\pi(r_e + r_e^{-1})$, $r_e = 1.6, k_2 = 11.2$.

out breaks. Note that the maximum GE on the average is decreasing more slowly than the decrease of maximum LE of laminar phase near the onset of intermittency and both tend to zero as k_2 is increased. The maximum LE of the chaotic bursts remain constant as expected. This also demonstrates the existence of the new type of class I intermittency and chaos.

It is well known that for the usual Class I intermittency, the average time taken to traverse the channel varies as $(k_2 - k_2^c)^{-0.5}$ where k_2^c is the critical parameter for the tangent bifurcation. In order to clarify the nature of the intermittency transition to chaos, we computed the scaling of the average length of the laminar phase with the excess of the critical value of the parameter over the control parameter very near to the tangent bifurcation at $k_2 = 12.44$ (in steps of 0.02) and found the exponent to be -0.60 as shown in Fig. 4.5. The scaling behaviour near the onset of bifurcation shows that the observed transition is a typical Class I intermittency. This was further confirmed by the

k_2	Local Lyapunov Exponent		Global Lyapunov Exponent
	Laminar Phase	Chaotic Bursts	
10.6	0.20	0.21	0.23
11.0	0.13	0.19	0.17
11.4	0.19	0.16	0.18
11.8	0.19	0.19	0.19
12.0	0.13	0.20	0.18
12.2	0.10	0.18	0.18
12.4	0.11	0.24	0.15
12.44	0.04	0.20	0.11
12.46	0.00	0.00	0.00

Table 4.1: The maximum values of the Local and Global Lyapunov exponent obtained for different values of k_2, $k_1 = k_3 = 0, \omega = J = 2\pi(r_e + r_e^{-1}), r_e = 1.6, \theta = \phi = 20°$

superposition of the return map of ϕ in the dynamics and the appropriate map, $\phi_{n-1} = \phi_n + {\phi_n}^2 + \epsilon$. Fig. 4.6 shows that the two maps coincide near the tangent bifurcation, where the map R_2 obtained from $\phi_{n+1} = \phi_n + {\phi_n}^2 + \epsilon$ is presented for ϵ equal to zero.

For detailed study we confined our results to $\theta = \phi = 20°$ and $10.6 \leq k_2 \leq 12.44$. We analyzed the return maps of ϕ by varying the control parameter for comparatively large steps of k_2, namely 0.2. In the return maps the points corresponding to the onset of the laminar phase fell on the curve between the points marked as A and B and remainder of the return maps correspond to the intermittent bursts as given in the Fig. 4.7. Fig. 4.7 shows the return maps of ϕ of the Poincaré Sections (stroboscopic plot) of 5000 iterations of the system for one set of initial conditions and value of k_2. Some points of a typical return map are plotted by joining all the points to establish the fact that the reinjection period is nearly constant and the plot is given in Fig. 4.8. The portion of the return map shown in Fig. 4.8 corresponding to the region between A and B corresponds to the laminar phase. An examination of Fig. 4.8 shows that once the system leaves the laminar phase, it is reinjected into the neighbourhood of

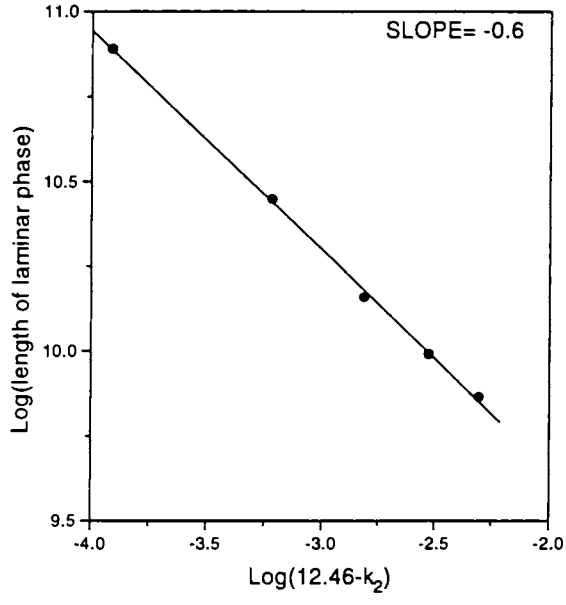

Figure 4.5: Plot of logarithm of average length of laminar phase as a function of logarithm of excess of control parameter showing scaling typical of Class I Intermittency.

the tangent bifurcation in approximately two or three periods. The reinjection time remains nearly unaffected by changes in control parameter whereas, as expected, the average length of the laminar phase increases as the system moves away from the tangent bifurcation.

The portion of the return maps shown in Fig. 4.7, which correspond to regions away from the laminar phase, namely the smooth curve below the line $\phi_{n+1} = \phi_n$ and the two intersecting straight lines, namely C_1, C_2 and C_3 and is explored during the bursts lies less often on these curves once the average length of the laminar phase increases. As a result, fewer points of the stroboscopic return map lie on these curves as k_2 increases. The points of intersection D and E with the line $\phi_{n+1} = \phi_n$ were confirmed to be non-attracting by starting the computation with initial conditions near the points of intersection of the curve D and E with the line $\phi_{n+1} = \phi_n$. To further establish the observation

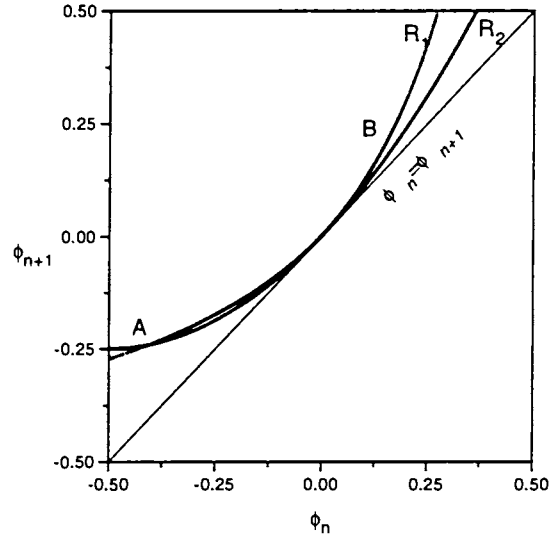

Figure 4.6: Superposition of the observed return map (R_1) obtained from Eq.2.21 at the point of tangent bifurcation and the classic map (R_2) exhibiting Class I Intermittency, where the return map, R_1 is presented for $k_2 = 12.44$, initial conditions $\theta = \phi = 20°$, $\omega = J = 2\pi(r_e + r_e^{-1})$, $r_e = 1.6$

of nearly regular reinjection process and the process is unaffected by variation in the control parameter, the return maps of ϕ for different values of k_2 were analyzed along with the line $\phi_{n+1} = \phi_n$. It can be seen in Fig. 4.9 that the reinjection process is unchanged by the variation in the control parameter.

Another interesting feature of this system is that the average length of the laminar phase varies smoothly with the excess of the critical parameter over the control parameter even when the system is relatively far away from the onset of intermittency. This was confirmed numerically by checking that the logarithm of the average life time of the laminar phase scaled linearly with the logarithm of $12.6 - k_2$ with a slope of -1.15 as shown in the Fig. 4.10. Interesting scaling behaviour is observed near the critical value of the control parameter as shown in Fig. 4.11 where the length of laminar phase scales linearly with $12.4 - k_2$.

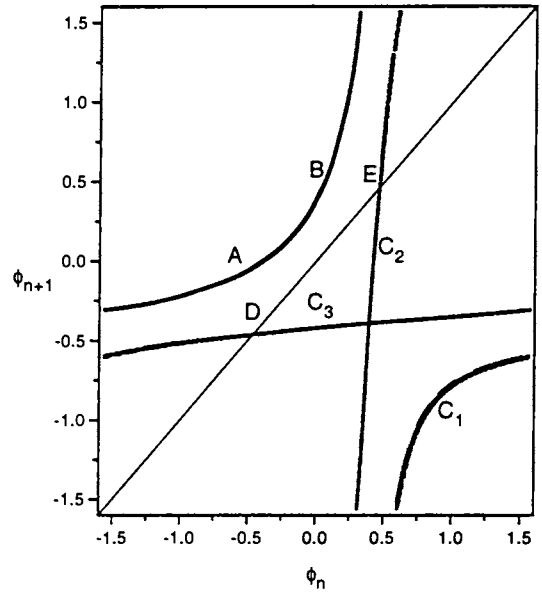

Figure 4.7: The return map ϕ for 5000 points of Poincaré section (stroboscopic plot) of the system for $k_2 = 11.0$, initial conditions $\theta = \phi = 20°$, $\omega = J = 2\pi(r_e + r_e^{-1})$, $r_e = 1.6$.

The number of the bursts as well as the number of occurrences of the laminar phase decreases as k_2 is increased. Further, the average length of the bursts is nearly constant and the average length of the laminar phase increases as k_2 increases. It is also found that length of the burst scales with control parameter near $k_2 = 12.4$ with zero slope. The number of bursts as well as the number of occurrences of the laminar phase decreases smoothly as k_2 increases. As a result, scaling behaviours of the average length of the laminar phase with $k_2 - 10.4$ are obtained. Class I intermittency behaviour with nearly constant reinjection period continued upto a value of k_2 equal to 12.44. Beyond k_2 equal to 12.44 this phenomenon disappeared and the system response becomes periodic.

The feature of the system studied which we feel is interesting to the nonlinear dynamics community is the existence of Class I intermittency with nearly constant reinjection period. This implies that the length of the burst between

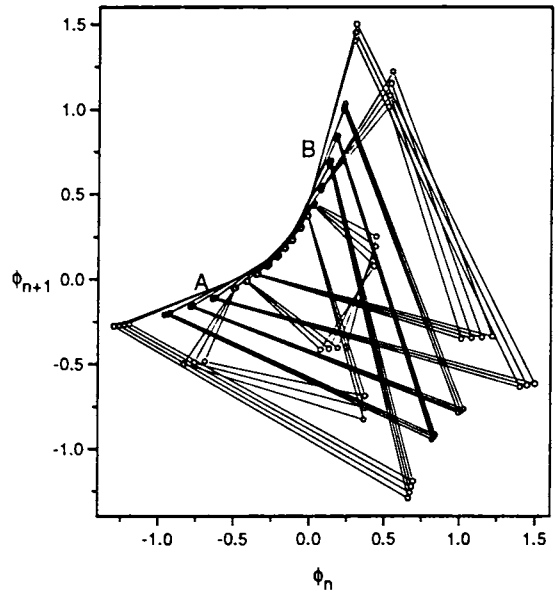

Figure 4.8: The return map ϕ for 100 connected points of Poincaré section (stroboscopic plot) of the system for $k_2 = 12.2$, initial conditions $\theta = \phi = 20°$, $\omega = J = 2\pi(r_e + r_e^{-1})$, $r_e = 1.6$ showing that the reinjection period is nearly constant.

two laminar phases is nearly constant. An analysis of the return maps for ϕ shown in Figs. 4.7 and 4.8 indicates that once the system leaves the neighbourhood of the tangency, it comes back to the neighbourhood of the tangency in nearly the same number of iterations. At k_2=12.44 the attractor is nearly regular. The system was purely periodic with period 6 at k_2=12.46.

Numerical evidence for Class I intermittency with nearly constant reinjection period has been presented near the onset of tangent bifurcation. New scaling behaviour which governs how the average life time of the laminar phase scales with control parameter away from the onset of intermittency is presented. The return maps of the stroboscopic plot for different values of k_2 given in Fig. 4.9 provide an explanation for this behaviour. The present system is one of the very few physically realizable systems which shows this phenomenon of

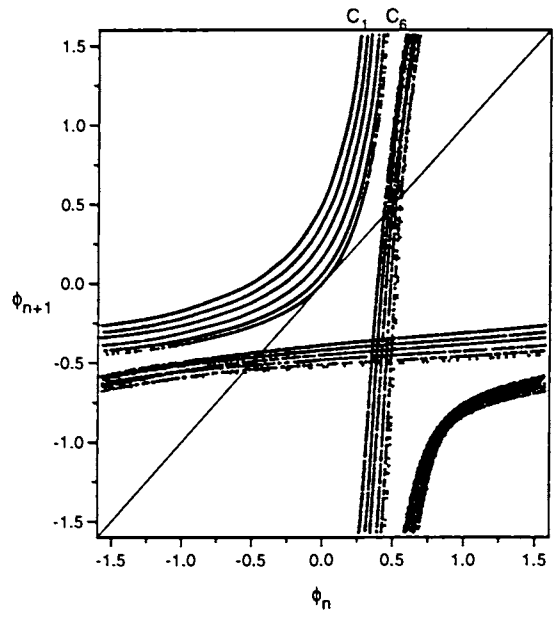

Figure 4.9: Superposition of return maps of ϕ for different values for k_2 =10.6, 11.0, 11.4, 11.8, 12.2, 12.44, initial conditions $\theta = \phi = 20°$, $\omega = J = 2\pi(r_e + r_e^{-1})$, $r_e = 1.6$. Curve C_1 is for k_2 =10.6, Curve C_6 is for k_2 =12.44 with the other curves representing values of k_2 in ascending order.

Class I intermittency with nearly constant reinjection period. Since this problem is technologically important as is evident from the literature cited in this work, the existence of the new behaviour in this system and the existence of the interesting transient behaviour may have important practical consequences, when operating near the regime considered in this work where this phenomenon may not be recognized as leading to chaos. An analysis of the original model equations to explain to some extent the behaviour presented in this work could be carried out. Price and Mullin (1991) and Aubry *et al.* (1988) have reported similar behaviour with other model equations. They have performed some preliminary analysis of their model equations in an attempt to explain the behaviour observed. A similar analysis of our model equations would be considerably more involved since our equations are non-autonomous and would

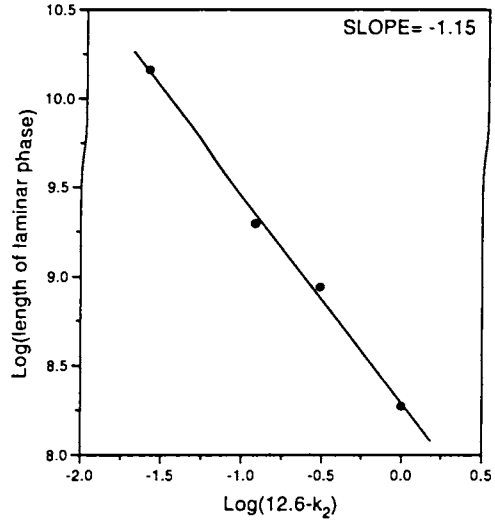

Figure 4.10: Plot of logarithm of average length of laminar phase as a function of logarithm of excess of control parameter showing scaling away from the tangent bifurcation.

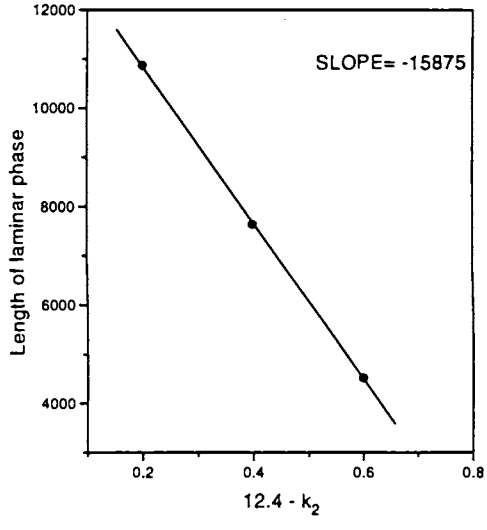

Figure 4.11: Plot of average length of laminar phase as a function of excess of control parameter showing linear scaling away from the tangent bifurcation.

not necessarily throw more light on the results than the analysis based on the return maps presented here.

One paper resulting from this work has been published in an international journal **Phys. Lett. A** (1997), The Netherlands.

Chapter 5

The Theory of Dynamics with Control

5.1 Introduction

The fact that a chaotic solution eliminates the possibility of long term prediction of system behaviour induced many reports in the literature of either quenching chaos or controlling chaos (Ott *et al.* 1990 and Ditto *et al.* 1995). Since chaotic attractors have embedded within them a dense set of unstable periodic orbits, any one of the unstable periodic orbits can be stabilized to obtain otherwise unattainable system behaviour. The essential idea is that a chaotic system explores a relatively large region of state space and the system can be brought to a desired stable state to improve the performance of the separation technique by a suitable control algorithm. The first method (OGY) of control of chaos proposed by Ott *et al.* (1990) generated appreciable interest in the literature of chaos. Thereafter, a large number of algorithms for controlling chaos have been reported in the literature (Ott and Spano 1995, Rhode *at al.* 1995, Christini and Collins 1995 and references therein). Broadly speaking there are two classes of algorithms for controlling chaos, namely (a) *Feedback Methods* (Ott *et al.* 1990) and (b) *Non-feedback Methods* (Güémez *et al.* 1994). The first method needs appreciable information about system behaviour but is comparatively simple to implement experimentally. The second method is theoretically simple and

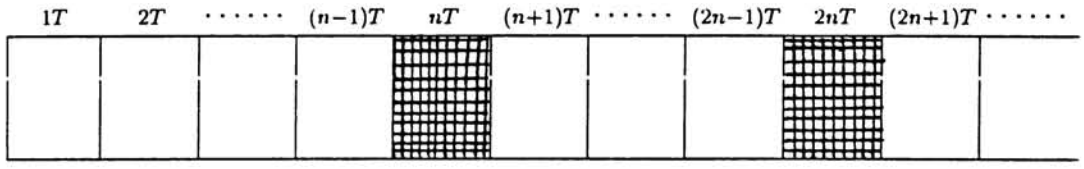

Figure 5.1: The schematic representation of the novel control strategy presented in this work. The control is active during the period corresponding to the shaded area and not active during the period corresponding to the blank area, where each box stands for the period. T of length $2\pi/\omega$.

hence it is easy to implement on a computer whereas it is difficult to implement experimentally in many systems.

The algorithm suggested in this work needs very little information about system behaviour but is rather easy to implement experimentally. This algorithm can be classified as a *Non-feedback control method.* Rajasekar and Lakshmanan (1993) have investigated the applicability and effectiveness of various approaches of controlling chaos in the BVP oscillator. Suppression of chaos by periodic parametric perturbations in an experimental set up of a Duffing oscillator is also reported in the literature by Fronzoni *et al.* (1991). In the method proposed in this section, the control parameter is perturbed for one period at fixed intervals of every integral multiple of the fundamental period. In the methods considered earlier in the literature (Lakshmanan and Murali 1996), the parameter was perturbed continuously rather than at fixed intervals. To implement the control strategy reported in the section 5.2, we apply a constant external force in addition to the periodic force for the duration of one period after every $n-1$ periods as shown in Fig. 5.1, where the length of one period (T) is equal to length of the fundamental period of the periodic force. If the system is perturbed after $n-1$ periods by applying an additional constant force, the system is found to be stabilized in a periodic orbit with a period equal to nT or with a period equal to an integral multiple of nT.

For example, if a represents the magnitude of the additional constant force,

then the control can be implemented by setting $a = 0$ if $j \not\equiv 0 \bmod(n)$ and $a \neq 0$ if $j \equiv 0 \bmod(n)$ where j represents iteration number and the time interval between two successive iterations is equal to the fundamental period T. That is, the system evolves without any modification for periods which are not multiples of n and with modification for periods which are multiples of n. A schematic representation of the control strategy is given in Fig. 5.1. The choice of n depends on the period-m solution we want to stabilize. The integer n can be either m or a divisor of m depending on the value of a and the choice of n.

5.2 A new algorithm for control of chaos

To incorporate the above idea of controlling the dynamics of the system, we modify Eq. 2.21 governing the dynamics of the system by introducing a constant force in addition to the periodic force along the direction of the periodic force for one period at the end of n forcing periods. Thus the resultant torque induced on the particle is given by $\boldsymbol{L} = (\boldsymbol{k}\cos(\omega t) + \boldsymbol{k}') \times \boldsymbol{u}$. Let k_1', k_2' and k_3' be the x, y, z components of $\boldsymbol{k}'$. After scaling all quantities appearing in the equations similarly as explained in the section 2.7, the Eq. 2.21 can be written as

$$\begin{aligned}
\frac{d\theta}{dt} &= \frac{P}{2}\sin 2\theta \sin 2\phi + R\left[(\cos\theta\cos\phi\, k_1 + \cos\theta\sin\phi\, k_2 - \sin\theta\, k_3)\cos(\omega t)\right] \\
&\quad + R\left[(\cos\theta\cos\phi\, k_1' + \cos\theta\sin\phi\, k_2' - \sin\theta\, k_3')\right] \\
\frac{d\phi}{dt} &= P\cos 2\phi - Q \\
&\quad + \frac{R}{\sin\theta}\left[(-\sin\phi\, k_1 + \cos\phi\, k_2)\cos(\omega t) + (-\sin\phi\, k_1' + \cos\phi\, k_2')\right] \qquad (5.1)
\end{aligned}$$

It is noted that the modified system of equations 5.1 reduces to Eq. 2.21 when $k_1' = k_2' = k_3' = 0$.

The application of an additional external forcing (constant) to control chaotic systems evolving under the effect of external forcing (periodic) has

been reported in the literature (Lakshmanan and Murali 1996). In this method the constant force is applied continuously. Our control strategy involves the application of the constant force for a period of finite length, T after a period of length, $(n-1)$T (where T=$2\pi/\omega$ is the fundamental period of the periodic forcing). Then, we lift the control for a period of finite length, $(n-1)$T and thereafter we apply the constant force of the same magnitude for a period of length, T and again we lift the control for a period of finite length, $(n-1)$T. This process is repeated. Under this process, the system is allowed to evolve according to the system of Eq. 2.21 upto the $(n-1)^{\text{th}}$ forcing period and evolve according to the system of Eqs. 5.1 at the n^{th} forcing period. This process is repeated every n^{th} period. While solving the Eqs. 5.1, this idea can be implemented by setting $k_1' = k_2' = k_3' = 0$ if $j \not\equiv 0 \bmod(n)$ and $k_1' = k_2' = k_3' \neq 0$ if $j \equiv 0 \bmod(n)$ where j represents iteration number and $T = 2\pi/\omega$ is the time interval between two successive iterations. We note that the above equations for $\dot{\theta}$ and $\dot{\phi}$ decouple in the absence of k_1, k_1' and k_2, k_2'. Hence the presence of an external force field with either k_1 or k_2 is necessary to obtain chaotic solutions in this system. In our calculations we kept $k_1 = k_3 = k_1' = k_3' = 0$. In almost all cases the system is stabilized to a periodic orbit with period n if the control is applied throughout the n^{th} period. In some cases the system is stabilized to a periodic orbit of period equal to an integral multiple of n. On the other hand if the control is applied continuously, we loose the flexibility of controlling the system to an orbit of desired period.

5.3 Results on separation technique with control

We have analyzed the properties of the system without control in chapter 3. We tentatively identified chaotic regimes of the parameter k_2 keeping $k_1 = k_3 = 0$. As a first step in analyzing the properties of the equations derived in this work,

we set $k_1 = k_3 = 0.$ in equations 2.21 and varied k_2 for particles of different aspect ratio within the range of r_e ranging from 0.2 to 2.0 in steps of 0.2 and kept ω equal to $J = 2\pi(r_e + r_e^{-1})$. We ran the program for 2500 points of the Poincaré section (stroboscopic plot) and deleted the first 2250 points to remove the transients. We started the trajectory with the initial conditions $\theta = o = 45°$. For each trajectory we evaluated 100 points in each cycle which resulted in 25000 points of the trajectory after the transients are removed. We selected $k_2 = 12.0$ and computed the solution of the equations for different r_e ranging within 0.2 to 2.0 in steps of 0.2. For $k_2 = 12.0$ the system given by Eq. 2.21 behaved chaotically for all the r_e considered except for r_e equal to 1.8 and 2.0. The Lyapunov exponents of the attractors were evaluated and found to be positive. The attractor and time series of a typical trajectory are shown in Fig. 5.2 and Fig. 5.3 for the case of r_e=1.2.

In chapter 3, it was reported that the results of the computations are very sensitive to the aspect ratio of the particle in some parameter regimes. In the case of constant external fields in the same parametric regimes we obtained regular behaviour. For $r_e > 1.0$, we obtained nearly the same fixed point for all initial conditions in the case of a constant force field. This indicates that in the sample application considered in this work, a periodic force field is necessary to effect particle separation for particles with $r_e > 1.0$ as explained in section 3.3. Tables. 3.1, 5.1 and 5.2 give a sample of the results obtained for zero force, a constant force of amplitude $k_2 = 12.0$ and a periodic force of amplitude $k_2 = 12.0$ respectively. In this case independent separation of particles is possible only for particles of aspect ratio r_e equal to 1.2. The existence of chaotic dynamics in this system allows control of its dynamics to a desired orbit and thus suggests the possibility of better separation of particles for almost all particles of aspect ratio ranging within 0.2 to 2.0. This is difficult to obtain in the case of regular behaviour or chaotic behaviour without control.

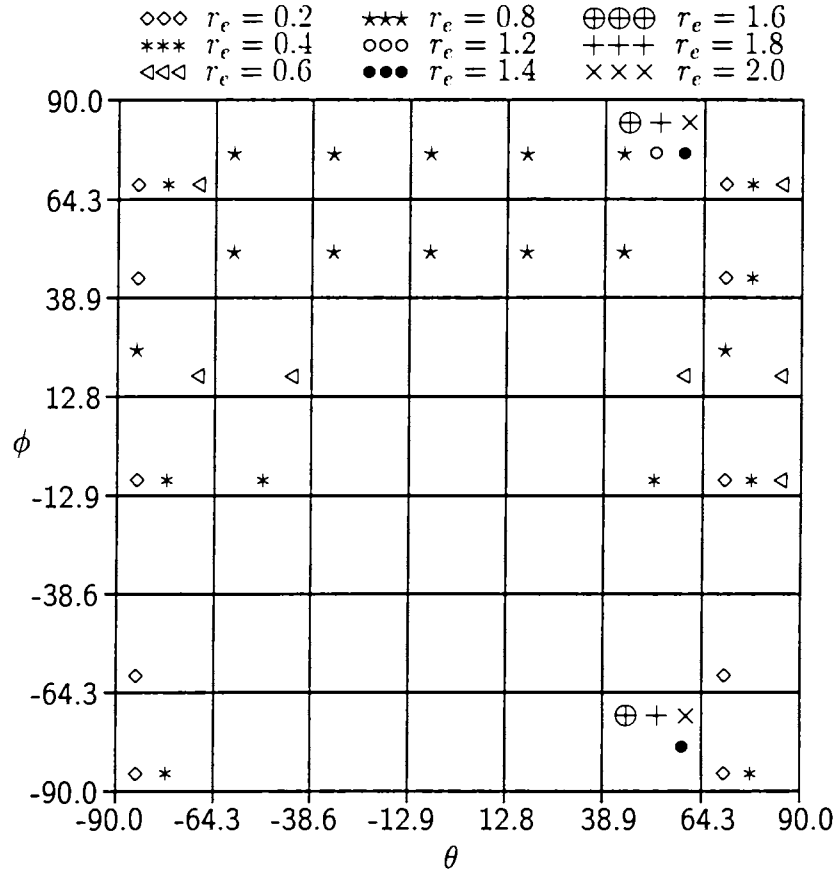

Table 5.1: Distribution of evolution of initially uniformly distributed particles of different aspect ratios for the case $k_2 = 12.0$, $\omega = 0$, $5 \leq l_1 \leq 49$ and $100 \leq l_2 \leq 1000$, where l_1 is the total number of particles in the grid on the average and l_2 is the total number of occurrences of the grid.

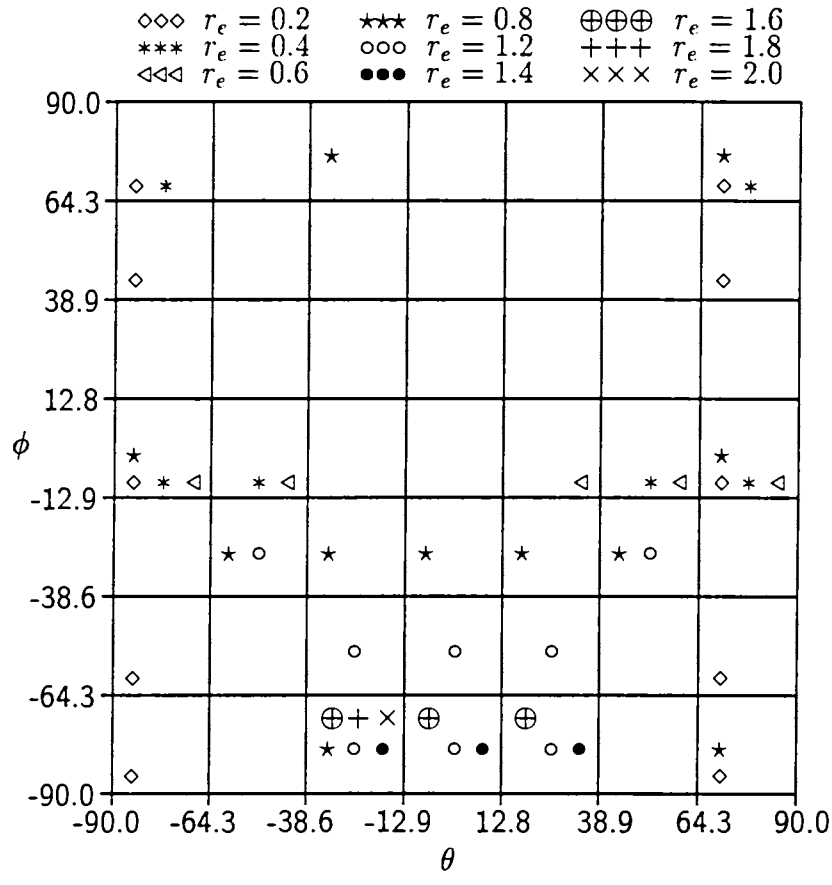

Table 5.2: Distribution of evolution of initially uniformly distributed particles of different aspect ratios for the case $k_2 = 12.0$, $\omega = J = 2\pi(r_e + r_e^{-1})$, $5 \leq l_1 \leq 49$ and $100 \leq l_2 \leq 1000$, where l_1 is the total number of particles in the grid on the average and l_2 is the total number of occurrences of the grid.

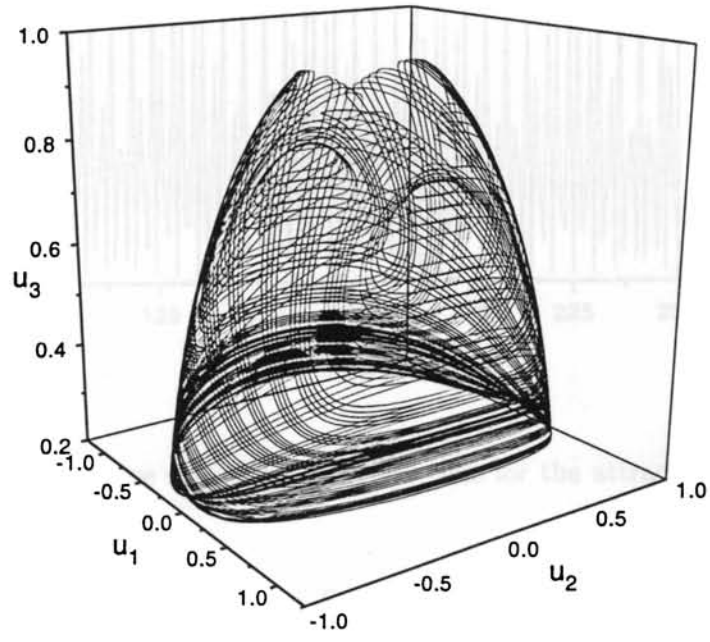

Figure 5.2: Trajectory (phase space) plot of $u_1 \times u_2 \times u_3$ for $k_2 = 12$, initial conditions $\theta = \phi = 45°$, $\omega = J = 2\pi(r_e + r_e^{-1}), r_e = 1.2$.

We stabilized the chaotic dynamics obtained at k_2=12.0 to a periodic behaviour of period equal to a multiple of the fundamental period, $2\pi/\omega$ to demonstrate the applicability of the method proposed. The time series of u_2 of the Poincaré section (stroboscopic plot) upto 4000 periods computed from Eq. 2.21 for r_e=1.6 is given in Fig. 5.4. It is demonstrated that the system can be controlled to periodic behaviour of any desired period by applying the same constant force. For example, the system could be controlled to period-2, period-3, period-4 and period-5 orbits by applying the same constant force equal to k_2'=5 as can be seen from Figs. 5.5. This is obtained by setting $k_1' = k_2' = k_3' = 0$ if $j \not\equiv 0 \bmod(n)$ and $k_1' = k_3' = 0$, $k_2' = 5.0$ if $j \equiv 0 \bmod(n)$ in the evolution of Eqs. 5.1 when the system is to be stabilized in a period-n orbit. The system

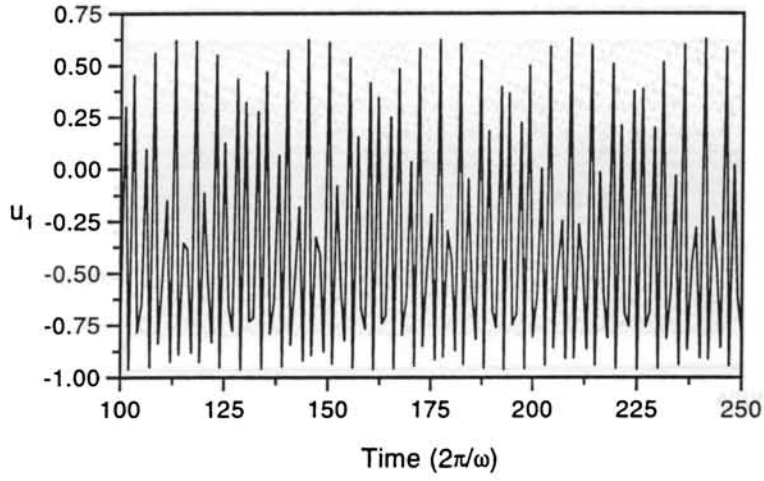

Figure 5.3: Phase space plot of u_1 vs. time for the attractor shown in Fig. 5.2.

evolves according to the evolution Eq. 2.21 for $j \not\equiv 0 \bmod(n)$ and according to the evolution Eqs. 5.1 for $j \equiv 0 \bmod(n)$. It is also possible to stabilize the system to qualitatively different periodic orbits of the same period by suitably changing the control parameter k_2' as can be seen from Fig. 5.6. In this example the control technique is applied after 1500 fundamental periods and the system is followed upto 3000 periods with control. Once the control is applied the system stabilizes rapidly to the appropriate periodic orbit as can be seen from the sample figures in Fig. 5.5. The magnitude of the perturbation required to stabilize the system was small compared to the magnitude of the periodic force for all aspect ratios except r_e= 0.2, 0.4 and 0.6. The magnitude of the constant force required for control depends on the aspect ratio of the particle and the desired period, n for aspect ratios less than or equal to 0.6.

One important advantage of the control algorithm outlined in this work is the possibility of switching over to different periodic solutions during a given run. This implies that a system in chaotic dynamics can be stabilized to one particular periodic orbit for a given time and to another periodic orbit of en-

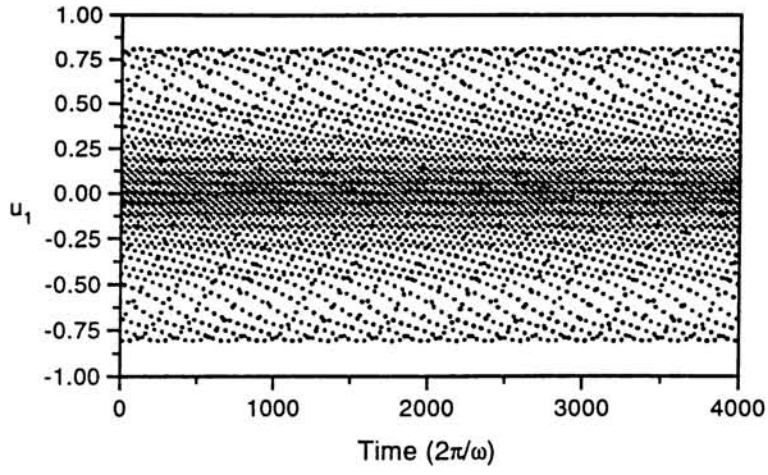

Figure 5.4: Trajectory plot of u_2 vs. time at every intersection of the trajectory with the Poincaré plane for $k_2 = 12$, initial conditions $\theta = \phi = 45°$, $\omega = J = 2\pi(r_e + r_e^{-1})$, $r_e = 1.6$.

tirely different period after a given time as shown in Fig. 5.7. In this example the control parameter $k_2' = 5.0$ is applied between 1001 and 2000 periods to stabilize the system to a period-2 orbit. Then control is lifted between 2001 and 3000 periods and again applied between 3001 and 4000 periods to stabilize the system to a period-3 orbit. Control was removed again between 4001 and 5000 periods. Thus the system oscillates in a period-2 orbit between 1001- 2000 periods and then oscillates in a period-3 orbit between 3001- 4000 periods as can be seen from Fig. 5.7. This figure also reveals the fact that once the control is lifted, the system returns to a chaotic state. Another advantage which is important from the point of view of the sample application proposed in this work is the possibility of changing the periodic behaviour to another orbit of the same period by changing the magnitude of the applied constant force. This allows us to bring a particle having a definite aspect ratio to a desired orbit by changing control parameters. It is also noted that all initially uniformly distributed particles of a given aspect ratio within the range $0.8 \leq r_e \leq 2.0$ can be concentrated in a given grid by applying a periodic force with control as can

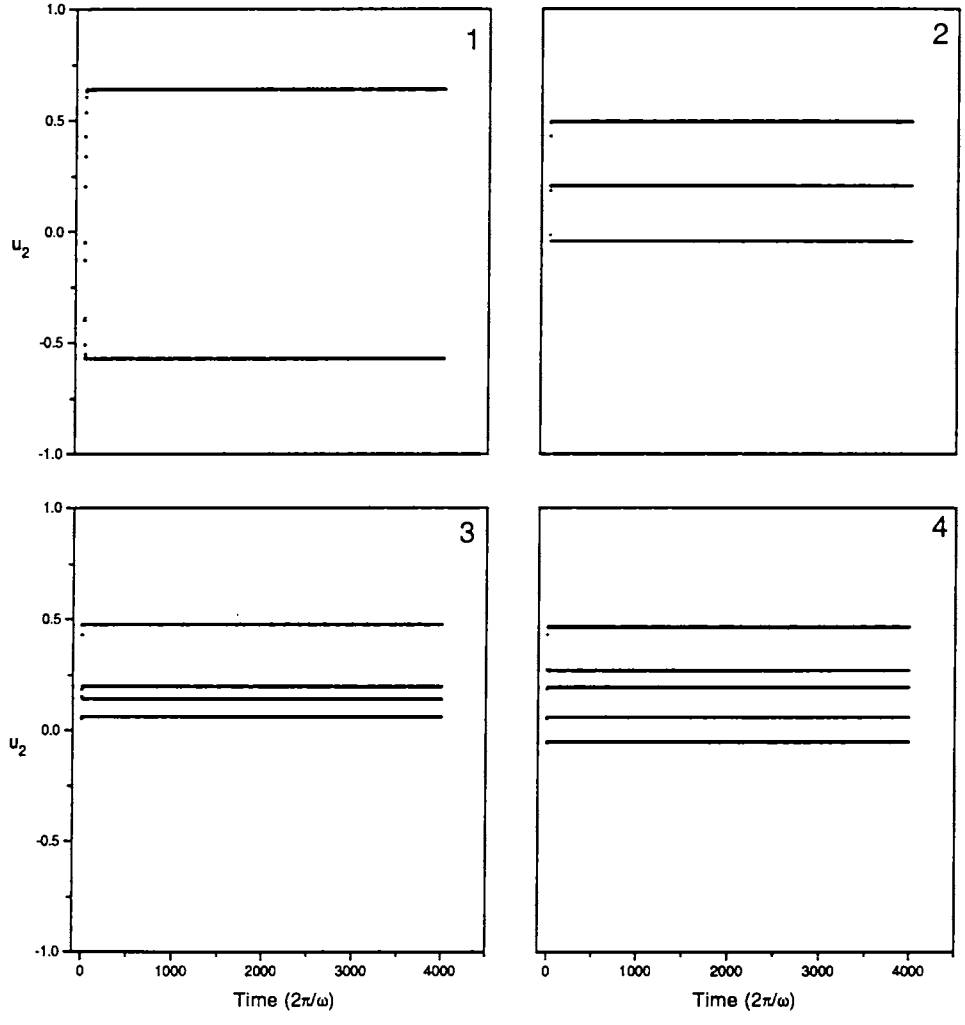

Figure 5.5: Stroboscopic plot with control for $k_2 = 12$, $k_2' = 5.0$, initial conditions $\theta = \phi = 45°$, $\omega = J = 2\pi(r_e + r_e^{-1})$, $r_e = 1.6$ showing (1). a period-2 solution with $n = 2$ (2). a period-3 solution with $n = 3$ (3). a period-4 solution with $n = 4$ (4). a period-5 solution with $n = 5$

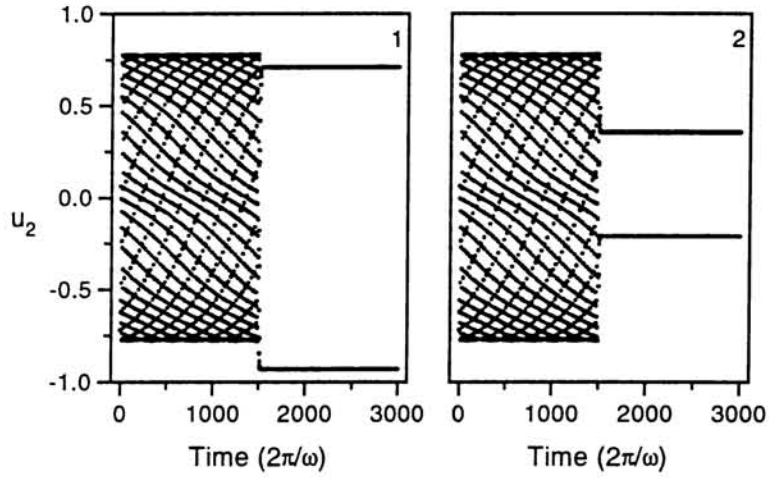

Figure 5.6: Stroboscopic plot with different controls showing two different period-2 orbits obtained for $k_2 = 12$, initial conditions $\theta = \phi = 45°$, $\omega = J = 2\pi(r_e + r_e^{-1})$, $r_e = 1.2$ with control (1) $k_2' = 4, n = 2$ (2) $k_2' = 5, n = 2$

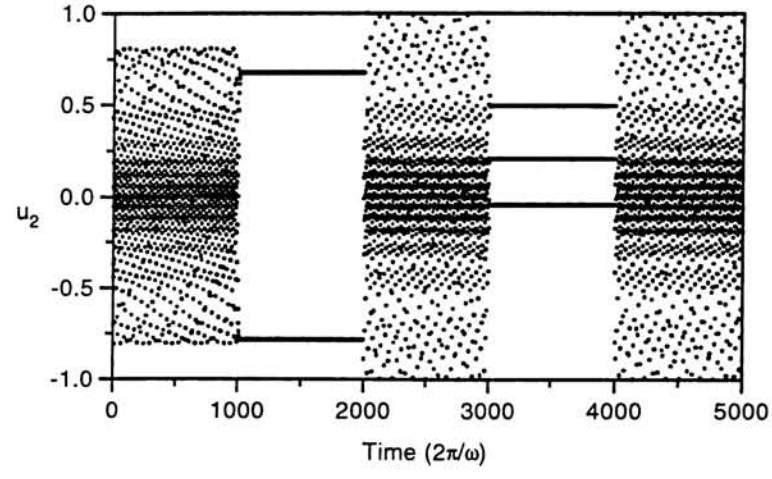

Figure 5.7: Stroboscopic plot showing period-2 and period-3 orbits successively obtained with control applied at every second and third periods respectively for $k_2 = 12$, initial conditions $\theta = \phi = 45°$, $\omega = J = 2\pi(r_e + r_e^{-1})$, $r_e = 1.6, k_2' = 5.0$.

be seen from Tables. 5.3, 5.4 and 5.5.

The observations made in this work suggest the possibility of separating particles more efficiently based on control of chaotic dynamics. We applied a control force (constant force) of magnitude $1 \leq k_2' \leq 5$. For this range of k_2', the chaotic dynamics of particles of all aspect ratio except r_e =0.2, 0.4 and 0.6 could be controlled to a desired orbit. This range of control force seems to be sufficient for efficient separation of particles by shape since particles of these aspect ratios alone can be brought to a desired position. To develop quantitative results based on this observation, we divided the range of possible orientations namely $[-90°\ ,\ 90°]$ in both θ and ϕ variables into 7 equal intervals resulting in 49 equal sized grids. We then computed the evolution of initially uniformly distributed particles of different aspect ratio within the range of r_e equal to 0.2 to 2 in steps of 0.2. In the section 3.3, we have already studied the evolution of the initially uniformly distributed particles in the same manner within the above range of particle axis ratios under the effect of constant, periodic and zero force fields. We observed that periodic forces are better than constant forces for separating particles especially of aspect ratio $r_e > 1$.

We followed the evolution of the ensemble of particles for 3000 iterations of the stroboscopic plot and deleted the first 1000 values to remove transients in the case of constant and zero forces and in the case of periodic forces with control and without control. In all cases we calculated the number of particles in each grid on every second iteration of the Poincaré section of the evolution equations resulting in a total of 1000 values. We noted the grids in which the total number of particles was greater than or equal to 5 and also noted the number of particles in each grid only if the particle occurred in that grid in more than 100 iterations in all cases. We denote these values as r_e, l_1, l_2 where r_e, l_1, l_2 denote the aspect ratio, total number of occurrences of the grid and total number of particles in the grid on the average respectively and prepared tables for these values. A particle of a given aspect ratio visiting a given grid

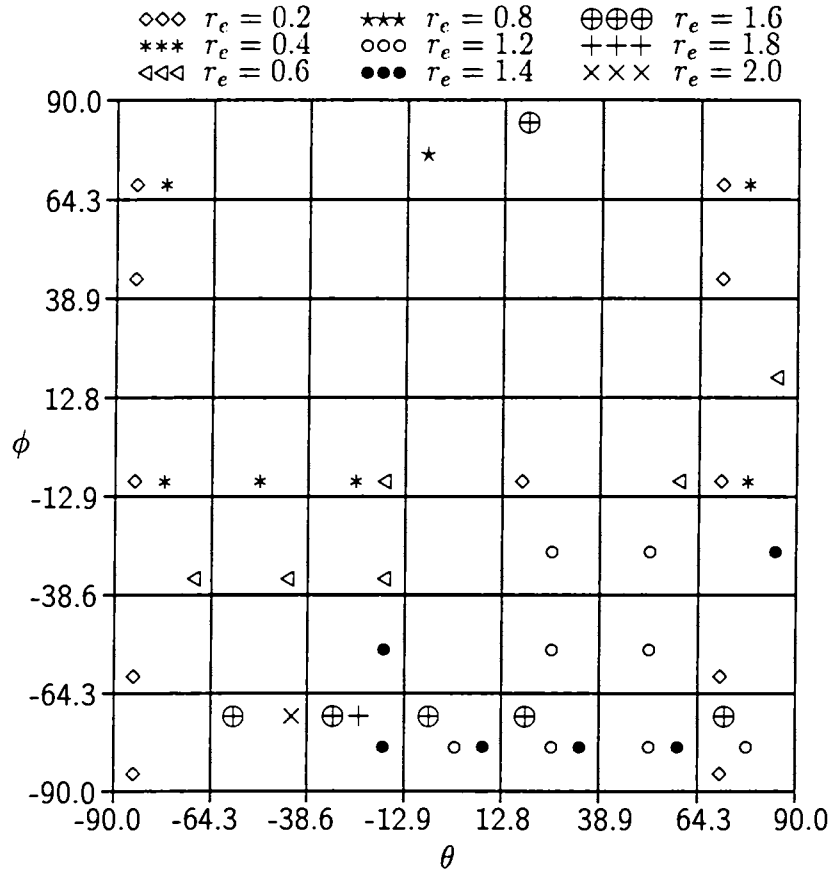

Table 5.3: Distribution of evolution of initially uniformly distributed particles of different aspect ratios for the case $k_2 = 12$, $\omega = J = 2\pi(r_e + r_e^{-1})$, $5 \leq l_1 \leq 49$ and $100 \leq l_2 \leq 1000$ with control $k_2' = 2$, where l_1 is the total number of particles in the grid on the average and l_2 is the total number of occurrences of the grid.

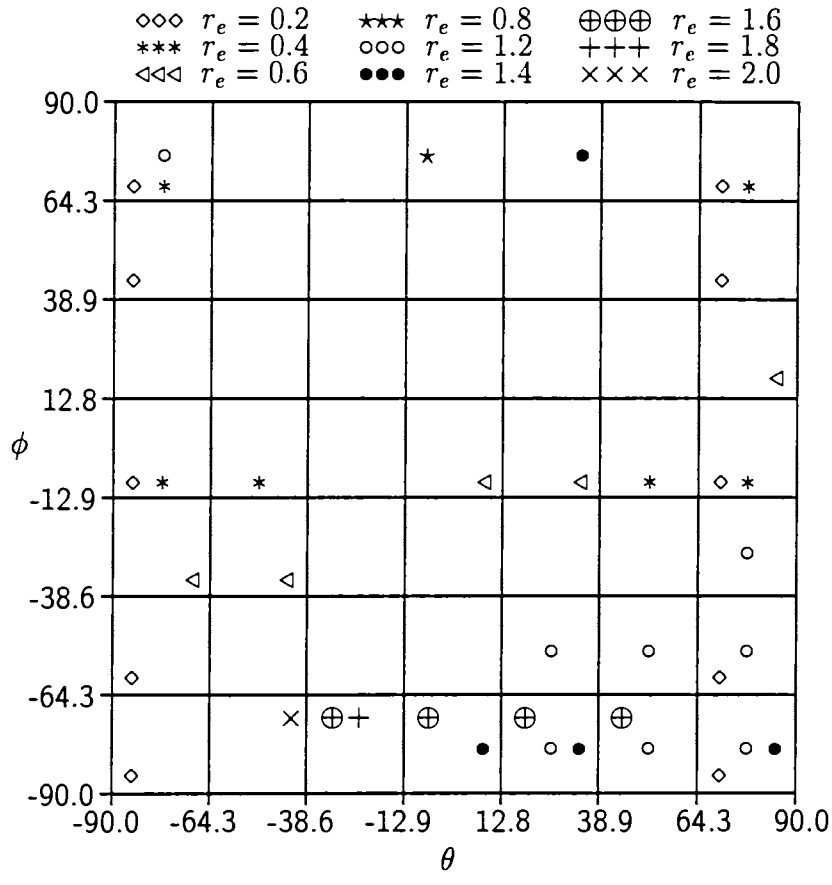

Table 5.4: Distribution of evolution of initially uniformly distributed particles of different aspect ratios for the case $k_2 = 12$, $\omega = J = 2\pi(r_e + r_e^{-1})$, $5 \leq l_1 \leq 49$ and $100 \leq l_2 \leq 1000$ with control $k_2' = 3$, where l_1 is the total number of particles in the grid on the average and l_2 is the total number of occurrences of the grid.

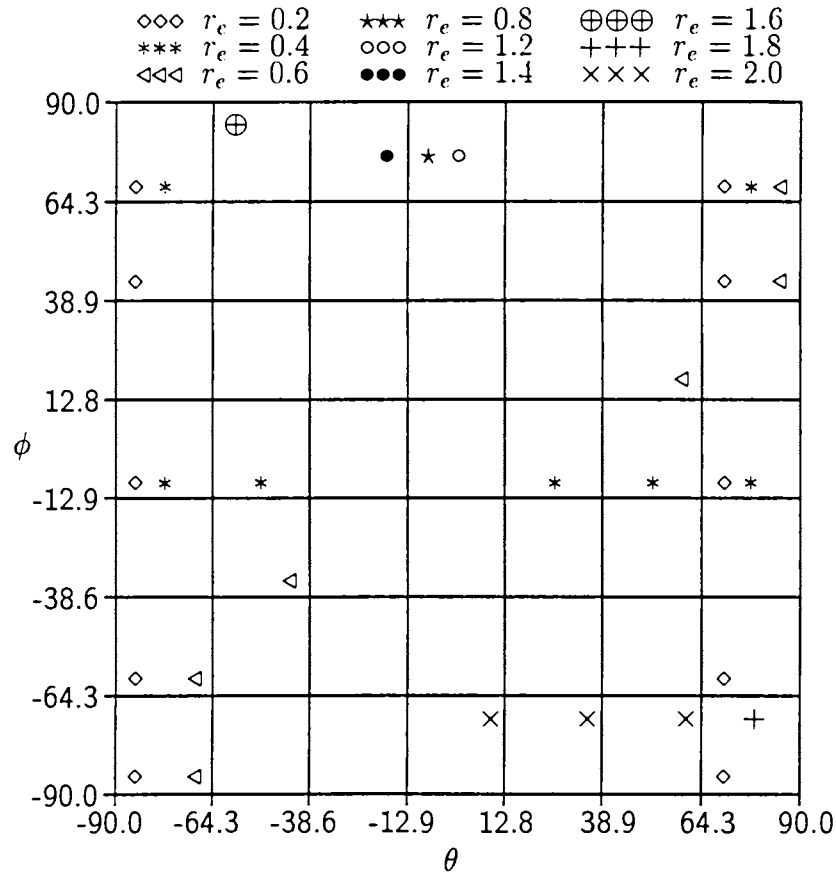

Table 5.5: Distribution of evolution of initially uniformly distributed particles of different aspect ratios for the case $k_2 = 12$, $\omega = J = 2\pi(r_e + r_e^{-1})$, $5 \leq l_1 \leq 49$ and $100 \leq l_2 \leq 1000$ with control $k_2' = 5$, where l_1 is the total number of particles in the grid on the average and l_2 is the total number of occurrences of the grid.

and the absence of particles of other aspect ratios visiting the same grid is more important than the number of visitations of a given grid and the number of particles visiting a grid from the point of view of particle separation. Since our earlier computations indicated the greatest sensitivity of the results to the aspect ratio near $k_2 = 10$, we selected k_2 equal to 12.0 for comparing the effects of periodic forces with and without control and as a magnitude of the constant force. Earlier we demonstrated (in section 3.3) the possibility of the potential application of the separation technique without control, where the magnitudes of the external periodic force were taken as $k_2 = 9.5, 10.0$ and 10.5 keeping $k_1 = k_3 = 0.0$.

We noted the evolution of the ensemble of particles at every 2nd iteration. We analyzed in detail the cases of periodic force with and without control and compared the results with the constant force and zero forces. The fact that a chaotic behaviour can be controlled to oscillate in a selected period resulted in more efficient separation enabling all initially and uniformly distributed particles to be directed to a desired grid by a suitably engineered control technique. For example, all the 49 initially uniformly distributed particles of aspect ratio $r_e = 1.2$ could be brought to the grids (1,4) or (7,4) by applying $k_2' = 4$. Under the same circumstances it was possible to bring all the 49 particles of aspect ratio $r_e = 1.2$ to the grids (1,3) or (7,1) by applying a control of constant force $k_2' = 5$. A sample of the results we obtained for zero force, a constant force and a periodic force both of magnitude $k_2 = 12.0$ and for a periodic force of magnitude $k_2 = 12.0$ with control forces k_2'=2, 3 and 5 are given in Tables 3.1, 5.1, 5.2, 5.3, 5.4 and 5.5. The tables presented in this work indicate that controlling chaotic dynamics is preferable to chaotic behaviour and regular behaviour for efficient separation of particles.

A detailed analysis of all the tables indicates that particles of aspect ratio 0.2 alone can be separated from a mixture containing particles of different aspect ratios ranging within 0.2 to 2.0 by applying a control force of magnitude

k_2'=1, 2, 3, 4 or 5 applied at every second period along with $k_2 = 12$, since particles of aspect ratio 0.2 alone occur in some grids as can be seen from the sample tables. In the case of periodic forces without control and constant and zero forces particles of aspect ratio 0.2 alone also occur along the boundary of the tables. We have suggested in the section 3.3 that particles of this aspect ratio alone could be separated by applying a constant force. However in the case of a periodic force with control, the occurrence of this particle alone are concentrated among a fewer number of grids and visit a given grid a larger number of times. In the case of zero forces the particles of this aspect ratio alone are concentrated among a fewer number of grids along with particles of higher aspect ratio. Thus, for the separation of the particles of this aspect ratio alone a periodic force of magnitude $k_2 = 12.0$ with control is preferable to any other possibility. Similar analysis of the tables shows that it is desirable to apply a periodic force with control for separating particles of aspect ratio 0.4. As can be seen from the sample tables particles of aspect ratio 0.6 alone and 0.8 alone also can separated individually by applying a periodic force with control. In the case of particles of aspect ratio 0.8, they can be brought to one of the extreme grids. Thus, a periodic force with control seems to be preferable to any other case considered for effective separation of particles in the case of aspect ratios $r_e < 1$.

In an earlier analysis made in section 3.3, we have demonstrated that periodic forces are preferable to constant forces and zero forces for separating particles of aspect ratio $r_e > 1$. In the analysis we observed that the occurrence of particles of aspect ratio $r_e > 1$ are spread among a large number of grids. However for particles of aspect ratio greater than or equal to 1.6 individual separation was not possible in the analysis. Further study of the tables prepared in this work indicate that a periodic force with control is once again preferable in such cases. In the case of particles of aspect ratio $r_e > 1.0$ all the initially uniformly distributed particles of the same aspect ratio could be brought to

one grid except for $r_e = 1.8$. Hence particles of aspect ratio within the range of r_e ranging from 1.2 to 2.0 except for r_e=1.8 can be easily separated as can be seen from the sample tables prepared. For particles of aspect ratio equal to 1.8 individual separation may not be possible in the cases considered in this work since particles of this aspect ratio appear in combination with particles of lower aspect ratio equal to 0.2 in some cases considered with control. Hence if particles of aspect ratio 0.2 have been separated out as explained earlier, particles of aspect ratio equal to 1.8 can be separated from the mixture. One advantage of periodic forces with control is that all particles of aspect ratio 1.8 can be brought to one grid in combination with the particles of aspect ratio 0.2 as shown in Table 5.5.

Note that the dynamics of periodically forced spheroids of aspect ratios $r_e = 1.8$ and 2.0 is non-chaotic when $k_2 = 12.0$. In this case we lose the flexibility of forcing the particles to oscillate in a desired orbit even though all the particles of these aspect ratios could be brought to a single grid. Hence it may be possible to separate out the particles of aspect ratios $r_e = 1.8$ and 2.0 alone by selecting some other values of k_2 for which the system behaves chaotically. In such cases more efficient separation of individual particles of these aspect ratios may also be possible by a suitable control strategy. This also shows that a chaotic behaviour of the dynamics with or without control is a must for the separation of particles individually.

In conclusion, it has been generally noted that control of chaotic behaviour gives better separation than chaotic and regular behaviour. One of the main features of the method suggested in this work is that all particles of the same aspect ratio can be concentrated in a previously desired grid. A detailed analysis of the problem can suggest suitable designs for separation of particles by aspect ratio to get a well characterized suspension of particles. As pointed out in the section 3.3, a possible design for this separation of particles from a mixture of particles of different aspect ratios based on the differences in the orientation of

the particle may consist of a base plate having grooves along different orientations so that when the particles are oriented in such directions, they settle in a particular groove and can be separated out at every integral multiple of the fundamental period.

Thus, even in the rather simple application considered in this work, control of chaos leads to greater efficiency. This suggests that the possibility of chaos control should be important in many of the applications mentioned in the introduction. The novel control of chaos technique suggested in this section has been demonstrated to be effective even in the relatively complex problem considered here. An additional feature of the control of chaos technique suggested is that the control is effected very rapidly and the behaviour of the concerned system can be switched from one desired period to another desired period very rapidly. One of the interesting results noted is the possibility to stabilize periodic orbits of period appreciably greater than by the Ott *et al.* method (Ott *et al.* 1990). This suggests that this control of chaos technique may be applied to other chaotic systems very effectively.

One paper resulting from this work is in press in the journal **Sadhana**, published by Indian Academy of Sciences.

We compared the new technique in three dynamical systems and found some advantages over two other techniques. A detailed comparative analysis of the new control of chaos algorithm on some physically realizable model systems will be presented in the next chapter.

Chapter 6

A Comparative Analysis of the New Control of Chaos Algorithm on Some Models

6.1 Introduction

In this work we have proposed a novel algorithm based on parametric perturbation for control of chaos. The method needs almost no information about the system. One of the main advantages of this control algorithm is the possibility of pre-targeting the length of the controlled period obtained by suitably engineering the control technique. In addition we demonstrate certain advantages of this technique over two well-known algorithms, namely, control by periodic parametric perturbation and control by addition of a second weak periodic force, such as the possibility of switching behaviour, pre-targeting the period, stabilizing high period orbits etc. We also demonstrate the applicability of the technique in certain numerical models of physical systems. We demonstrate the successful application of the new algorithm in a rather difficult model problem, namely, the control of the dynamics and the rheological parameters of periodically forced suspensions of slender rods in simple shear flow. We have also implemented the algorithm and controlled chaos in another interesting model of a dynamical system *i. e.* the Bonhoeffer-Van der Pol (BVP) oscillator.

The existence of chaotic parametric regimes and the possibility of control of chaotic behaviour (Ott *et al.* 1990) allows the possibility of many applications including the development of computer controlled intelligent rheology (Kumar *et al.* 1998) and new processing technologies (Zumbrunnen *et al.* 1996). Another possible application of control of chaos is further fine-tuning the separation of particles by aspect ratio than is possible with other methods (ref. section 3.3). The essential idea underlying control of chaos as a tool to obtain novel system behaviour is that a chaotic system may explore a relatively large region of state space and the system can be brought to a desired stable state to improve the performance of the system by a suitable control algorithm. This may lead to system behaviour which heretofore had been impossible to achieve. As new possibilities are offered by chaotic systems, a lot of interest has been generated in chaos and control of chaos. The first method (OGY) of control of chaos proposed by Ott *et al.* (1990) generated appreciable interest in the literature of chaos. Various techniques to alter the behaviour of a chaotic system were proposed by many researchers (Huberman and Lumer 1990, Jackson and Hübler 1990, Shinbrot *et al.* 1993a, Shinbrot 1993b and references therein), but some of these algorithms are system dependent and difficult to implement experimentally. The method introduced by Huberman and Lumer (1990) achieves the desired behaviour by changing the parameter. Thereafter, a large number of algorithms for controlling chaos have been reported in the literature (Schiff *et al.* 1994, Rhode *et al.* 1995 and Christini and Collins 1995). The algorithm proposed by Ott *et al.* (1990) needs information about the system and leads to difficulties in stabilizing higher multiples of the fundamental period. There are are two classes of algorithms for controlling chaos, namely (a) *Feedback methods* (Ott *et al.* 1990) and (b) *Non-feedback methods* (Güémez 1994), as explained in Chapter. 5.

The method proposed in this work is explained in detail in section 5.2. The algorithm presented in section 5.2 is classified as a *Non-feedback control*

method. If the system is perturbed at the end of n forcing periods, the system is found to be stabilized in a periodic orbit with a period equal to n or an integral multiple of n. We have successfully implemented the algorithm proposed in this chapter in certain model equations and find certain advantages when compared with two other methods, namely, (1) perturbing a control parameter and (2) adding a second weak periodic term. The examples we have considered are the dynamics and rheology of periodically forced slender rods, the Bonhoeffer-Van der Pol (BVP) oscillator and the dynamics of periodically forced spheroids. The models other than the dynamics of periodically forced spheroids are considered only to demonstrate the applicability and compare the efficiency of the novel control of chaos technique. The dynamics of periodically forced spheroids was analyzed in detail in earlier chapters.

A variety of mechanisms have been investigated in detail in different dynamical systems (Rajasekar and Lakshmanan 1993). However, an analysis of chaos control by different algorithms in a single dynamical system is essential and important to understand the capability, applicability, efficiency, consistency, and nature of the orbit after implementing various mechanisms of chaos control. In what follows, we report a brief analysis of the new controlling technique and two other techniques in the dynamical systems mentioned above separately. We present these results in the hope that they may excite experimental interest in the problems considered.

6.2 The dynamics and rheology of slender rods

Most of the simple algorithms available in the literature are very difficult to implement on this system of equations, particularly when the system is started off with a uniform initial distribution. For a brief description of the relevance of this problem, see Kumar and Ramamohan (1995). Therefore it is desirable to study the feasibility of control of chaos algorithms in this system. One of the

interesting results noted in this system is the possibility of obtaining complex nonsinusoidal periodic rheological parameters.

The evolution equation of slender rods in simple shear flow has been developed by Ramamohan *et al.* (1994) following Berry and Russel (1987). The undisturbed velocity profile is given as

$$\boldsymbol{V} = \dot{\gamma} y \boldsymbol{i}_x \tag{6.1}$$

where $\dot{\gamma}$ is the shear rate, y is the y-coordinate and $\boldsymbol{i}_x$ is the unit vector along the x-axis. The second phase particle is modeled as a slender rigid rod of radius a and length $2l$. Let $\boldsymbol{u}$ be a unit vector fixed along the symmetry axis of the particle, representing its orientation. The magnetic or electric dipole $\boldsymbol{m}$ is assumed to be oriented parallel to the particle axis, *i. e.* $\boldsymbol{m} = m\boldsymbol{u}$. The periodic external force is taken to be $\boldsymbol{H}\cos(\omega t)$ where ω is the frequency of the periodic driver. The x, y, z components of the orientation independent part of the torque $\boldsymbol{k} = m\boldsymbol{H}$ induced on the slender rods are represented by k_1, k_2, k_3 respectively. The reader is referred to Kumar and Ramamohan (1995) for the details and assumptions of the model. We demonstrate the applicability of the novel control strategy in their model. The novel algorithm for control of chaos of the rheological parameters is described as follows. We apply a constant external force other than the periodic force for the duration of one period $(2\pi/\omega)$ after every $(n-1)$ periods. In order to accomplish this we modify the dynamical system given by them as follows.

$$\begin{aligned}
\dot{\theta} &= \sqrt{2}\sin\theta\cos\theta\sin\phi\cos\phi + [(k_1\cos(\omega t) + k_1')\cos\theta\cos\phi \\
&\quad + (k_2\cos(\omega t) + k_2')\cos\theta\sin\phi - (k_3\cos(\omega t) + k_3')\sin\theta] \\
\dot{\phi} &= -\sqrt{2}\sin^2\phi + \left[-(k_1\cos(\omega t) + k_1')\frac{\sin\phi}{\sin\theta} + (k_2\cos(\omega t) + k_2')\frac{\cos\phi}{\sin\theta}\right]
\end{aligned} \tag{6.2}$$

where k_1', k_2', k_3' are the x, y, z components of the scaled constant force. Accordingly we modify the rheological parameters.

$$
\begin{aligned}
[\eta_1] &= \lim_{\substack{\Phi\to 0 \\ r\to\infty}} \left(\frac{(\sigma_{xy} - \eta_s\dot{\gamma})100B_H}{\Phi\eta_s\dot{\gamma}} \right) \\
&= 75\langle \sin^4\theta \, \sin^2 2\phi\rangle + 300\sqrt{2}\,[\\
&\quad -(k_1\cos(\omega t) + k_1')(\langle \sin\theta \, \sin\phi\rangle - \langle \sin^3\theta \, \sin\phi\rangle + \langle \sin^3\theta \, \sin^3\phi\rangle) \\
&\quad -(k_2\cos(\omega t) + k_2')(\langle \sin^3\theta \, \cos^3\phi\rangle - \langle \sin^3\theta \, \cos\phi\rangle) \\
&\quad -(k_3\cos(\omega t) + k_3')(\frac{1}{2}\langle \cos^3\theta \, \sin 2\phi\rangle - \frac{1}{2}\langle \cos\theta \, \sin 2\phi\rangle)\,]
\end{aligned}
$$

$$
\begin{aligned}
[\eta_2] &= \lim_{\substack{\Phi\to 0 \\ r\to\infty}} \left(\frac{(\sigma_{yx} - \eta_s\dot{\gamma})100B_H}{\Phi\eta_s\dot{\gamma}} \right) \\
&= 75\langle \sin^4\theta \, \sin^2 2\phi\rangle + 300\sqrt{2}\,[\\
&\quad -(k_1\cos(\omega t) + k_1')(\langle \sin^3\theta \, \sin^3\phi\rangle - \langle \sin^3\theta \, \sin\phi\rangle) \\
&\quad -(k_2\cos(\omega t) + k_2')(\langle \sin\theta \, \cos\phi\rangle - \langle \sin^3\theta \, \cos\phi\rangle + \langle \sin^3\theta \, \cos^3\phi\rangle) \\
&\quad -(k_3\cos(\omega t) + k_3')(\frac{1}{2}\langle \cos^3\theta \, \sin 2\phi\rangle - \frac{1}{2}\langle \cos\theta \, \sin 2\phi\rangle))\,]
\end{aligned}
$$

$$
\begin{aligned}
[\tau_1] &= \lim_{\substack{\Phi\to 0 \\ r\to\infty}} \left(\frac{(\sigma_{xx} - \sigma_{zz})100B_H}{\Phi\eta_s\dot{\gamma}} \right) \\
&= \frac{75}{2}\langle \sin^4\theta \, \sin 4\phi\rangle + 225\langle \sin^4\theta \, \sin 2\phi\rangle - 150\langle \sin^2\theta \, \sin 2\phi\rangle + 300\sqrt{2}\,[\\
&\quad -(k_1\cos(\omega t) + k_1')(2\langle \sin\theta \, \cos\phi\rangle - \langle \sin^3\theta \, \cos^3\phi\rangle - \langle \sin^3\theta \, \cos\phi\rangle) \\
&\quad -(k_2\cos(\omega t) + k_2')(\langle \sin^3\theta \, \sin^3\phi\rangle - 2\langle \sin^3\theta \, \sin\phi\rangle + \langle \sin\theta \, \sin\phi\rangle) \\
&\quad -(k_3\cos(\omega t) + k_3')(\frac{1}{2}\langle \sin 2\theta \, \sin\theta \, \sin^2\phi\rangle - \langle \sin 2\theta \, \sin\theta\rangle)\,]
\end{aligned}
$$

$$
\begin{aligned}
[\tau_2] &= \lim_{\substack{\Phi \to 0 \\ r \to \infty}} \left(\frac{(\sigma_{yy} - \sigma_{zz}) 100 B_H}{\Phi \eta_s \dot{\gamma}} \right) \\
&= \frac{-75}{2} \langle \sin^4\theta \, \sin 4\phi \rangle + 225 \langle \sin^4\theta \, \sin 2\phi \rangle - 150 \langle \sin^2\theta \, \sin 2\phi \rangle + 300\sqrt{2} \, [\\
&\quad -(k_1 \cos(\omega t) + k_1')(\langle \sin\theta \, \cos\phi \rangle + \langle \sin^3\theta \, \cos^3\phi \rangle - 2\langle \sin^3\theta \, \cos\phi \rangle) \\
&\quad -(k_2 \cos(\omega t) + k_2')(2\langle \sin\theta \, \sin\phi \rangle - \langle \sin^3\theta \, \sin^3\phi \rangle - \langle \sin^3\theta \, \sin\phi \rangle) \\
&\quad -(k_3 \cos(\omega t) + k_3')(\frac{-1}{2} \langle \sin 2\theta \, \sin\theta \rangle - \frac{1}{2} \langle \sin 2\theta \, \sin\theta \, \sin^2\phi \rangle) \,] \qquad (6.3)
\end{aligned}
$$

where η is the effective viscosity, σ_{xy}, σ_{yx}, $\sigma_{xx}, \sigma yy, \sigma zz$ are the components of the total stress tensor, η_s is the viscosity of the suspending liquid and Φ is the volumetric concentration of the suspended particles, θ and ϕ are the azimuthal angle and the polar angle corresponding to a given vector $\boldsymbol{u}$. Here B_H is a function of the shape of the particle and r is the aspect ratio of the particle.

It may be noted that when $k_1' = k_2' = k_3' = 0$, the system evolves without any modification as given in Kumar and Ramamohan (1995).

Under the operation of the new control technique, the system is allowed to evolve according to the system of equations 6.3 with $k_1' = k_2' = k_3' = 0$ upto the $(n-1)^{\text{th}}$ forcing period and evolve according to the system of equations 6.3 with $k_1' = k_2' = k_3' \neq 0$ at the n^{th} forcing period. This can be implemented by setting $k_1' = k_2' = k_3' = 0$ if $j \not\equiv 0 \bmod(n)$ and $k_1', k_2', k_3' \neq 0$ if $j \equiv 0 \bmod(n)$ where j represents iteration number. That is the system evolves without any modification for periods which are not multiples of n. The choice of n depends on the period-m solution we want to stabilize. The integer n can be either m or a divisor of m depending on the magnitude of the constant force. In this work, we kept $k_1 = k_3 = 0$ and varied k_2 in the original equations obtained before the modification for finding chaotic regimes. The equations 6.3 reduces to the original equations as given by Ramamohan *et al.* (1994), when $k_1' = k_2' = k_3' = 0$. We selected a value of k_2 from the chaotic regime. To demonstrate the applicability of the novel control technique, we put different values for k_2' in the

manner explained above. In our calculations we kept $k_1 = k_3 = k_1' = k_3' = 0$ throughout. In general, k_1, k_2, k_1' and k_3' can also be set to non-zero values similar to k_2 and k_2'.

The numerical procedure discussed in Kumar and Ramamohan (1995) was adopted to calculate the orientation distribution function and hence the various orientation averages involved in the rheological parameters. Kumar and Ramamohan (1995) have reported earlier the behaviour of the rheological parameters for the parameter range from $k_2 = 0.0$ to $k_2 = 0.30$ keeping $k_1 = k_3 = 0.0$ starting off from a uniform initial distribution. We selected a value of k_2 in a chaotic regime between $k_2 = 0.3$ and $k_2 = 1.0$ and stabilized periodic solutions of periods upto ten times the fundamental period $2\pi/\omega$ to demonstrate the applicability of the method proposed. The control technique is applied from the very beginning and the system is followed upto 400 cycles of the fundamental period. For the trajectory we evaluated 100 points in each cycle. The trajectory plot of a chaotic attractor and the time series of $[\tau_1]$ observed at a stroboscopic period of $2\pi/\omega$ of the chaotic behaviour without control for $k_1 = k_3 = 0.0$, $k_2 = 0.44$, $k_1' = k_2' = k_3' = 0$ is shown in Fig. 6.1 and 6.2 for the uniform distribution. The time interval between successive values of the time series noted is $2\pi/\omega$ in the stroboscopic plot.

The initial orientation distribution is taken to be uniform and $k_1' = k_3' = 0.0$, $k_1 = k_3 = 0.0$ for all the results reported in this work. The time series of $[\tau_2]$ for $k_2 = 0.44$ is shown in Fig. 6.3 which represents a controlled period-6 behaviour. In this case, for every i^{th} period of evolution the magnitude of k_2' was assigned to be $k_2' = 0.05$ if $i \equiv 0 \pmod 6$ and was set to be $k_2' = 0.0$ if $i \not\equiv 0 \pmod 6$. Except for the period i with $i \equiv 0 \pmod 6$ the system evolves without any modification. In the case shown in Fig. 6.2, the control was applied after 500 periods. As can be seen from Fig. 6.3 the system stabilizes rapidly once the control is applied.

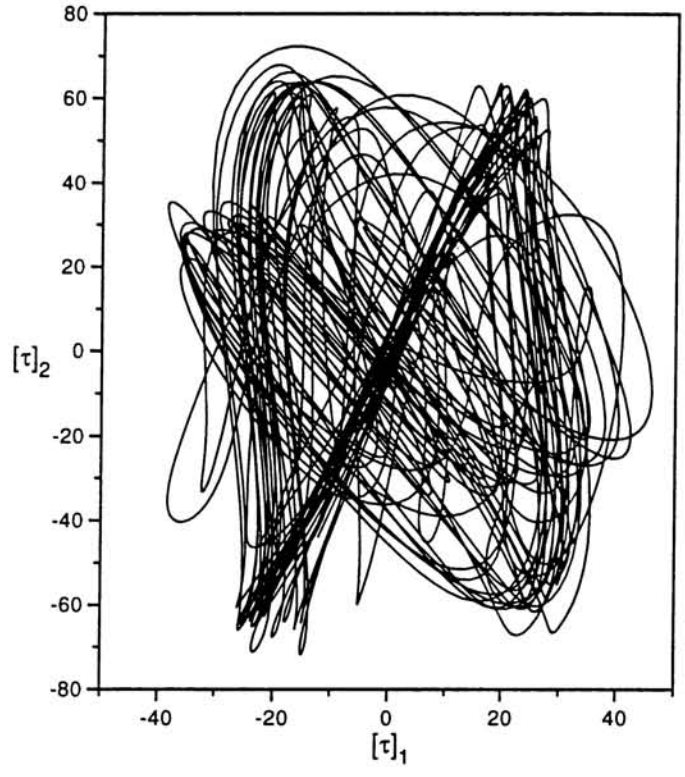

Figure 6.1: Trajectory plot of the attractor ($[\tau_1] \times [\tau_2]$) for $k_1 = k_3 = 0$, $k_2 = 0.44$, $\omega = 1$ and uniform initial orientation distribution.

For the case $k_2 = 0.44$ the system without control behaves chaotically (Fig. 6.1). The time series of $[\tau_1]$ for $k_2 = 0.44$ which was stabilized to a period-5 behaviour is shown in Fig. 6.4, the control was applied from the very beginning with $k_2' = 0.03$ and $n = 5$. For the same k_2 value, *i. e.* $k_2 = 0.44$, the system stabilized to period-27 behaviour when the control was applied with $k_2' = 0.08$ and $n = 9$ and the system stabilized to period-36 behaviour when the control was applied with $k_2' = 0.10$ and $n = 9$. At the same time a period-8 behaviour is obtained when the control was applied with $k_2' = 0.08$ and $n = 8$. That is, the value of n should be chosen to be the desired periodicity or a divisor. Besides, the magnitude of k_2' is related to n. The details of the different periods stabilized from a chaotic regime are given in Table. 6.1. The magni-

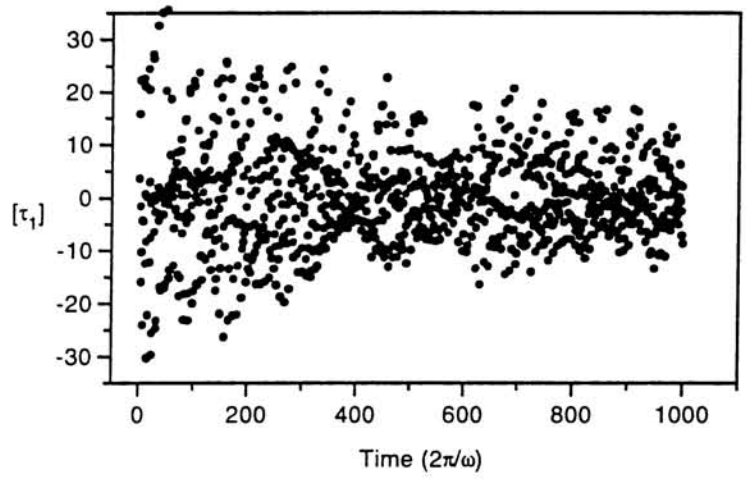

Figure 6.2: Time series of $[\tau_1]$ of the trajectory plot shown in Fig. 6.2 observed at a stroboscopic period of length $(2\pi/\omega)$.

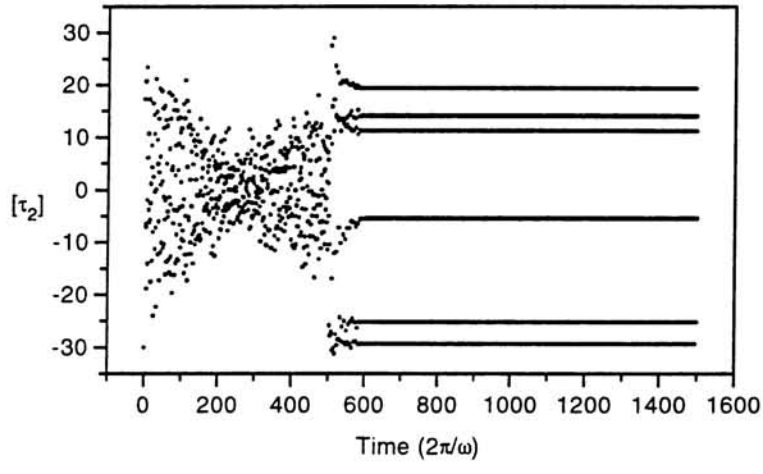

Figure 6.3: Stroboscopic plot with the novel control technique showing a period-6 solution for $k_2 = 0.44$, $\omega = 1$, uniform initial orientation distribution with $k_2' = 0.05$, $n = 6$.

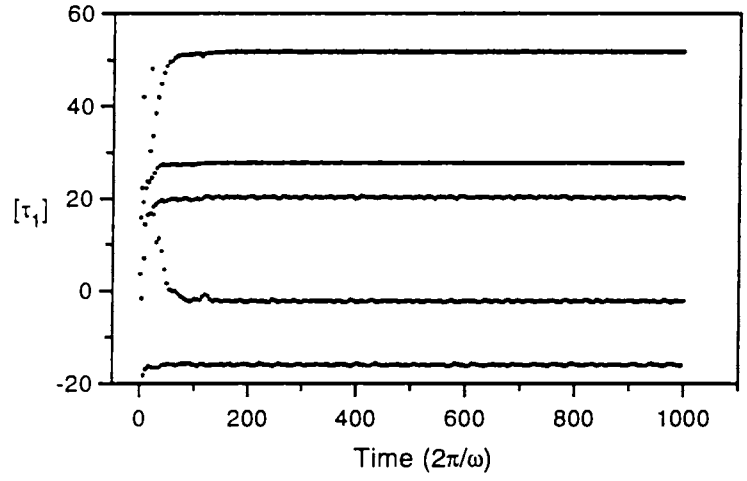

Figure 6.4: Stroboscopic plot with the novel control technique showing a period-5 solution for $k_2 = 0.44$, $\omega = 1$, uniform initial orientation distribution with $k_2' = 0.03$, $n = 5$.

tude of the constant force required is comparatively high for stabilizing the lower period orbit as can be seen from Table. 6.1. For the value of $k_2 = 0.44$, the system stabilized to a lower period orbit of period-1, when the control was applied with $k_2' = 0.2$ and $n = 1$.

We have noted earlier that, a period-m orbit can be stabilized by choosing the value n as m or a divisor of m. For example a period-8 orbit can be stabilized for $k_2 = 0.44$ by applying a control either with $k_2' = 0.08$ and $n = 8$ or with $k_2' = 0.09$ and $n = 4$.

One advantage of the control of chaos method followed in this work is that it is possible to switch over to different periodic solutions, *i. e.*, a chaotic solution can be stabilized to a particular periodic solution for some time and then to another solution with entirely different period. For example, for $k_2 = 0.44$ the control with $k_2' = 0.11$ and $n = 3$ was applied from the 500^{th} period to the 1000^{th} period for which the system stabilized to a period-3 behaviour. Then the control was lifted and was again applied from the 1500^{th} period to the 2000^{th} period with $k_2' = 0.07$ and $n = 2$ afterwards for which the system stabilized to

	n									
k_2'	1	2	3	4	5	6	7	8	9	10
0.03				4	5					
0.04				4	5					
0.05				8	5	6				10
0.06				4	5	6	14	8	27	
0.07		2	3	4	5	6	14	8	27	
0.08		2	3	8	5	6	14	8	27	
0.09	3	2	3	8	5	6	14	8	27	10
0.10		2	3	8	5	6	14	8	36	10

Table 6.1: A two way tabulation of controlled periods of the rheological parameters obtained with the novel control technique for different values of k_2' and different values of n, where $k_2 = 0.44$, $k_1 = k_3 = 0$, $\omega = 1$, uniform initial orientation distribution.

period-2 behaviour. Thus the system oscillates in a period-3 orbit between the 500^{th} period and the 1000^{th} period and then it oscillates in a period-2 orbit after the 1500^{th} period. This is shown in Fig.6.5.

One of the interesting observations made in this work is the possibility of obtaining complex nonsinusoidal periodic rheological parameters by control of chaos techniques. It is also possible to alter the nature of the controlled periodic rheological parameters dramatically by a small change in the constant control force. These complex periodic rheological parameters may not be obtained by other by other methods. The large variation in the apparent viscosity obtainable during one cycle of the complex periodic orbit may perhaps be used to absorb complex vibrations in and to impart complex motions to a rotor.

We also applied the method of periodic parametric perturbations (Rajasekar and Lakshmanan 1993) to attempt to control the rheological parameters for comparative study. In this method we perturb one of the parameters periodically. We adopt this technique in the computations by replacing the term $k_i \cos(\omega t) + k_i'$ in Eqs. 6.3 with $k_i[1+\eta(\cos\omega_1 t]\cos\omega t$, where η is the magnitude, ω_1 is the frequency of the parametric perturbation and i=1 or 2 or 3. Note that

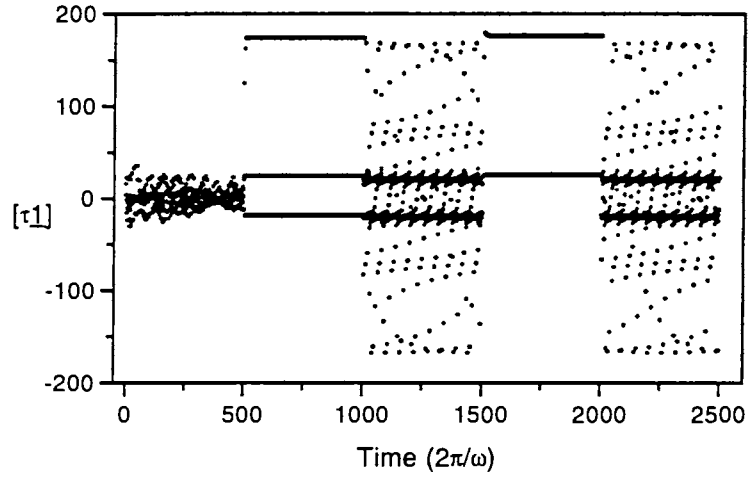

Figure 6.5: Stroboscopic plot with the novel control technique showing switching between a period-3 solution and a period-2 solution for $k_2 = 0.44$, $\omega = 1$, uniform initial orientation distribution, where $k_2' = 0.11$, $n = 3$ is applied from 500 to 1000 periods and $k_2' = 0.07$, $n = 2$ is applied from 1500 to 2000 periods.

usual rheological parameters will be recovered for η=0 and $k_1' = k_2' = k_3' = 0$. To demonstrate the technique we put $k_1 = k_3 = 0 = k_1' = k_3'$, $k_2 = 0.44$ and varied η after replacing $k_2 \cos(\omega t) + k_2'$ in equation 6.3 with $k_2(1 + \eta \cos(\omega_1 t)) \cos(\omega t)$. Starting from the chaotic state (η=0), the effect of parametric perturbations on the dynamics and rheology of periodically forced slender rods was explored by considering a range of values of η. By changing the values of η the system may or may not be controlled as desired. We found that in almost all cases the system is controlled to a 2-period orbit or a 5-period orbit or a 8-period orbit or a 12-period orbit or control with a high degree of disturbance. The system with control showed the same behaviour for all the considered values of ω_1 and η ranging between $0 < \omega_1 \leq 1$ and $0 < \eta \leq 0.35$. Typical plots are given in Figs. 6.6 for 2-period and 5-period solutions and for control with disturbance. Switching between two different periodic orbits seems to be very difficult with this method. The amount of perturbation required is high compared to the ad-

	ω_1							
η	0.2	0.25	0.4	0.5	0.6	0.75	0.8	1
0.05					5			
0.10	5	12	5		5		5	
0.15	5	12	5		5		5	
0.20	5	12	5		5	8	5	
0.25	5	12	5	2	5	8	5	
0.30	5	12	5	2	5	8		

Table 6.2: A two way tabulation of controlled periods of the rheological parameters obtained with the control technique of periodic parametric perturbation method for different values of η and different values of ω_1, where $k_2 = 0.44$, $k_1 = k_3 = 0$, $\omega = 1$, uniform initial orientation distribution.

ditional constant force required in the new control technique. A list of periodic behaviour obtained for different values of η and different values of ω_1 is given in Table. 6.2.

We tried one more method for controlling chaos in this problem. In this method we add a second weak periodic force instead of the constant force described above. The equations governing the dynamics and rheological parameters can be obtained by replacing the term $k_i \cos(\omega t) + k_i'$ with $k_i \cos(\omega t) + k_i' \cos(\omega_1 t)$, i=1, 2, 3. To demonstrate the the applicability of the technique we kept $k_1 = k_3 = k_1' = k_3' = 0$ and $k_2 = 0.44$ and varied k_2' for small steps. Since we deal with introduction of a weak periodic force in this method we applied a certain percentage of the original external force, $k_2 = 0.44$ with different frequencies. As an example we kept $\omega = 1$ and varied ω_1 as $\omega_1 = 0.2$, 0.25, 0.5, 0.6, 0.75 and 0.9. In this method we could not control chaos in the system for the considered values of k_2' upto $k_2' = 0.0132$ (3% of k_2). For certain cases control is obtained with a high degree of disturbance as can be seen from Fig. 6.7. However there is considerable reduction in the disturbance when k_2' is increased. In this method there is no possibility of switching between the

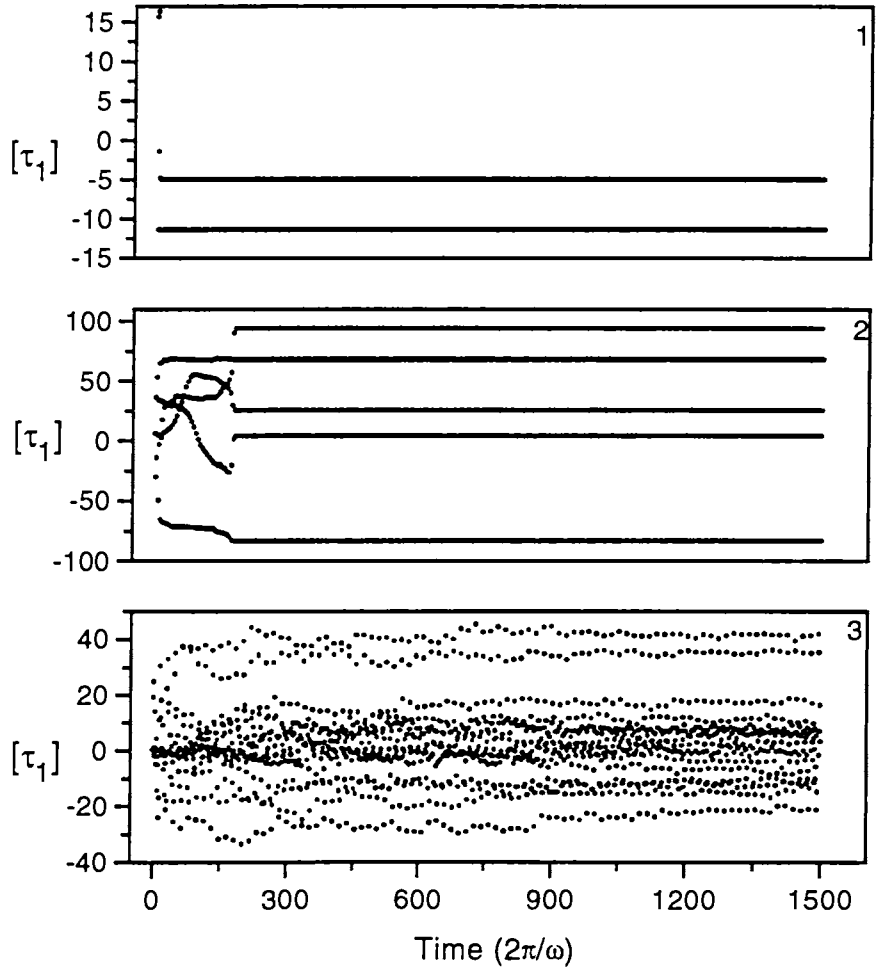

Figure 6.6: Stroboscopic plot for $k_2 = 0.44$, $\omega = 1$, uniform initial orientation distribution with the method of periodic parametric perturbation, (1) showing a 2-period orbit when η=0.3 and ω_1=0.5 (2) showing a 5-period orbit when η=0.1 and ω_1=0.4 (3) showing control with disturbance when η=0.1 and ω_1=1

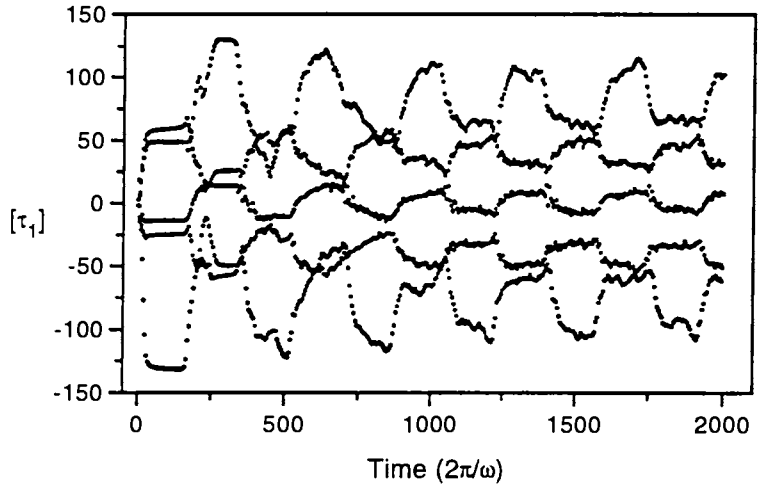

Figure 6.7: Stroboscopic plot for $k_2 = 0.44$, $\omega = 1$, uniform initial orientation distribution with the method of addition of a second weak periodic force, showing control with disturbance when k_2'=0.0176 and ω_1=0.2

orbits stabilized. Finally periodic solutions of period-5, period-8, period-10 and period-12 are obtained for k_2' equal to 10% of k_2 and the different frequencies. We got a period-36 behavior for a weak periodic force of magnitude, k_2' equal to 4% of k_2 after a long transient. We also got a period-5 and a period-8 behaviors for a weak periodic force of magnitude, k_2'= 5% of k_2. In all cases the periods obtained are multiples of either 4 or 5 as can be seen from Table. 6.3.

6.3 The Bonhoeffer-Van der Pol (BVP) oscillator

Rajasekar and Lakshmanan (1992, 1993) have analyzed an interesting dynamical system of considerable biological and physical significance and established the existence of chaos. They have investigated the applicability of various approaches of controlling chaos in the BVP oscillator. The BVP oscillator with a periodic membrane current of magnitude A_1 as given by them is

	ω_1					
k_2'	0.2	0.25	0.5	0.6	0.75	0.9
0.0044						
0.0088						
0.0132						
0.0176					36	
0.0220	5	8				
0.0440	5	8		5	12	10

Table 6.3: A two way tabulation of controlled periods of the rheological parameters obtained with the control technique by the method of addition of second weak periodic force for different values of k_2' and different values of ω_1, where $k_2 = 0.44$, $k_1 = k_3 = 0$, $\omega = 1$, uniform initial orientation distribution.

$$\begin{aligned} \dot{x} &= x - \frac{1}{3}x^3 - y + A_1(\cos\omega t) \\ \dot{y} &= c(x + a - by) \end{aligned} \tag{6.4}$$

where A_1 is the magnitude of periodic bias with frequency ω.

In this section we investigate the efficiency and applicability of the novel control of chaos techniques for the BVP oscillator. The dynamical behaviour of the system 6.4 is chaotic for the choice of the parameters $a = 0.7$, $b = 0.8$, $c = 0.1$, A_1=0.74 and $\omega = 1.0$. A typical trajectory plot of a chaotic attractor and the time series of the x-coordinate of the Poincaré section of the chaotic attractor are given in Fig. 6.8 and 6.9 as given by Rajasekar and Lakshmana (1993). They demonstrated the applicability of various control algorithms in this model. In what follows we compare the results of the novel control of chaos technique with the results given by them.

To incorporate the novel control of chaos technique in the dynamics of the BVP oscillator, we modify the above Eq. 6.4 governing the dynamics with periodic membrane A_1, introducing a constant bias A_o in addition to the periodic

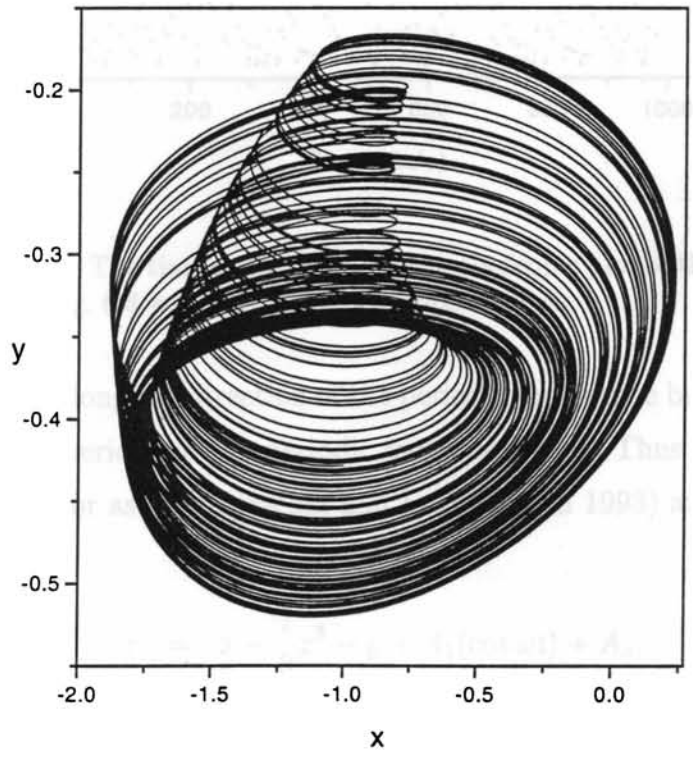

Figure 6.8: The phase portrait of a chaotic attractor of the BVP oscillator for $a = 0.7, b = 0.8, c = 0.1, A_1 = 0.74$ and $\omega = 1$, initial conditions $x = -0.3$ and $y = 0$ (Rajasekar and Lakshmanan 1992, 1993).

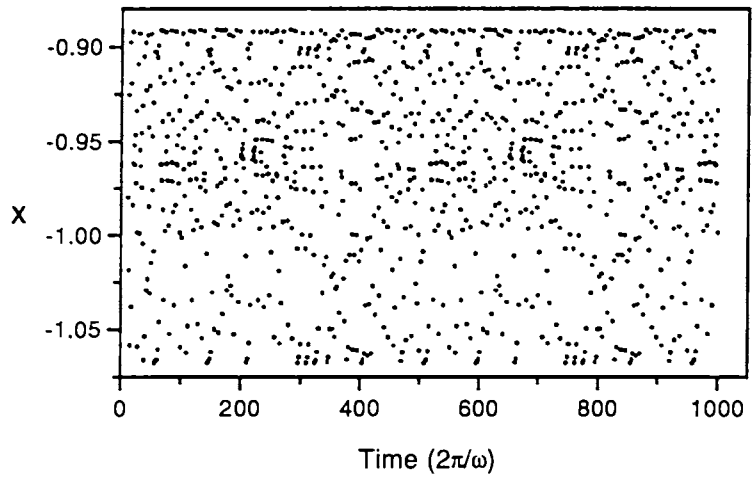

Figure 6.9: The time series of x of the stroboscopic plot of the attractor shown in Fig. 6.8 with stroboscopic period = $2\pi/\omega$.

membrane bias along the direction of the periodic membrane bias for one period at the end of n periods of the periodic membrane bias. Thus the equations of the BVP oscillator as in (Rajasekar and Lakshmanan 1993) are given by

$$\begin{aligned} \dot{x} &= x - \frac{1}{3}x^3 - y + A_1(\cos\omega t) + A_o \\ \dot{y} &= c(x + a - by) \end{aligned} \tag{6.5}$$

where A_o is the magnitude of the constant membrane bias. The set of equations given in Eqs. 6.5 is exactly same as the equation given in Rajasekar and Lakshmanan (1993) with the modification that the Eqs. 6.5 evolve as follows. The system is allowed to evolve according to the system of Eqs. 6.4 upto the $(n-1)^{\text{th}}$ period and evolve according to the system of Eqs. 6.5 at the n^{th} period. This process is repeated every n^{th} period. While solving the Eqs. 6.5, this idea can be implemented by setting $A_o = 0$ if $j \not\equiv 0 \bmod(n)$ and $A_o \neq 0$ if $j \equiv 0 \bmod(n)$ where j represents iteration number. In almost all cases the system is stabilized to a periodic orbit with period n if the control is applied

throughout the n^{th} period. In some cases the system is stabilized to a periodic orbit of period equal to an integral multiple of n. One of the advantages of control through this method is the possibility of fixing the length of the period required whereas in other methods the system itself will control the length of the period. For example, the system could be controlled to the predetermined periods of period-5, period-4 and period-3 orbits by applying a constant bias as can be seen from Figs. 6.10. This is implemented by setting $A_o = 0$ if $j \not\equiv 0$ mod(n) and $A_o \neq 0$ if $j \equiv 0$ mod(n) where j represents iteration number. For a small constant force of magnitude $A_o = 0.02$ compared to the value $A_1 = 0.74$, the system could be controlled to a periodic solution. As explained in the problem of controlling the chaotic rheological parameters, one important advantage of the control algorithm outlined in this work is the possibility of switching over to different specified periodic solutions during a given run. Another advantage is that once the control is applied the system stabilises rapidly to the appropriate periodic orbit as can be seen from the Figs. 6.10. A table of results obtained with the novel control technique is given in Table. 6.4.

The effect of periodic parametric perturbation on the chaotic dynamics of the BVP oscillator is studied extensively by Rajasekar and Lakshmanan (1993). As given by them, the BVP equations with periodic parametric perturbation can be expressed as

$$\begin{aligned} \dot{x} &= x - \frac{1}{3}x^3 - y + A_1(\cos\omega t) \\ \dot{y} &= c(1 + \eta\cos\omega_1 t)(x + a - by) \end{aligned} \tag{6.6}$$

where η is the magnitude and ω_1 is the frequency of the perturbation. We reproduced their results. On comparison of the results obtained in this method with that by the new algorithm, it is clear that the new method shows some advantages. With the new method, the system can be controlled to almost all periods of different lengths as can be seen from Table. 6.4. Rajasekar and Lakshmanan (1993) showed that regular motions may occur only for some ranges

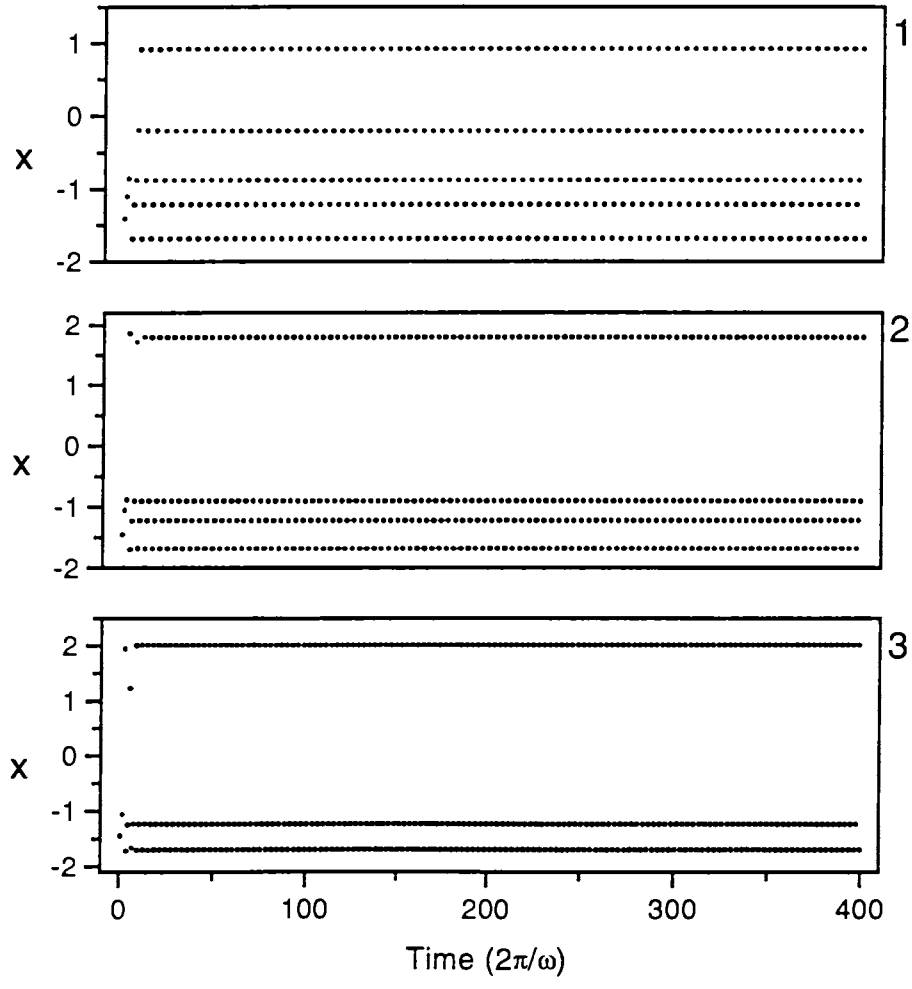

Figure 6.10: The stroboscopic plot of the controlled orbits of the BVP oscillator shown in Fig. 6.9 with stroboscopic period $= 2\pi/\omega$, where $a = 0.7, b = 0.8, c = 0.1, A_1 = 0.74$, $\omega = 1$ and initial conditions $x = -0.3$ and $y = 0$, (1) showing 5-period orbits when $A_o = 0.03$ and $n = 1$ (2) showing 4-period orbits when $A_o = 0.04$ and $n = 4$ (3) showing 3-period orbits when $A_o = 0.05$ and $n = 3$.

	n									
A_o	1	2	3	4	5	6	7	8	9	10
0.02					10					20
0.03	5				10	6				10
0.04	4		12	4	10	6				10
0.05	4	4		4	10	6	35	8		10
0.06	4	4		4	10	6		8		10
0.07	4	4	15	4	10	6		8		10
0.08	4	4	9	4	10	6		8		10
0.09	4	4	15	4	10	6		8		10
0.10	4	4		4	10	6		8		10
0.20	4	4	9	4	10	6	14	8		10
0.30	4	4	9	4		6	14	8	9	10
0.40	4	4	9	4	5	6	7	8	9	10
0.50	4	4	3	4	5	6	7	8	9	10
1.00	25	2	3	4	5	6	7	8	9	10

Table 6.4: A two way tabulation of controlled periods of the BVP oscillator obtained with the novel control technique for different values of A_o and different values of n, where $a = 0.7, b = 0.8, c = 0.1, A_1 = 0.74$, $\omega = 1$, initial conditions $x = -0.3, y = 0.0$

of magnitude (η) and frequency (ω_1) of the perturbation and the period of the controlled orbit depends on the applied values of η and ω_1. With the new control algorithm it is possible to pretarget the length of the period after control, whereas this appears to be very difficult with the method of periodic parametric perturbation. Another important aspect of the new algorithm which may be difficult to obtain with the periodic parametric perturbation method is the possibility of switching behaviour between different periods and the possibility of stabilizing high period solutions. The amount of constant force required in the new method is also comparatively less than the amount of perturbation required in the the periodic parametric perturbation method.

The effect of second periodic force is also considered for controlling the BVP oscillator with a second periodic force is given in (Rajasekar and Lakshmanan

1993) as

$$\begin{aligned} \dot{x} &= x - \frac{1}{3}x^3 - y + A_1(\cos\omega t) + \eta\cos\omega_1 t \\ \dot{y} &= c(x + a - by) \end{aligned} \tag{6.7}$$

where η is the magnitude of the additional weak periodic force of frequency ω_1. In this method we varied η and ω_1 and reproduced their results. The advantages found in the stabilization of chaotic behaviour with the new control algorithm presented in this chapter over the method of addition of second weak periodic force are evident in this system also.

6.4 The dynamics of periodically forced spheroids

In this section we demonstrate that control of the chaotic dynamics of periodically forced spheroids by the novel control technique which needs little information about the system and is easy to implement is also possible. Utilizing the flexibility of controlling chaotic dynamics in a orbit, there is the possibility of many applications such as the development of computer controlled intelligent rheology.

The modifications to incorporate the idea of the new control of chaos algorithm presented in earlier sections of this chapter in the dynamics of periodically forced spheroids of finite aspect ratio in simple shear flow are given in section 5.2. The modified equations given in section 5.2 are

$$\begin{aligned} \frac{d\theta}{dt} &= \frac{P}{2}\sin 2\theta\sin 2\phi + R\left[(\cos\theta\cos\phi\ k_1 + \cos\theta\sin\phi\ k_2 - \sin\theta\ k_3)\cos(\omega t)\right] \\ &\quad + R\left[(\cos\theta\cos\phi\ k_1' + \cos\theta\sin\phi\ k_2' - \sin\theta\ k_3')\right] \\ \frac{d\phi}{dt} &= P\cos 2\phi - Q \\ &\quad + \frac{R}{\sin\theta}\left[(-\sin\phi\ k_1 + \cos\phi\ k_2)\cos(\omega t) + (-\sin\phi\ k_1' + \cos\phi\ k_2')\right] \end{aligned} \tag{6.8}$$

The expressions of P, Q and R are given in section 2.7 as function of r_e. The maximum scaled value of ω is taken as $\omega = J = 2\pi(r_e + r_e^{-1})$ as given in section 2.8 Note that the system of equations 6.8 reduces to the system of equations 6.2 by carrying out the scaling as given in (Ramamohan *et al.* 1994) in the limiting case of r_e tends to infinity. The details of the method of solution of equations 6.8 are given in Chapter 5. The scheme of implementing the method of the new control strategy is also explained in section 5.2.

While solving Eqs. 6.8, the new idea of control can be implemented by setting $k_1' = k_2' = k_3' = 0$ if $j \not\equiv 0 \bmod(n)$ and $k_1' = k_3' = 0$ and $k_2' \neq 0$ if $j \equiv 0 \bmod(n)$ where j represents iteration number. In this calculations we kept $k_1 = k_3 = 0$. In almost all cases the system is stabilized to a periodic orbit with period n if the control is applied throughout the n^{th} period, as obtained in the other two models explained earlier. In some cases the system is stabilized to a periodic orbit of period equal to an integral multiple of n. As discussed in the section 6.1 the system evolves without any modification if we set $k_1' = k_2' = k_3' = 0$.

In section 5.3 we have demonstrated that controlling the chaotic dynamics of periodically forced particles by the new control technique can lead to the possibility of better separation than otherwise possible. An example of the importance of chaos control is the possibility of novel techniques to separate particles having the same size but different shapes much more efficiently than was demonstrated in section 5.3 by controlling the chaotic dynamics of such systems.

The chaotic attractor and the time series of u_2 of the Poincaré section (stroboscopic plot) of the chaotic attractor computed from Eq. 2.21 for r_e=1.6 are given in Figs. 6.11 and 6.12. It is demonstrated in chapter 5 that the system can be controlled to periodic behaviour of any desired period. For example, the system could be controlled to period-3, period-4, period-5 and period-6 orbits by applying a constant force as can be seen from Figs. 6.13. This is obtained

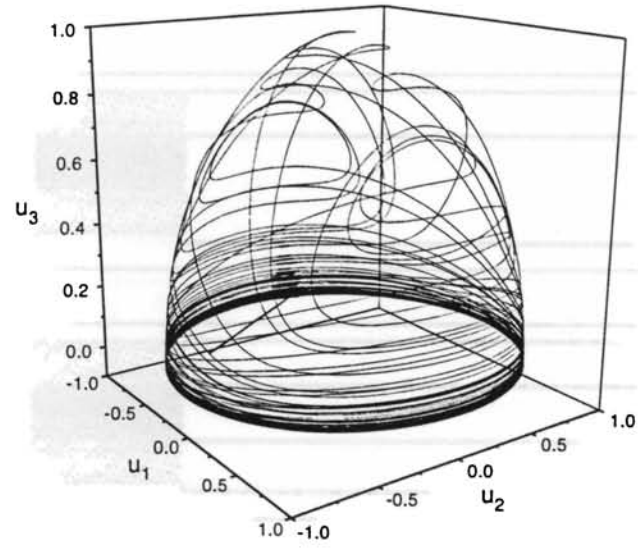

Figure 6.11: The chaotic attractor (trajectory plot) of the dynamics of the particle for $k_2 = 12$, initial conditions $\theta = \phi = 45°$, $\omega = J = 2\pi(r_e + r_e^{-1})$, $r_e = 1.6$.

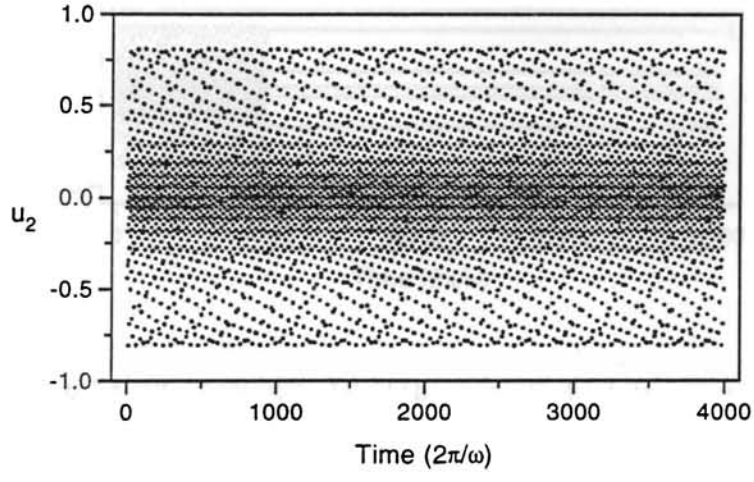

Figure 6.12: Trajectory plot of u_2 vs. time at every intersection of the trajectory shown in 6.11 with the Poincaré plane of the corresponding attractor, where stroboscopic period is $2\pi/\omega$.

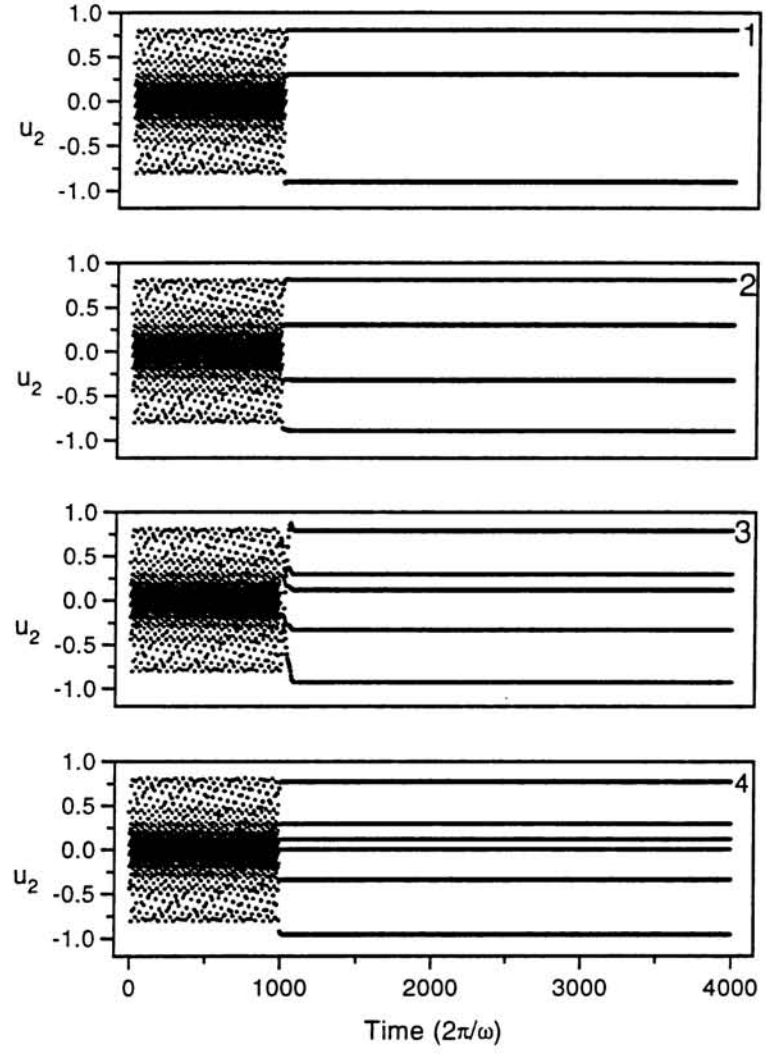

Figure 6.13: Stroboscopic plot of the controlled orbits with period $2\pi/\omega$ for $k_2 = 12$, initial conditions $\theta = \phi = 45°$, $\omega = J = 2\pi(r_e + r_e^{-1})$, $r_e = 1.6$. (1). showing 3-period orbits when $k_2' = 4.0$ and $n = 3$ (2). showing 4-period orbits when $k_2' = 3.0$ and $n = 4$ (3). showing 5-period orbits when $k_2' = 2.5$ and $n = 5$ (4). showing 6-period orbits when $k_2' = 1.0$ and $n = 6$.

	n									
k_2'	1	2	3	4	5	6	7	8	9	10
1.0						42	7			
1.5						66	7			
2.0		22		12		6	7			
2.5				16	5	6	7			
3.0			9	4	5	6	7			
3.5				4	5	6	7		18	
4.0			3	4	5	6	7			10
4.5		12	3	4	5	6	7	24		10
5.0	2	2	3	4	5	6	7	8	9	10

Table 6.5: A two way tabulation of controlled periods of the dynamics of periodically forced spheroids obtained with the novel control technique for different values of k_2' and different values of n, where $k_2 = 12.0$, $k_1 = k_3 = 0, r_e = 1.6, \omega = J = 2\pi(r_e + r_e^{-1}), \theta = \phi = 45°$.

by setting $k_1' = k_2' = k_3' = 0$ if $j \not\equiv 0$ mod(n) and $k_1' = k_3' = 0$, $k_2' \neq 0.0$ if $j \equiv 0$ mod(n) in the evolution of Eqs. 6.8 when the system is to be stabilized in a period-n orbit. In all cases the control was applied after 1000 periods. It is also demonstrated that periodic behaviour of different periods can be obtained by applying the same constant force as can be seen from Figs. 5.5. A list of the periodic orbits obtained is listed in the Table. 6.5. It is also possible to stabilize a given chaotic system to different n-period orbits by suitably changing the control parameter k_2'. As an example, the time series of the Poincaré Section corresponding to two 3-period solutions embedded in a chaotic system is given in Fig. 6.14. It is also noticed that once control is applied the system stabilizes rapidly to the appropriate periodic orbit as can be seen from Fig. 6.13 and 6.14.

The possibility of switching over to different periodic solutions during a given run is another important advantage of the novel control algorithm. This switching behaviour may have technological importance. An example showing switching behavior is given in Fig. 6.15. The observations made in this work suggest the possibility of separating particles more efficiently based on control

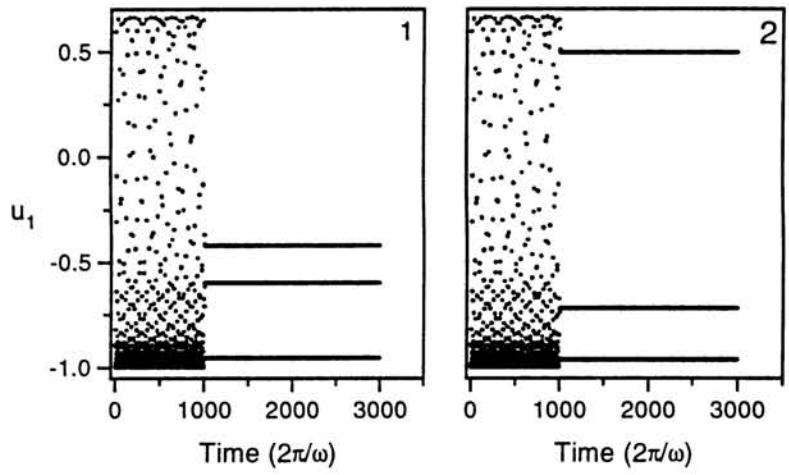

Figure 6.14: Stroboscopic plot with different controls showing two different period-3 orbits obtained for $k_2 = 12$ initial conditions $\theta = \phi = 45°$, $\omega = J = 2\pi(r_e + r_e^{-1})$, $r_e = 1.6$ with control (1). $k_2' = 4$, $n = 3$ (2). $k_2' = 4.5$, $n = 3$.

of chaotic dynamics as explained in section 5.3. Thus, even in the rather simple application suggested in section 5.3 the new control of chaos algorithm leads to greater efficiency than otherwise possible.

We also attempted to control the dynamics of periodically forced spheroids of finite aspect ratio with the other two methods, namely, periodic parametric perturbation and addition of a second weak periodic force for comparing the feasibility of the new control algorithm. The modifications made to implement the other methods of control in a model of the dynamics of periodically forced spheroids is exactly the same as in the other two models given in sections 6.2 and 6.3.

To study the effect of periodic parametric perturbation and the effect of addition of a second weak periodic force on the chaotic motion of the dynamics of periodically forced spheroids we modified the given equations 2.21 as given below. With a periodic parametric perturbation of k_2, the modified equations are exactly same as the equations 2.21 with the change that k_2 is replaced

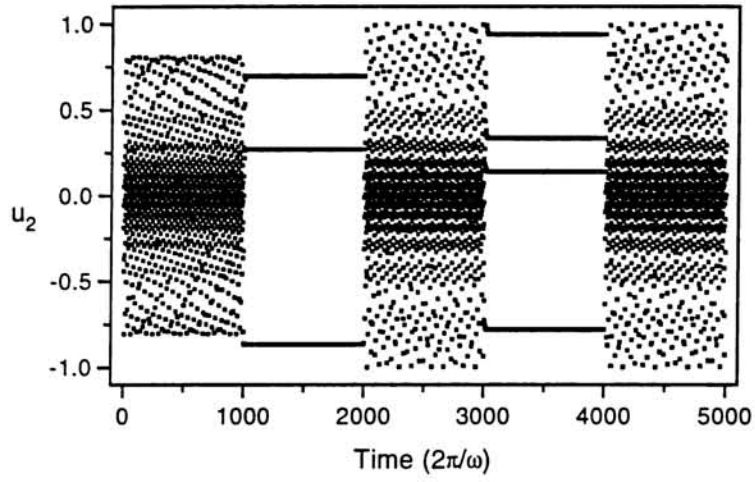

Figure 6.15: Stroboscopic plot showing period-3 and period-4 orbits successively obtained with control applied at every third and fourth periods respectively for $k_2 = 12$, initial conditions $\theta = \phi = 45°$, $\omega = J = 2\pi(r_e + r_e^{-1})$, $r_e = 1.6$ with $k_2' = 4.5$ and $k_2' = 3.5$ respectively.

by $k_2(1 + \eta\cos(\omega_1 t)$, where η is the amplitude and ω_1 is the frequency of the periodic parametric perturbation. The system was analysed for control by using different values of η and ω_1. Similarly the equations for the dynamics of periodically forced spheroids with the addition of a second weak periodic force are obtained by replacing $k_2\cos(\omega t)$ in 2.21 by $k_2\cos(\omega t) + k_2'\cos(\omega_1 t)$. This system was analysed for the values of k_2' ranging between 1% to 10% of the value of k_2. In both methods, the values of ω_1 were selected as 0.2J, 0.25J, 0.4J, 0.5J, 0.6J, 0.75J, 0.8J and 1J, where $J = 2\pi(r_e + r_e^{-1})$. We also kept $k_1 = k_3 = 0$ in both methods.

In this model also, as in the other two models considered earlier, the new control algorithm was found to be advantageous compared to the other two methods. A sample of the results obtained from three methods of control are given in Tables. 6.5, 6.6 and 6.7. As can be seen from Tables. 6.5, it is possible to force the system to oscillate in a required period by applying

	ω_1							
η	0.2J	0.25J	0.4J	0.5J	0.6J	0.75J	0.8J	1J
0.05		48						
0.10	5				35	28	35	
0.15	5	4	25	26				
0.20	5	4	45	6		84	65	
0.25	5	4	5	22				
0.30	5	4						5

Table 6.6: A two way tabulation of controlled periods of the dynamics of periodically forced spheroids obtained with the control technique of periodic parametric perturbation method for different values of η and different values of ω_1, where $k_2 = 12.0$. $k_1 = k_3 = 0, r_e = 1.6, \omega = J = 2\pi(r_e + r_e^{-1}), \theta = \phi = 45°$

the new control of chaos algorithm. We have demonstrated the possibility of periodic orbits of length equal to 1 to 10 times the fundamental period, $2\pi/\omega$. At the same time only periodic orbits of length equal to multiples of the fundamental period are obtained in the other two methods in which most periods are of two digit multiples of the fundamental period. With the methods of periodic parametric perturbation and addition of second weak periodic force, only orbits of period 1, 4, 5 and 6 times (considering only single digit multiples) the fundamental period are obtained as can be seen from the Tables. 6.6 and 6.7. Thus for stabilizing a periodic orbit of period equal to a single digit multiple of the fundamental period, the novel control of chaos algorithm is advantageous compared to the other two methods. Switching between two different multiples of the fundamental period is possible with the new control algorithm, whereas this appears to be very difficult with the other two methods.

The new control of chaos method proposed in this work is comparatively easy to implement and needs almost no information about the system. We have demonstrated some advantages of the novel technique over two well-known algorithms such as control by periodic parametric perturbation and control by

	ω_1							
k_2'	0.2J	0.25J	0.4J	0.5J	0.6J	0.75J	0.8J	1J
0.12								17
0.24								
0.36							20	
0.48					35		25	
0.60		28	35	14	55	32		1
0.72	35	28	90				5	1
0.84							5	1
0.96							5	1
1.08					25		5	1
1.20			45			4	5	1

Table 6.7: A two way tabulation of controlled periods of the dynamics of periodically forced spheroids obtained with the control technique of addition of second periodic force for different values of η and different values of ω_1, where $k_2 = 12.0$, $k_1 = k_3 = 0, r_e = 1.6, \omega = J = 2\pi(r_e + r_e^{-1}), \theta = \phi = 45°$

addition of a second periodic force. We have successfully implemented the new algorithm in a rather difficult problem such as the control of the dynamics and rheology of periodically forced suspensions of slender rods in simple shear flow. One of the interesting results noted is the possibility to stabilize periodic orbits of period appreciably greater than by the Ott *et al.* method (Ott *et al.* 1990). We have also implemented the algorithm and controlled chaos successfully in an interesting dynamical system, namely, the Bonhoeffer-Van der Pol (BVP) oscillator (Rajasekar and Lakshmanan 1992). We have compared the new technique with two other techniques for two dynamical systems and found some advantages of the new technique over them. The dynamics of periodically forced spheroids of different aspect ratios in simple shear flow has also been controlled successfully and we have suggested a possible application. Based on the results outlined in this work, it is felt that the new control of chaos technique may exhibit some advantages over many other control of chaos techniques. The

method may also successfully and perhaps, profitably, be applied to problems other than the ones considered in Chapter 5. We hope that these preliminary results will excite experimental interest also in this control of chaos technique.

Chapter 7

Conclusions and Future Work

7.1 Conclusions

We have numerically analyzed a fluid dynamic system, namely, the dynamics of a periodically forced spheroid in simple shear flow. This system is physically realizable and technologically important. During the computations we observed several practically and fundamentally important phenomena like strong dependence of the results on aspect ratio, a new Class I intermittency, *etc.* We have also proposed a new control algorithm. We have analyzed the results of our computations in detail and projected the aspect ratio dependence as a potential tool to segregate particles of a given shape from a suspension of particles having different shapes but similar sizes. We also have observed that the approach used by Strand(1989) for the strong Brownian limit is inappropriate in the chaotic regimes corresponding to the weak Brownian limit. Our results indicate a strong dependence of the solutions obtained on the aspect ratio of the spheroids. This strong dependence on the aspect ratio can be utilized to separate particles from a suspension of particles having different shapes but similar sizes.

In addition to the technological interest in the problem we have reported certain aspects of the problem that are of interest to the nonlinear dynamics community also. In this work we have reported a physically realizable system

in which the possibility of an interesting and novel type of Class I intermittency has been demonstrated, namely it is an example of one of the very few physically realizable chaotic systems showing the phenomenon of a non hysteretic form of Class I intermittency with nearly regular reinjection period. Price and Mullin (1991) have observed experimentally a similar type of phenomenon in which a hysteretic form of intermittency with extreme regularity of the bursting is observed. The system described in this work appears to be one of the very few ODE systems describing a physically realizable system showing a non hysteretic form of Class I intermittency with nearly regular reinjection period. The regularity of the bursting is unaffected by variation in the control parameter. The maximum Lyapunov exponents of the bursts and laminar phase are estimated separately and indicate existence of chaos. The length of the laminar phase shows scaling behaviour typical of Class I intermittency near the tangent bifurcation and also shows new scaling behaviour. Return maps of the dynamical system are presented to explain the behaviour observed. The system also demonstrates some interesting features such as new scaling behaviour away from the onset of intermittency and the number of the bursts during a particular realization varying smoothly with the control parameter. The results are presented in terms of the evolution of the orientation of a spheroid subjected to an external periodic force immersed in a simple shear flow.

We also have demonstrated that controlling the chaotic dynamics of periodically forced particles by a suitably engineered novel control technique which needs little information about the system and easy to implement leads to the possibility of better separation than otherwise possible. In this work we have demonstrated that controlling the chaotic dynamics of periodically forced particles leads to the possibility of better separation. Utilizing the flexibility of controlling chaotic dynamics in a desired orbit irrespective of initial state, it is demonstrated that it is theoretically possible to separate particles much more

efficiently than otherwise possible from a suspension of particles having different shapes but similar sizes especially for particles of aspect ratio $r_e > 1.0$. The strong dependence of the controlled orbit on the aspect ratio of the particles demonstrated in this work may have many applications such as the development of computer controlled intelligent rheology. The results of this work also suggest that control of chaos in this problem may have many applications.

We have proposed a novel algorithm based on parametric perturbation for control of chaos in this work. The method proposed is comparatively easy to implement and needs almost no information about the system. One of the main advantages of this control algorithm is the possibility of pre-targeting the length of the controlled period obtained by suitably engineering the control technique. In addition we demonstrate certain advantages of this novel technique over two well-known algorithms, namely control by periodic parametric perturbation and control by addition of a second weak periodic force, such as the possibility of switching behaviour, pre-targeting the period, stabilizing high period orbits *etc.* We have also demonstrated the applicability of the technique in certain numerical models of physical systems. We have demonstrated the successful application of the new algorithm in a rather difficult problem, namely, the control of the dynamics and the rheological parameters of periodically forced suspensions of slender rods in simple shear flow and also in the Bonhoeffer-Van der Pol (BVP) oscillator.

7.2 Future work

It has been demonstrated that the dynamics of periodically forced spheroids can have complex chaotic behaviour. Since the above problem is virtually unexplored in the chaos literature and since within a period of nearly four years we have found a wealth of interesting results with technological potential, it is desirable to continue the work with more realistic assumptions such as

inclusion of Brownian motion, interaction of particles *etc.* In this work we have considered only one component of the external force *i. e.* k_2. The problem can be analyzed for new properties and behaviour by considering the other two components of the force, namely, k_1 and k_3 or combinations of these parameters. It is also desirable to study the effect of change in the frequency of the external force.

The present analysis is based on certain assumptions. We have considered the dynamics of dilute suspensions of spheroids of finite aspect ratio in simple shear flow under the action of a periodically induced external force, where Brownian motion is weak. There are some fundamental questions raised by our problem such as how does one include the effects of Brownian motion in the chaotic case? We have identified some errors in the approach of Strand(1989). What is the alternative technique to solve such problems? The problem can further be analyzed by changing or manipulating the assumptions made in the model given in this thesis. The underlying flow is another important factor that matters. It is possible to develop a theory for another classic cases of linear flows, namely, uniaxial extensional flow. The dynamics of interacting particles under certain conditions is another important problem in the field of non-linear dynamics which could be considered in future work.

Nomenclature

a	=	polar radius
b	=	equatorial radius
$\boldsymbol{i}_x, \boldsymbol{i}_y, \boldsymbol{i}_z$	=	The unit vectors in x, y and z directions
J	=	$2\pi(r_e + {r_e}^{-1})$
$\boldsymbol{k}$	=	The periodic force field
$\boldsymbol{k}'$	=	The constant force field
${}^{c}\hat{\mathsf{K}}$	=	The intrinsic properties of the particle, which depend upon the geometric configuration of its wetted surface
${}^{r}\hat{\mathsf{K}}, \hat{\tau}$	=	The intrinsic properties of the particle, which depend upon the geometric configuration of its wetted surface
l_1	=	Total number of particles in the grid on the average
l_2	=	Total number of occurrences of the grid
$\boldsymbol{L}$	=	The torque about the centre of the particle exerted by the fluid on the particle
n	=	The period of at which the control is active
m	=	The obtained period of the control
r_e	=	The particle aspect ratio given by $r_e = a/b$
S	=	The rate of deformation tensor given by $\mathsf{S} = \frac{1}{2}\left[\nabla \boldsymbol{V} + \nabla \boldsymbol{V}^{\mathrm{T}}\right]$
$\boldsymbol{u}$	=	The unit vector along the axis of symmetry which determines the orientation of the spheroids with components u_1, u_2, u_3
$\boldsymbol{U}$	=	The translational velocity
$\boldsymbol{U} - \boldsymbol{V}$	=	The translational slip velocity
y	=	The y coordinate
$\dot{\gamma}$	=	The shear rate
μ_o(or η_s)	=	The viscosity of the fluid
θ, ϕ	=	The polar angle and the azimuthal angle corresponding to a given vector $\boldsymbol{u}$ respectively
$\dot{\theta}$	=	The time derivative of θ
$\dot{\phi}$	=	The time derivative of ϕ

ω	=	The frequency of the driving force
$\mathbf{\Omega}$	=	The angular velocity of the particle
$\mathbf{\Omega} - \boldsymbol{\omega}$	=	The rotational slip velocity
∇	=	The del operator
P_e	=	The Peclet number
R_e	=	The Reynolds number
D_r	=	Rotary diffusivity
V_p	=	The volume of the spheroid
δij	=	The Kronocker delta function
ϵijk	=	The permutation symbol
$\mathbf{G}$	=	The velocity gradient tensor
$\mathbf{S}$	=	The rate of shear tensor
$\boldsymbol{\omega}$	=	The vorticity tensor

Program Listing[1]

The source code (Fortran) for finding the orbit and the stroboscopic plot is given below for the dynamics of periodically forced particles. We do not include the program used for control of chaos since the following program can easily be modified for the same purpose.

```
external derivs
external rkqc
external rk4
character*2 i01
dimension y(2)
common /area1/w1,ak1,ak2,ak3,v,re
common /path/kmax,kount,dxsav,xp(200),yp(2,200)
open(unit=7,file="traj.dat")
open(unit=8,file="poin.dat")
v=0.5
pi=3.141592653589793
re=1.6
ak1 =0.0
ak2 =12.44
ak3 =0.0
thint=20.0
phint=20.0
w1=2.0*pi*(re+1.0/re)
akc=1
x1=0.0
pi2=pi/2.0
thint=2.0*pi*thint/360.0
phint=2.0*pi*phint/360.0
y(1)=thint
y(2)=phint
nvar=2
eps =0.000001
kmax=2
h1=2.0*pi/w1/100.0
```

[1]Subroutine odeint is adapted from Press *et al.* (1986)

```
        dx2=h1
        dxsav=dx2/20.0
        x2=x1+dx2
        hmin=h1/200000.0
        do 1 j=1,505000
        i01="OK"
        call odeint(i01,y,nvar,x1,x2,eps,h1,hmin,nok,nbad)
        q1=sin(y(1))*cos(y(2))
        q2=sin(y(1))*sin(y(2))
        q3=cos(y(1))
        qmod=q1*q1+q2*q2+q3*q3
        i1=1
        if(q1.lt.0.0) i1=-1
        arg1=i1*sqrt((q1*q1+q2*q2))/q3
        y(1)=atan(arg1)
        y(2)=atan(q2/q1)
        if(j.ge.5001) write(7,101)float(j)/100,q1,q2,q3,qmod
100     format(i7,4(x,f9.5),A5)
101     format(f10.3,x,4(x,f9.5))
        x1=x2
        x2=x2+dx2
        if(mod(j,100).eq.0) then
        x1=0.0
        x2=x1+dx2
        if(j.ge.5001) write(8,101)float(j)/100,q1,q2,q3,qmod
        endif
1       continue
        close(7)
        close(8)
        stop
        end
        subroutine derivs(x,y,yprime)

c       user defined routine called  by ode integrator

        dimension y(2),yprime(2)
        common /area1/w1,ak1,ak2,ak3,v,re

c       simple sheal flow
c       spheroids for any value of re

        pi=3.141592653589793
```

```
      if(re.lt.1.0) go to 5
      sq2 = re*re-1.0
      beta=(alog(re + sqrt( sq2 ))) / (re*sqrt( sq2 ))
      go to 6
5     beta=(acos(re))/(re*sqrt(1.0-re*re))
6     continue
      cc =2.0*re*re-1.0
      aaa=pi*(re*re-1.0)/re
      bbb=pi*(re*re+1.0)/re
      ccc=(3.0*re*re*re*(cc*beta - 1.0))/(8.0*(re*re-1.0))
      d1=cos(x*w1)
      a1=cos(y(1))*cos(y(2))*ak1+
     !    cos(y(1))*sin(y(2))*ak2-sin(y(1))*ak3
      a2=(cos(y(2))*ak2-sin(y(2))*ak1)/sin(y(1))
      yprime(1)=0.5*aaa*sin(2.0*y(1))*sin(2.0*y(2)) + ccc*a1*d1
      yprime(2)=aaa*( cos(2.0*y(2)) ) - bbb + ccc*a2*d1
      return
      end

      subroutine odeint(i01,ystart,nvar,x1,x2,eps,h1,hmin,
     ! nok,nbad)
c     runge kutta driver with adaptive stepsize control.
c     Integrate the nvar starting values ystart from x1
c     to x2 with accuracy eps, storing intermediate results
c     in the common block /path/ h1 should be set as a guessed
c     first stepsize. hmin as the minimum allowed stepsize
c     (can be zero). On output nok and nbad are the number
c     of good and bad (but retried and fixed) steps taken,
c     and ystart is replaced by values at the end of the
c     integration interval. derivs is the user supplied
c     subroutine while rkqc is the name of the stepper routine
c     to be used. path contains its own information about
c     how often an intermediate value is to be stored.
      external derivs
      external rkqc
      character*2 i01
      parameter (maxstp=1000000,nmax=2,two=2.0,zero=0.0,
     ! tiny=1.e-30)
      common /path/kmax,kount,dxsav,xp(200),yp(2,200)
      common /area1/w1,ak1,ak2,ak3,v,re

c     user storage for intermediate results. Preset
```

```
c       dxsav and kmax

        dimension ystart(nvar),yscal(nmax),y(nmax),dydx(nmax)
        x=x1
        h=sign(h1,x2-x1)
        nok=0
        nbad=0
        kount=0
        do 11 i=1,nvar
        y(i)=ystart(i)
11      continue
        if(kmax.gt.0) xsav=x-dxsav*two

c       assures storage of first step

        do 16 nstp=1,maxstp

c       take at most maxstp steps

        call derivs(x,y,dydx)
        do 12 i=1,nvar

c       scaling used to monitor accuracy. This general purpose
c       choice can be modified if need be

        yscal(i)=abs(y(i))+abs(h*dydx(i))+tiny
12      continue
        if(kmax.gt.0) then
        if(abs(x-xsav).gt.abs(dxsav)) then
        if(kount.lt.kmax-1) then
        kount=kount+1
        xp(kount)=x
        do 13 i=1,nvar
        yp(i,kount)=y(i)
13      continue
        xsav=x
        endif
        endif
        endif
        if((x+h-x2)*(x+h-x1).gt.zero) h=x2-x

c       if step can overshoot end, cut down stepsize
```

```
        call rkqc(i01,y,dydx,nvar,x,h,eps,yscal,hdid,hnext)
        if(hdid.eq.h) then
        nok=nok+1
        else
        nbad=nbad+1
        endif
        if((x-x2)*(x2-x1).ge.zero) then

c       are we done?

        do 14 i=1,nvar
        ystart(i)=y(i)
14      continue
        if(kmax.ne.0) then
        kount=kount+1

c       save final step

        xp(kount)=x
        do 15 i=1,nvar
        yp(i,kount)=y(i)
15      continue
        endif
        return

c       normal exit

        endif
        if(abs(hnext).lt.hmin) i01="N1"
        h=hnext
16      continue
        i01="N2"
        return
        end

        subroutine rkqc(i01,y,dydx,n,x,htry,eps,yscal,hdid,hnext)

c       fifth order runge-kutta step with monitoring of local
c       truncation error to ensure accuracy and adjust stepsize.
c       Input are the dependent variable vector y of length n and
c       its derivative dydx at the starting value of the
```

```
c       independent variable x. Also input are the stepsize to be
c       attempted htry, the required accuracy eps, and the vector
c       yscal against which the error is scaled. On output, y and
c       x are replaced by their new values, hdid is the stepsize
c       which was actually accomplished, and hnext is the estimated
c       next stepsize. derivs is the user supplied subroutine that
c       computes the right hand side derivatives.

        character*2 i01
        parameter (nmax=2,pgrow=-0.2,pshrink=-0.25,fcor=1.0/15.0,
     !  one=1.0,safety=0.9,errcon=6.e-04)

c       the value errcon equals (4/safety)**(1/pgrow), see use below

        external derivs
        common /area1/w1,ak1,ak2,ak3,v,re
        dimension y(n),dydx(n),yscal(n),ytemp(nmax),ysav(nmax),
     !  dysav(nmax)
        xsav=x

c       save initial values

        do 11 i=1,n
        ysav(i)=y(i)
        dysav(i)=dydx(i)
11      continue
        h=htry

c       set stepsize to the initial trial value

1       hh=0.5*h
        call rk4(ysav,dysav,n,xsav,hh,ytemp)
        x=xsav+hh
        call derivs(x,ytemp,dydx)
        call rk4(ytemp,dydx,n,x,hh,y)
        x=xsav+h
        if(x.eq.xsav) i01="NO"
        call rk4(ysav,dysav,n,xsav,h,ytemp)

c       take the large step

        errmax=0.0
```

```
c       evaluate accuracy

.       do 12 i=1,n
        ytemp(i)=y(i)-ytemp(i)
        errmax=max(errmax,abs(ytemp(i)/yscal(i)))
12      continue

c       ytemp now contains the error estimate

        errmax=errmax/eps
        if(errmax.gt.one) then
        h=safety*h*(errmax**pshrink)

c       truncation error too large, reduce stepsize

        go to 1
        else

c       step succeeded. compute size of next step

        hdid=h
        if(errmax.gt.errcon) then
        hnext=safety*h*(errmax**pgrow)
        else
        hnext=4.0*h
        endif
        endif
        do 13 i=1,n

c       mop up fifth order truncation error

        y(i)=y(i)+ytemp(i)*fcor
13      continue
        return
        end

        subroutine rk4(y,dydx,n,x,h,yout)

c       given values for n variables y and their derivatives
c       dydx known at x, use the fourth order runge kutta method
c       to advance the solution over an interval h and return
```

```
c       the incremented variables as yout, which need not be a
c       distinct array from y. The user supplies the
c       subroutine derivs(x,y,dydx) which returns derivatives
c       dydx at x.

        external derivs
        parameter(nmax=2)

c       set to the maximum number of functions

        common /area1/w1,ak1,ak2,ak3,v,re
        dimension y(n),dydx(n),yout(n),yt(nmax),dyt(nmax),
     !  dym(nmax)
        hh=0.5*h
        h6=h/6.0
        xh=x+hh
        do 11 i=1,n
        yt(i)=y(i)+hh*dydx(i)
11      continue
        call derivs(xh,yt,dyt)
        do 12 i=1,n
        yt(i)=y(i)+ hh*dyt(i)
12      continue
        call derivs(xh,yt,dym)
        do 13 i=1,n
        yt(i)=y(i)+h*dym(i)
        dym(i)=dym(i)+dyt(i)
13      continue
        call derivs(x+h,yt,dyt)
        do 14 i=1,n
        yout(i)=y(i)+h6*(dydx(i)+dyt(i)+2.0*dym(i))
14      continue
        return
        end
```

Appendix A

Phase Diagrams of types of attractors of the governing eqs.

In this work, numerical computations have been reported for various values of k_2 and r_e for $\omega = J$. Below we present a detailed investigation of the k_2 vs. r_e space for values of $0.5 \leq k_2 \leq 6.0$ in steps of 0.5 and r_e varying between 0 and 2 in steps of 0.2.

We ran the program for 2500 points of the Poincaré section (stroboscopic plot) and deleted the first 2250 points to remove the transients. All runs were started with the initial conditions $\theta = \phi = 45°$. We obtained similar results when ϕ was replaced by $-\phi$. As a test case when we ran the program for $\theta = 90°$ the trajectory plot reduced to a continuous curve, indicating regular behaviour for all the values of k_2 and r_e considered. At $k_2 = 0.03$ for $r_e = 1.6$, the attractor slowly begins to broaden from a continuous curve and the Lyapunov exponent first becomes positive. There are a number of regular regimes in between the chaotic regimes. In our system, chaos usually appears as a broadening of the attractor as can be seen from the example given in Fig. 3.1. In certain regimes as in Ramamohan *et al.*, (1994) the attractor broadens to such an extent that a subset of the phase space is completely filled.

	k_2											
r_e	0.5	1.0	1.5	2.0	2.5	3.0	3.5	4.0	4.5	5.0	5.5	6.0
0.2	1	1	1	1	1	1	1	1	1	1	1	1
0.4	1	1	1	1	1	1	1	1	1	1	1	1
0.6	1	1	1	1	1	1	1	1	1	1	1	1
0.8	1	1	1	1	1	1	1	1	1	1	1	1
1.2	1	1	1	1	1	1	4	1	1	1	1	1
1.4	1	1	1	1	1	1	1	1	4	5	1	1
1.6	1	1	1	1	1	1	1	1	1	2	1	1
1.8	1	1	1	1	1	1	1	1	1	2	3	3
2.0	1	1	1	1	1	1	1	1	2	2	3	3

Table A.1: A Phase diagram of k_2 vs. r_e for $\omega = J$, initial conditions $\theta = 30°, \phi = 45°$

For a comprehensive study of the chaotic behaviour of the system considered in this work we have analysed the problem for two different initial conditions. In both cases we varied the parameter r_e ranging from 0 to 2 in steps of 0.2 and k_2 ranging from 0 to 5 in steps of 0.5. We obtained different types of attractors for these ranges of the parameters and we have classified them into 6 types. These attractors are given in Fig. A.1 of this appendix. The corresponding phase diagrams in $k_2 - r_e$ space are given in Tables. A.1 and A.2.

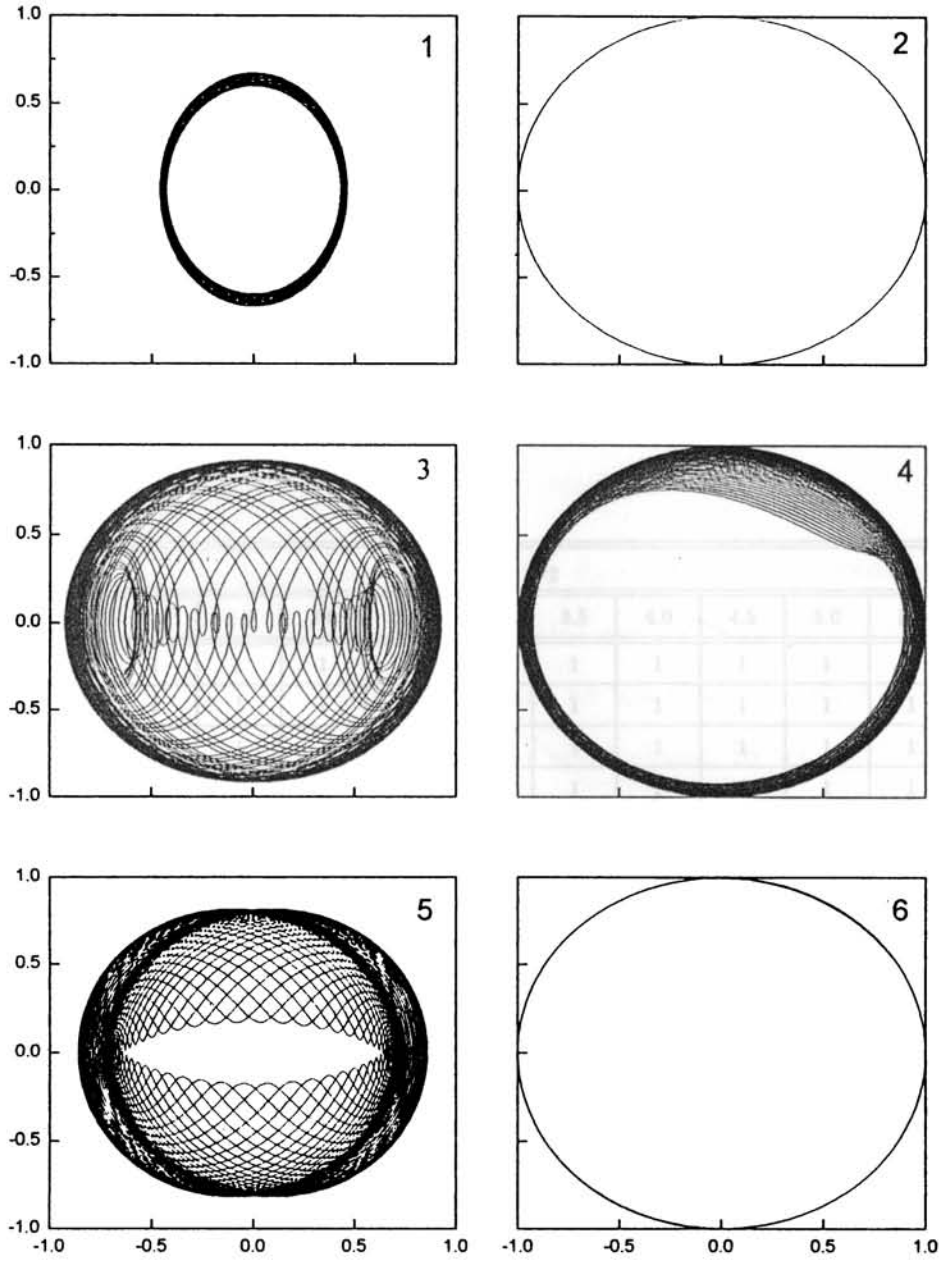

Figure A.1: Attractors of different types for different values of k_2: (1) $\theta = 30°, \phi = 45°, r_c = 0.6, k_2 = 4.0$ (2) $\theta = 30°, \phi = 45°, r_c = 1.8, k_2 = 5.0$ (a regular attractor with two fixed points in the Poincaré section) (3) $\theta = 30°, \phi = 45°, r_c = 1.8, k_2 = 6.0$ (4) $\theta = 30°, \phi = 45°, r_c = 1.4, k_2 = 4.5$ (5) $\theta = 30°, \phi = 45°, r_c = 1.4, k_2 = 5.0$ (6) $\theta = 75°, \phi = 30°, r_c = 2.0, k_2 = 6.0$ (a regular attractor with more than two fixed points in the Poincaré section)

	k_2											
r_e	0.5	1.0	1.5	2.0	2.5	3.0	3.5	4.0	4.5	5.0	5.5	6.0
0.2	1	1	1	1	1	1	1	1	1	1	1	1
0.4	1	1	1	1	1	1	1	1	1	1	1	1
0.6	1	1	1	1	1	1	1	1	1	1	1	1
0.8	1	1	1	1	1	1	1	1	1	1	1	1
1.2	1	1	1	1	1	1	2	1	1	1	1	1
1.4	1	1	1	1	1	1	1	1	2	2	1	1
1.6	1	1	1	1	1	1	1	1	1	2	2	1
1.8	1	1	1	1	1	1	1	1	1	2	1	1
2.0	1	1	1	1	1	1	1	1	2	2	1	6

Table A.2: A Phase diagram of k_2 vs. r_e for $\omega = J$, initial conditions $\theta = 75°, \phi = 30°$

Appendix B

Similarities and Differences with the thesis of K. Satheesh Kumar

In this thesis, we have reviewed chaotic dynamics and suspension rheology briefly. Since the problem considered in this work and the problem handled by K. Satheesh Kumar lie in these two areas, he has also reviewed these two areas briefly. In these reviews there are some similarities. In what follows we have included in this appendix the similarities and differences of this thesis with the thesis entitled *studies on the chaotic rheological parameters of periodically forced suspensions of weak Brownian slender bodies in simple shear flow* submitted to the Cochin University of Science and Technology by K. Satheesh Kumar (1997)[1]

The main thrust of this thesis is the demonstration of chaos and a study of its properties in a physically realizable fluid dynamic system. That is, the chaotic evolution of the orientations of individual particles of finite aspect ratio ranging from 0 to 2 is analysed in detail. Similarly, K. Satheesh Kumar has analyzed, in his thesis, the effect of evolution of the orientations of individual particles of infinite aspect ratio. In short, the dynamics of periodically forced particles of finite aspect ratio is analyzed in this thesis whereas K. Satheesh

[1]studies on the chaotic rheological parameters of periodically forced suspensions of weak Brownian slender bodies in simple shear flow, Kumar, KS (1997)

Kumar has studies the rheology of a suspension of long slender rods (of infinite aspect ratio).

The analysis of dynamics in this thesis is of dilute suspensions of periodically forced spheroids in the presence of weak or negligible Brownian motion in simple shear flow. K. Satheesh Kumar has considered slender rods instead of spheroids keeping the other assumptions on the suspensions the same. In fact there is no similarity in the main contributions of this thesis with that of K. Satheesh Kumar. To get overall idea of the differences and similarities we list out the features of this thesis which differ from that of K. Satheesh Kumar.

We have numerically analysed a fluid dynamic system, namely, the dynamics of periodically forced spheroids in simple shear flow. This system is physically realizable and technologically important. During the computations we observed several practically and fundamentally important phenomena like strong dependence of the results on aspect ratio, a new Class I intermittency, *etc.* We have also proposed a new control algorithm.

The main contributions of this thesis can be summarised as follows. Firstly, we have analysed the results of our computations in detail and projected the aspect ratio dependence as a potential tool to segregate particles of a given shape from a suspension of particles having different shapes but similar sizes. We also have observed that the approach used by Strand(1989) for the strong Brownian limit is inappropriate in the chaotic regimes corresponding to the weak Brownian limit. Our results indicate a strong dependence of the solutions obtained on the aspect ratio of the spheroids. This strong dependence on the aspect ratio can be utilized to separate particles from a suspension of particles having different shapes but similar sizes.

Secondly, we have reported certain aspects of the problem that are of interest to the nonlinear dynamics community also. In this work we have reported a physically realisable system in which the possibility of an interesting and novel type of Class I intermittency has been demonstrated, namely it is an example of one of the very few physically realisable chaotic systems showing the phenomenon of a non hysteretic form of Class I intermittency with nearly regular reinjection period. Price and Mullin (1991) have observed experimentally a similar type of phenomenon in which a hysteretic form of intermittency with extreme regularity of the bursting is observed. The system described in this work appears to be one of the very few ODE systems describing a physically realisable system showing a non hysteretic form of Class I intermittency with nearly regular reinjection period. The regularity of the bursting is unaffected by variation in the control parameter. The maximum Lyapunov exponents of the bursts and laminar phase are estimated separately and indicate existence of chaos. The length of the laminar phase shows scaling behaviour typical of Class I intermittency near the tangent bifurcation and also shows new scaling behaviour. Return maps of the dynamical system are presented to explain the behaviour observed. The system also demonstrates some interesting features such as new scaling behaviour away from the onset of intermittency and the number of the bursts during a particular realization varying smoothly with the control parameter. These results are presented in terms of the evolution of the orientation of a spheroid subjected to an external periodic force immersed in a simple shear flow.

Thirdly, we have demonstrated that controlling the chaotic dynamics of periodically forced particles by a suitably engineered novel control technique which needs little information about the system and is easy to implement leads

to the possibility of better separation than otherwise possible. In this work we have demonstrated that controlling the chaotic dynamics of periodically forced particles leads to the possibility of better separation. Utilizing the flexibility of controlling chaotic dynamics in a desired orbit irrespective of initial state, it is demonstrated that it is theoretically possible to separate particles much more efficiently than otherwise possible from a suspension of particles having different shapes but similar sizes especially for particles of aspect ratio $r_e > 1.0$. The strong dependence of the controlled orbit on the aspect ratio of the particles demonstrated in this work may have many applications such as the development of computer controlled intelligent rheology. The results of this work also suggest that control of chaos in this problem may have many applications.

Finally, we have proposed a novel algorithm based on parametric perturbation for control of chaos in this work. The method proposed is comparatively easy to implement and needs almost no information about the system. One of the main advantages of this control algorithm is the possibility of pre-targeting the length of the controlled period obtained by suitably engineering the control technique. In addition we demonstrate certain advantages of this novel technique over two well-known algorithms, namely control by periodic parametric perturbation and control by addition of a second weak periodic force, such as the possibility of switching behaviour, pre-targeting the period, stabilising high period orbits *etc.* We have also demonstrated the applicability of the technique in certain numerical models of physical systems. We have demonstrated the successful application of the new algorithm in a rather difficult problem, namely, the control of the dynamics and the rheological parameters of periodically forced suspensions of slender rods in simple shear flow and also in the Bonhoeffer-Van der Pol (BVP) oscillator.

As part of considering different systems to test the applicability and suitability of the new control of chaos algorithm developed during this work, we have considered the case of chaotic rheological parameters of periodically forced slender rods only to compare the efficiency of the new control algorithm with some other control algorithms. The control of chaos algorithm developed in this work is used to control chaotic rheological parameters in the work of K. Satheesh Kumar, but the thrust in his work is on the possibility of obtaining novel rheological parameters and not on the control algorithm. In short, we have just reproduced the expressions of the rheological parameters from the thesis of K. Satheesh Kumar, as chaotic rheological parameters happen to be one of the different systems we considered to test the novel control of chaos algorithm for efficiency.

The other similarity is the assumptions of the model of the suspension considered in these two thesis are similar with deviation from the thesis of K. Satheesh Kumar in the particle shape. We developed the orientation evolution equations based on Brenner (1974) and his scaling. At the same time, the development of the orientation evolution equations in the work of K. Satheesh Kumar is based on the approach of Strand and Kim (1992) and the scaling in his thesis is also different from that of ours.

Except for these two similarities all other results are the original contributions of this thesis which has been published in international referred journals.

Literature Cited

Altan, M. C., S. G. Advani, S. I. Guceri and R. B. Pipes, "On the description of the orientation state for fibre suspensions in homogeneous flows," J. Rheol. **33**, 1129–1155 (1989).

Anczurowski, E. and S. G. Mason, "The kinetics of flowing dispersions: II. Equilibrium orientations of rods and discs," J. Coll. Int. Sci. **23**, 522–532 (1967).

Anishchenko, V. S., *Dynamical chaos -models and experiments, Appearance routes and structure of chaos in simple dynamical systems* (World scientific, Singapore 1995).

Aubry, N., P. Holmes, J. L. Lumley and E. Stone, "The dynamics of coherent structures in the wall region of a turbulent boundary layer," J. Fluid Mech. **192**, 115–173 (1988).

Bird, R. B., R. C. Armstrong and O. Hassager, *Dynamics of Polymeric Liquids: Vol 1 Fluid Mechanics* (John Wiley & Sons, Inc., New York, 1987a).

Bird, R. B., R. C. Armstrong and O. Hassager, *Dynamics of Polymeric Liquids: Vol 2 Kinetic Theory* (John Wiley & Sons, Inc., New York, 1987b).

Brenner, H., "Suspension rheology," Proc. Heat and Mass Transfer **5**, 89–129 (1972).

Brenner, H., "Rheology of a dilute suspension of axisymmetric Brownian particles," Int. J. Multiphase Flow **1**, 195–341 (1974).

Bergé, P., Y. Pomeau and C. Vidal, *Order Within Chaos* (Wiley, New York, 1986).

Bretherton, F. P., "The motion of rigid particles in a shear flow at low Reynolds number," J. Fluid Mech. **14**, 284–304 (1962).

Buevich Yu A., S. V. Syutkin and V. V. Tetyukhin, "Theory of a developed magnetofluidized bed," Magnetohydrodynamics **20**, 333–339 (1984).

Cebers, A., "Chaos in polarization relaxation of a low-conducting suspension of anisotropic particles," J. Magnetism and Magnetic Materials **122**, 277–280 (1993a).

Cebers, A., "Chaos: new trend of magnetic fluid research," J. Magnetism and Magnetic Materials **122**, 281–285 (1993b).

Berry, D. H. and W. B. Russel, "The rheology of dilute suspensions of slender rods in weak flows," J. Fluid Mech. **180**, 475–494 (1987).

Christini, D.J., and J.J. Collins, "Controlling nonchaotic neuronal noise using chaos control techniques," Phys. Rev. Lett. **75(14)**, 2782–2785 (1995).

Cvitanovic, P., *Universality in Chaos* (Adam Hilger, Bristol, England, 1989).

Ditto, W. L., M. L. Spano and Lindner, "Techniques for the control of chaos," Physica D **86**, 198–211 (1995).

Einstein, A., *Theory of Brownian Movement* (New York, Dover 1956).

Einstein, A., "Eine neue Bestimmung der Molekuldimension," Ann. Phys. **19**, 286–306 (1906).

Einstein, A., "Berichtigung zu meiner Arbeit: Eine neue Bestimmung der Molekuldimension," *ibid.* **34**, 591– (1911).

Eckmann, J. P. and D. Ruelle, "Ergodic theory of chaos and strange attractors," Rev. Mod. Phys. **57**, 617–656 (1985).

Fronzoni, L., M. Giocondo and M. Pettini, "Experimental evidence of suppression of chaos by resonant parametric perturbations," Phys. Rev. A **43** 6483–6487 (1991).

Ginder, J. M. and J. L. Sproston, "The performance of field-controllable fluids and devices," ACTUATOR 96 (5th international conference on new actuators) , 313–319 (1996).

Glass, L. and M. C. Mackey, *From clocks to chaos, the rhythms of life* (Princeton University press, Princeton, NJ, 1988)

Güémez, J., J. M. Gutiérrez, A. Iglesias and M. A. Matias, "Stabilization of periodic and quasiperiodic motion in chaotic systems through changes in the system variables", Phys. Lett. A, **190**, 429–433 (1994).

Happel, J. and H. Brenner, *Low Reynolds Number Hudrodynamics with Special Applications to Particulate Media* (Martinus Nijhoff Publishers, Dordrecht, 1986)

Hao Bai-lin, *Directions in chaos*, Vol 2 (World Scientific, NJ, 1988).

Hao Bai-lin, *Elementary symbolic dynamics and chaos in dissipative systems* (World Scientific, Singapore 1989).

Heffernan, D. M., P. Jenkins, M. Daly, B. J. Hawdon and J. O'Gorman, "Characterization of chaos," International Journal of Theoretical Physics **31**(8), 1345–1362 (1992).

Hilborn, R.C., *Chaos and nonlinear dynamics* (Oxford University Press, New York 1994).

Huberman, B. A. and E. Lumar, "Dynamics of adaptive systems," IEEE Trans. Circ. Syst. **37**, 547–550 (1990).

Ignatenko, N. M., Melik-Gaikazyan I. Yu, V. M. Polunin and A. O. Tsebers, "Excitation of ultrasonic vibrations in a suspension of uniaxial ferromagnetic particles by volume magnetostriction," Magnetohydrodynamics **20**, 237–240 (1984).

Jackson, E. A. and A Hübler, "Periodic entrainment of chaotic logistic map dynamics," Physica D, **44**, 407–420 (1990)

Jeffery, G. B., "The motion of ellipsoidal particles immersed in a viscous fluid," Proc. Roy. Soc. (Ser. A) **102**, 161–179 (1922).

Kantz, H., "A robust method to estimate the maximal Lyapunov exponent of a time series," Phys. Lett. A **185**, 77–87 (1994).

Kashevskii B.É., "Torque and rotational hysteresis in a suspension of single-domain ferromagnetic particles," Magnetohydrodynamics **22**, 161–168 (1986).

Kim, S. and S. J. Karrila, *Mycrohydrodynamics: Principles and Selected Applications* (Butterworth–Heinemann, Stoneham, MA, 1991)

Knudsen, C., R. Feldberg, H. True, "Bifurcations and chaos in a model of a rolling railway wheelset," Phil. Trans. R. Soc. Lond. A **338**, 455–469 (1992).

Knudsen, C., E. Slivsgaard, M. Rose, H. True, R. Feldberg, "Dynamics of a model of a railway wheelset," Nonlinear Dynamics **6**, 215–236 (1994).

Kumar, K. S. and T. R. Ramamohan, "Chaotic rheological parameters of periodically forced slender rods in simple shear flow," J. Rheol. **39(6)** 1229–1241 (1995).

Kumar, K. S., S. Savithri and T. R. Ramamohan, "Review of chaotic behaviour of suspensions of slender rods in simple shear flow," C4, Dynamics of Complex fluids Eds: M. J. Adams, A. R. Rennie, R. A. Mashelkar and J. R. A. Pearson (Imperial College Press, The Royal Society, 1998) (In press).

Lakshmanan, M. and K. Murali, *Chaos in nonlinear oscillator: controlling and synchronization* (World Scientific, Singapore 1996)

Lindner, J. F. and W. L. Ditto, "Removal, suppression and control of chaos by nonlinear design," Appl. Mech. Rev. **48**(12) part 1, 795–808 (1995).

Leal, L. G., and E. J. Hinch, "The effect of weak Brownian rotations on particles in shear flow," J. Fluid Mech. **46**, 685–703 (1971).

Lorenz, E. N., "Deterministic non-periodic flows," J. Atmos. Sci. **20**, 130–141 (1963).

Macmillan, E. H., "Slow flows of anisotropic fluids" J. Rheol. **33**, 1071–1105 (1989).

Manneville, P. and Y. Pomeau, "Intermittency and the Lorenz model," Phy. Lett. A **75** 1–2 (1979).

May, R., "Simple Mathematical Models with very very complicated dynamics," Nature **261** 45–67 (1976).

Nayfeh, A. H. and B. Balachandran, *Applied Non-linear Dynamics - Analytical, Computational and Experimental Methods* (John Wiley and Sons, Inc., New York, 1995)

Ott, E., C. Grebogi and J. A. Yorke, "Controlling chaos," Phys. Rev. Lett. **64**, 1196–1199 (1990).

Ott, E., *Chaos in Dynamical Systems* (Cambridge University Press, Cambridge, 1993)

Ott, E. and M. Spano, "Controlling chaos," Physics Today , 34–40 (May, 1995).

Parker, T. S. and L. O. Chua, *Practical numerical algorithms for chaotic systems* (Springer-Verlag, New York 1989).

Petrikevich, A. V., and Raikher Yu. L, "Rheological characteristics of magnetic suspension in alternating magnetic field," Magnetohydrodynamics **20**, 122–127 (1984).

Pomeau, Y. and P. Manneville, "Intermittent transition to turbulence in dissipative dynamical systems," Comm. Math. Phys. **74**, 189–197 (1980).

Press, W. H., B. P. Flannery, S. A. Teukolsky and W. T. Vetterling, *Numerical Recipes, The Art of Scientific Computing* (Cambridge University press, Cambridge 1986).

Price, T.J., T. Mullin, "An experimental observation of a new type of intermittency," Physica D, **48**, 29–52 (1991).

Rajasekar, S. and M. Lakshmanan, "Controlling of chaos in Bonhoeffer-van der Pol oscillator," Int. J. Bifur. Chaos, **2(1)**, 201–204 (1992).

Rajasekar, S. and M. Lakshmanan, "Algorithms for controlling chaotic motion: application for the BVP oscillator," Physica D, **67**, 282–300 (1993).

Ramamohan, T.R., C. Chandra Shekara Bhat, S. K. Vijayalakshmi, and K. Rajalekshmy Ammal, "Effects of some external force fields on the orientation of a slender rod in simple shear flow," Developments in Mechanics, Vol.16, University of Missouri, Rolla, (R.C.Batra and B.F.Armaly ,Eds.), 501–502 (1991)

Ramamohan, T. R., S. Savithri, R. Sreenivasan and C. C. S. Bhat, "Chaotic dynamics of a periodically forced slender body in a simple shear flow," Phys. Lett. A **190**, 273–278 (1994).

Rhode, M.A., R.W. Rollins, A.J. Markworth, K.D. Edwards, K. Nguyen, C.S. Daw and J.F. Thomas, "Controlling chaos in a model of thermal pulse combustion," J. Appl. Phys., **78(4)**, 2224–2232 (1995).

Schuster, H. G., *Deterministic Chaos, an Introduction* (VCH Verlagsgesellschaft mbH, Weinheim, Federal Republic of Germany, 1989)

Schiff, S. J., K. Jorger, D. H. Duong, T. Chang, M. L. Spano and W. L. Ditto, "Controlling chaos in the brain," Nature **370**, 615–620 (1994).

Shinbrot, T., C. Grebogi, E. Ott and J. A. Yorke, "Using small perturbations to control chaos," Nature **363**, 441–417 (1993a).

Shinbrot, T., "Chaos: unpredictable yet controllable," Nonlinear Science Today **3**(2), 1–8 (1993b).

Shul'man, Z. P., B. M. Khusid and E. A. Zal'tsgendler, "Motion of an axisymmetric magnetically soft particle in hydrodynamic flow under the action of a strong rotating magnetic field," Magnetohydrodynamics **22**, 288–293 (1986).

Sprott, J. C., "How common is chaos?," Phys. Lett. A **173**, 21–24 (1993).

Strand, S. R., *Dynamic rheological and rheo-optical properties of dilute suspensions of dipolar Brownian particles* (Ph.D Dissertation, University of Wisconsin, Madison 1989).

Strand, S. R. and S. Kim, "Dynamics and rheology of a dilute suspensions of dipolar nonspherical particles in an external field: Part 1. Steady shear flows," Rheol. Acta **31**, 94–117 (1992).

Szeri, A. J., W. J. Milliken and L. G. Leal, "Rigid particles suspended in time-dependent flows: irregular versus regular motion, disorder versus order," J. Fluid Mech. **237**, 33–56 (1992).

Tsebers, A. O., "Numerical modelling of the dynamics of a drop of magnetizable liquid in constant and rotating magnetic fields," Magnetohydrodynamics **22**, 345–351 (1986).

Zhang Shu-Yu, *Bibliography on Chaos (Directions in chaos Vol. 5)* (World Scientific, Singapore, 1991)

Zibol´d, A.F., A.B. Kapusta, V.F. Keskyula, G.N. Petrov, O.A. Remizov, "Hydrodynamic phenomena accompanying the growth of single crystals by Czochralski's method in a rotating magnetic field," Magnetohydrodynamics, **22**, 202-206 (1986).

Zumbrunnen, D. A., K. C. Miles and Y. H. Liu, "Auto-processing of very fine-scale composite materials by chaotic mixing of melts," Composites Part A **27A**(1), 37–47 (1996).

List of Publications

1. **C.V. Anil Kumar**, K. Satheesh Kumar, T.R. Ramamohan, *Chaotic dynamics of periodically forced spheroids in simple shear flow with potential application to particle separation*, Rheol. Acta, **34(5)**, 504-512 (1995).

   (This paper is listed in the Current World Literature section of Current Opinion in Colloid and Interface Science 1/4, 1996)

2. **C.V. Anil Kumar** and T.R. Ramamohan, *New type I intermittency in the dynamics of periodically forced spheroids in simple shear flow*, Phys. Lett. A, **227**, 72-78 (1997).

3. **C.V. Anil Kumar** and T.R. Ramamohan, *Controlling chaotic dynamics of periodically forced spheroids in simple shear flow: Results for an example of a potential application*, Sadhana. India (In press).

4. **C.V. Anil Kumar** and T.R. Ramamohan, *Dynamics and rheology of periodically forced particles in simple shear flow: part I. Dynamics*, 19th ICTAM, Japan (1996).

5. **C.V. Anil Kumar**, K. Satheesh Kumar, T.R. Ramamohan, *Erratum: "Chaotic dynamics of periodically forced spheroids in simple shear flow with potential application to particle separation, Rheol. Acta, 34(5), 504-512 (1995)"*, Rheol. Acta. **35** 523-523 (1997).

6. **C.V. Anil Kumar** and T. R. Ramamohan, *Comparative analysis of a new control of chaos algorithm on some model systems* (communicated).